Julius-Maximilians-Universität Würzburg

Fakultät für Biologie

Vaccinia virus mediated expression of human erythropoietin in colonized human tumor xenografts results in faster tumor regression and increased red blood cell biogenesis in mice

Dissertation

Zur Erlangung des naturwissenschaftlichen Doktorgrades der

Julius-Maximilians-Universität Würzburg

vorgelegt von

Duong Hoang Nguyen

aus Vietnam

Würzburg, November 2012

Eingereicht am: _____

Mitglieder der Promotionskommission:

Vorsitzender: _____

Erstgutachter: _____

Zweitgutachter: _____

Tag des Promotionskolloquiums: _____

Doktorurkunde ausgehändigt am: _____

Erklärung gemäß § 4 Absatz 3 der Promotionsordnung der Fakultät für Biologie der Bayerischen Julius-Maximilians-Universität Würzburg

Hiermit erkläre ich, die vorgelegte Dissertation selbständig angefertigt zu haben und keine anderen als die von mir angegebenen Quellen und Hilfsmittel verwendet zu haben.

Des Weiteren erkläre ich, dass die vorliegende Arbeit weder in gleicher noch in ähnlicher Form bereits in einem anderen Prüfungsverfahren vorgelegt wurde.

Zuvor habe ich neben dem akademischen Grad “Master of Science“ keine weiteren akademischen Grade erworben.

Die vorliegende Arbeit wurde von Prof. A. A. Szalay betreut.

Würzburg, den 10.11.2012 ----------

This thesis is dedicated to the memory of my father, Nguyen Tien Quang.

TABLE OF CONTENTS

ZUSAMMENFASSUNG 9

SUMMARY 13

1. INTRODUCTION 16

1.1 Overview on cancer 16

1.2 Lung cancer carcinoma 17

1.3. Vaccinia virus 17

1.3.1 An overview on vaccinia virus 17

1.3.2 Vaccinia virus molecular biology 18

1.3.3 Vaccinia virus as an oncolytic agent 20

1.4 Erythropoietin 26

1.4.1 An overview 26

1.4.2 Structure of erythropoietin 28

1.4.3 Mechanism of action of erythropoietin 32

1.4.4 Erythropoietin therapy in cancer anemia 35

1.4.5 EPO functions beyond erythopoiesis 37

1.4.6 Safety concerns of using rhEPO 39

2. MATERIALS AND METHODS 41

2.1 Materials 41

2.1.1 Equipments 41

2.1.2 Reagents 44

2.1.3 Kits 47

2.1.4 Solutions and buffers 48

2.1.5 Cell lines and culture media 49

2.1.6 Antibodies 49

2.1.7 Oligonucleotides 50

2.1.8 Animal use 51
2.1.9 Recombinant vaccinia virus 51
2.2 Methods 52
2.2.1 Culture of monolayer cells 52
2.2.2 Virus titration assay 53
2.2.3 Virus infection and replication assay 54
2.2.4 Cell viability assay (MTT assay) 54
2.2.5 Protein isolation 55
2.2.6 Western blotting 56
2.2.7 Real-time quantitative polymerase chain reaction (Q-PCR) 56
2.2.8 Enzyme-Linked Immunosorbent Assay (ELISA) 58
2.2.9 Detection of hEPO isoforms 59
2.2.10 Tumorigenicity and tumor therapy 60
2.2.11 Hemoglobin test and total blood cell counts 61
2.2.12 Cytokine and chemokine profiling 62
2.2.13 Immunohistological staining 62
2.2.14 Measurement of fluorescent intensity 64
2.2.15 Measurements of vessel density and vessel diameter 65
2.2.16 Statistical analysis 65
3. RESULTS 66
3.1 Characterization of recombinant vaccinia viruses expressing hEPO in cell culture 66
3.1.1 Construction of hEPO-encoding recombinant VAVCs 66
3.1.2 Detection of Ruc-GFP, *lacZ* and *gusA* expression by western blotting 67
3.1.3 Detection of Ruc-GFP expression via fluorescent microscopy 69
3.1.4 Detection of hEPO expression by western blotting 70
3.1.5 Transcription of *hEPO* in cells infected with different EPO-VACVs 71

3.1.6 Quantification of hEPO expression by ELISA 72
3.1.7 Replication of EPO-VACVs and GLV-1h68 in A549 and NCI-H1299 74
3.1.8 Cytotoxicity of EPO-VACVs and GLV-1h68 in A549 and NCI-H1299 75
3.1.9 Effect of hEPO on oncolytic potential in hypoxia and normaxia 76
3.2 Therapy of A549 xenografts with EPO-VACVs 79
3.2.1 EPO-VACVs enhance tumor regression 79
3.2.2 Increase of hemoglobin caused by virus-mediated expression of hEPO 80
3.2.3 Effects of treatment with EPO-VACVs on organ weights 82
3.2.4 Virus distribution in organs 84
3.2.5 Animal toxicity after treatment with different VACVs 85
3.3 Functional expression of hEPO in A549 tumor xenografts 87
3.3.1 Quantification of hEPO expression in tumor and serum 87
3.3.2 Detection of hEPO isoforms 88
3.3.3 Effects of EPO-VACV treatment on cell populations of the blood 89
3.3.4 Assessment of hemoglobin levels during the course of treatment 92
3.3.5 Confirmation of virus-mediated hEPO expression in tumor xenografts 93
3.4 Effects of EPO-VACVs treatment on micro tumor environment 94
3.4.1 Effects of EPO-VACVs treatment on the expression of immune-related antigens in tumors 94
3.4.2 Assessment of immune cell infiltration in tumors after treatment with VACVs 97
3.4.3 Assessment of tumor oxygenation after treatment with VACVs 99
3.4.4 Assessment of tumor vascularization after treatment with VACVs 100
4. DISCUSSION 103
4.1 The different expression levels of hEPO with four EPO-VACV constructs do not negatively affect oncolytic capacities of the viruses in cell culture. 104
4.2 EPO-VACVs express functional hEPO with different patterns of isoforms in tumors and sera 106

4.3 EPO-VACVs enhance blood vessel dilatation and tumor regression without evidence of hEPO promoting tumor growth in the A549 tumor xenograft model 107

4.4 The degree of tumor immune infiltration is proportionate to virus infection but is independent of hEPO expression 110

4.5 Toxicity concerns related to virus-mediated over-expression of hEPO 111

ABBREVIATIONS 113

ACKNOWLEDGEMENTS 114

CURRICULUM VITAE 116

LIST OF PUBLICATIONS 117

REFERENCES 118

ZUSAMMENFASSUNG

Vaccinia Virus (VACV) ist zweifelsohne eines der sichersten Viren, welches, als Ergebnis seiner Verabreichung als Impfstoff gegen Pocken in mehr als 200 Millionen Menschen, intensiv in seiner Molekularbiologie und Pathogenese studiert wurde. Es besitzt einen natürlichen Tropismus für Tumorzellen und da sein gesamter Lebenszyklus im Zytoplasma der Wirtszelle abläuft, besteht keine Gefahr einer Integration von viralen Genen ins Wirtszellgenom. Darüber hinaus kann VACV mehrere grosse Transgene aufnehmen, was es dem Virus erlaubt, diagnostische und therapeutische Gene zu enthalten ohne damit drastisch die virale Replikation zu verlangsamen. GLV-1h68 is ein genetisch stabiles VACV, das durch die Einfügung von drei Genkassetten, RUC-GFP Fusion, β-Galaktosidase und β-Glucuronidase in das Genom des LIVP Stammes hergestellt wurde. In vorklinischen Studien wurde GLV-1h68 erfolgreich benutzt, um verschiedene Tumormodelle zu therapieren, wo es spezifisch Tumorzellen infizierte, sich in ihnen replizierte und diese letztendlich zerstörte ohne gesundes Gewebe zu beschädigen. Kürzlich wurde eine klinische Studie der Phase I mit GL-ONC1 (die klinische Version von GLV-1h68) in Patienten mit fortgeschrittenen soliden Tumoren abgeschlossen, die ohne Anzeichen für Toxizität erste Anzeichen einer anti-tumoralen Wirkung aufwies.

Blutarmut stellt eine häufige Begleiterscheinung in Krebspatienten dar. Anämie beeinträchtigt die normale mentale und körperliche Funktionsfähigkeit mit Symptomen wie Übelkeit, Kopfschmerzen oder Depression. Menschliches Erythropoetin (hEPO), ein Glykoprotein-Hormon, welches die Bildung roter Blutzellen reguliert, ist klinisch zur Behandlung von Krebs-induzierter Blutarmut zugelassen. Wenn es zur Behandlung eingesetzt wird, verbessert hEPO bei anämischen Patienten den Gesundheitszustand und damit die LebensqualitätDes Weiteren führt der Einsatz von hEPO zu Erfolgen bei derBestrahlungs- und Chemotherapie von Krebspatienten. Verschiedene klinische Studien haben jedoch darauf hingewiesen, dass rekombinantes hEPO (rhEPO) das Tumorwachstum anregen kann, was die Frage nach Sicherheit der Anwendung von rhEPO aufbringt. In anderen Studien hingegen, gab es keine Anzeichen für eine Tumorwachstum anregenden Wirkung

oder für ein Eingreifen in krebsspezifische Signalwege. Die genaue Funktion von rhEPO in Tumormodellen bleibt umstritten und muss durch weitere Studien untersucht weren.

Ausgehend vom GLV-1h68 Rückgrat wurden die verschiedenen hEPO-exprimierende rekombinante VACV Stämme GLV-1h210, GLV-1h211 und GLV-1h213, (EPO-VACV) hergestellt, in welchen die *lacZ* Expressionskassette im J2R Lokus durch das *hEPO* Gen unter der Kontrolle von verschiedenen Vaccinia Promotoren, p7.5, pSE und pSL, ersetzt wurde. Ebenfalls wurde GLV-1h209 hergestellt, welches ähnlich zu GLV-1h210 ist, jedoch ein mutiertes (R103A) und nicht-funktionelles EPO Protein exprimiert. Alle EPO-VACV Stämme wurden bezüglich ihrer onkolytischen Funktion in A549 Zellkultur-Experimenten sowie in *in vivo* Tumormodellen charakterisiert. Gleichzeitig wurden die Effekte von lokal exprimiertem hEPO auf Virusvervielfältigung, Immuninflitration durch den Wirt, Tumorvaskularisierung sowie Tumorwachstum analysiert.

Die Expression der zwei Markergene (*ruc-gfp* und *gusA*) war in Zellkultur sowie in Tumorxenograften für alle EPO-VACV vergleichbar mit der des parentalen GLV-1h68 Virus. Unterschiede in hEPO Transkription und Translation der EPO-VACV war deutlich abhängig von der Promotorstärke und stieg promoter-abhängig von p7.5, über pSE und pSL zu pSEL 12 h nach Infektion von Zellen an. Darüberhinaus hatte die Insertion von hEPO in das virale Genom keinen Einfluss auf Replikation oder Zytotoxizität aller EPO-VACV in A549 oder NCI-H1299 Zelllinien, obwohl zu frühen Zeitpunkten (24-48 hpi) die Replikation der EPO-VACV etwas höher war, als die des GLV-1h68 Virus. Die A549 Zellen war zugänglicher für virale Infektion durch alle untersuchten Viren als die NCI-H1299 Zellen. Von besonderem Interesse ist, dass hypoxische Bedingungen (2% O_2) die Replikation und damit Expression des Markergens *gusA*, sowie Zytotoxizität für alle untersuchten VACV unabhängig von hEPO Expression verlangsamte.

Wie erwartet, erhöhten alle injizierten EPO-VACV die Bildung von roten Blutzellen (RBC) in Mausmodellen. Anzahl and RBCs sowie Hämoglobin (Hb) Level waren signifikant erhöht in Mäusen, die mit EPO-VACV behandelt wurden im Vergleich zu unbehandelten oder GLV-1h68 behandelten Mäusen. Die Durchschnittsgröße einer RBC sowie der Hämoglobinanteil hingegen waren unverändert. Darüberhinaus hatte die Expression von hEPO keinen signifikanten Einfluss auf Lymphozyten,

Monozyten, Leukozyten oder Blutplättchen im peripheren Blut. Die Expression von hEPO in EPO-VACV kolonisierten Tumoren wurde durch immunohistologische Färbungen bestätigt. Interessanterweise konnten 9-10 EPO Isoformen in Tumoren, Zellen oder Zellüberständen gefunden werden, während im Blutserum 3-4 basische Isoformen fehlten und nur 6 Isoformen auftraten.

Tumortragende Mäuse, die mit EPO-VACV behandelt wurden, wiesen im Vergleich zu GLV-1h68 behandelten Mäusen eine erhöhte Tumorregression auf. Ausserdem waren virale Titer in EPO-VACV behandelten Tumoren 3-4-fach höher also in denen, die mit GLV-1h68 behandelt wurden. Kein signifikanter Unterschied hingegen wurde zwischen viralen Titern der verschiedenen EPO-VACV in Tumoren gefunden. Tumorale Blutgefäße waren im Vergleich zu GLV-1h68 behandelten Mäusen deutlich vergrößert, wohingegen die Dichte an Blutgefäßen unverändert war, was andeutet, dass keine Proliferation von Endothelzellen angeregt wurde. Rekombinant hergestelltes Epoetin alfa in klinisch relevanten Dosen allein oder in Kombination mit GLV-1h68 hatte keinen Einfluss auf Verbesserung der Tumorregression verglichen mit unbehandelten oder GLV-1h68 behandelten Mäusen. Diese Ergbnisse legen nahe, dass weder Angiogenese noch Tumorwachstum durch hEPO im A549 Tumormodell angeregt wurde.

Humanes EPO spielt eine Rolle als Immunmodulator. In dieser Studie hingegen wurde kein Einfluss von hEPO im Bezug auf Zytokin- oder Chemokinexpression sowie Immunzellinfiltration (Leukozyten, B-Zellen, Makrophagen und dentritischen Zellen) in Tumore nachgewiesen. Das Ausmaβ an Immunzellinfiltratrion und Zytokinexpression konnte direkt mit der Anzahl an viralen Partikeln korreliert werden. Eine erhöhte Virusreplikation führte zu einer erhöhten Zahl an rekrutierten Immunzellen und sekretierten Zytokinen/Chemokinen. Es wurde angenommen, dass Tumorregression zumindest teiweise durch eine Aktivierung des angeborenen Immunsystems bedingt ist.

Zusammenfassend kann gesagt werden, dass durch die neuartigen EPO-VACV die Bildung von RBC, die Level an Hb und die virale Replikation signifikant angeregt wurden sowie eine erhöhte Tumorregression im A549 Xenograftmodell auftrat. Darüberhinaus leitete lokal exprimiertes hEPO keine Tumorangiogenese oder Tumorwachstum ein, aber führte zu einer Vergrößerung von Tumorblutgefäßen, was die virale Ausbreitung erleichtern könnte. Es ist vorstellbar, dass anämische

Patienten von einer möglichen klinischen Anwendung der EPO-Viren profitieren würden, da sie als eine Art „Wellness-Pille“ fungieren könnten, die die Symptome der Blutarmut lindern und dabei gleichzeitig den Tumor angreifen könnten.

SUMMARY

Vaccinia virus (VACV) is arguably one of the safest viruses, which has been intensively studied in molecular biology and pathogenesis as a vaccine for the eradication of smallpox in more than 200 million people. VACV possesses natural tumor tropism and its life cycle is entirely restricted to the cytoplasm, which prevents its genome from integrating into the host genome. Moreover, the VACV genome is able to carry multiple large transgenes, which allows the virus to include diagnostic and therapeutic genes without dramatically affecting virus replication. GLV-1h68 is a genetically stable engineered VACV constructed by insertion of three gene cassettes, RUC-GFP fusion, β-galactosidase and β-glucuronidase into the genome of LIVP strain. GLV-1h68 has been successfully used to treat many types of cancer in various preclinical models, where it has been shown to selectively infect, replicate in and destroy tumor cells without harming healthy cells. Recently, the first phase I clinical trial with GL-ONC1 (the clinical version of GLV-1h68) in patients with advanced solid tumors was finished, demonstrating the initial evidence of antitumor activity without toxicity concerns.

Cancer-related anemia is prevalent in cancer patients. Anemia negatively affects normal mental and physical function capacity with common symptoms like fatigue, headache, or depression. Human erythropoietin (hEPO), a glycoprotein hormone regulating red blood cell formation, is approved for the treatment of cancer-related anemia. It has shown benefits in correcting anemia, and subsequently improving health-related quality of life and/or enhancing radio-, and chemotherapy. Several recent clinical trials have suggested that recombinant hEPO (rhEPO) may promote tumor growth which raises questions concerning the safety of using rhEPO for cancer treatment. However, in other studies, such effects were not indicated. As of today, the direct functional effect of rhEPO in tumor models remains controversial and needs to be further analyzed.

Based on the GLV-1h68 backbone, the hEPO-expressing recombinant VACV strains (EPO-VACVs) GLV-1h210, GLV-1h211, GLV-1h212 and GLV-1h213 were generated by replacing the *lacZ* expression cassette at the *J2R* locus with *hEPO*

under the control of different vaccinia promoters p7.5, pSE, pSEL, pSL, respectively. Also, GLV-1h209 was generated, which is similar to GLV-1h210 but expresses a mutated (R103A) and non-functinal EPO. The EPO-VACV strains were characterized for their oncolytic efficacy in lung (A549) cancer cells in culture and tumor xenografts. Concomitantly, the effects of locally expressed hEPO in tumors on virus replication, host immune infiltration, tumor vascularization and tumor growth were also evaluated.

All EPO-VACVs were shown to be similar to the parental virus GLV-1h68 in expression of the two marker genes (*ruc-gfp* and *gusA*) in both cell cultures and tumor xenografts. The differences in the *hEPO* transcription and translation among EPO-VACVs were clearly promoter strength-dependent in an increasing order of p7.5, pSE, pSL and pSEL at 12 hpi in infected cells. Moreover, the insertion of hEPO did not significantly affect the replication and cytotoxicity of all EPO-VACVs in the A549 and NCI-H1299 cell lines, although at early time points (24-48 hpi), the replication of EPO-VACVs was higher than that of GLV-1h68. In addition, A549 cells were more susceptible to all tested viruses than NCI-H1299 cells. Notably, hypoxic condition (2% O_2) delayed the viral replication and therefore marker gene (*gusA*) expression as well as cytotoxicity for all analyzed VACV strains irrespective of hEPO expression.

As expected, EPO-VACVs enhanced red blood cell (RBC) formation in lung xenograft model. The number of RBCs and hemoglobin (Hb) levels were significantly increased in EPO-VACVs-treated mice compared to GLV-1h68-treated or untreated control mice. However, the mean size of RBC or Hb content per RBC remained normal. Furthermore, over-expression of hEPO did not significantly affect numbers of lymphocytes, monocytes, neutrophils or platelets in the peripheral blood stream. The expression of hEPO in colonized tumors of mice treated with EPO-VACVs was demonstrated by immunohistological staining. Interestingly, there were 9 - 10 hEPO isoforms detected either in tumors, cells, or supernatants, while 3-4 basic isoforms were missing in blood serum, where only six hEPO isoforms were found.

Tumor-bearing mice showed enhanced tumor regression after treatment with EPO-VACVs compared to GLV-1h68. The virus titers in tumors in EPO-VACVs-treated mice were 3-4 fold higher compared to GLV-1h68-treated mice. Nevertheless, no significant differences in virus titers among EPO-VACVs were found. The blood

vessels in tumors were significantly enlarged while the blood vessel density remained unchanged compared to the GLV-1h68 treated mice, indicating that hEPO did not affect endothelial cell proliferation in this model. Meanwhile, rhEPO (Epoetin alfa) alone or in combination with GLV-1h68 did not show any signs of enhanced tumor growth when compared to untreated controls and GLV-1h68 groups, while doses used were clinical relevant (500 U/kg). These findings suggested that hEPO did not promote angiogenesis or tumor growth in the A549 tumor xenograft model.

Human EPO has been reported to function as an immune modulator. In this study, however, we did not find any involvement of hEPO in immune cytokine and chemokine expression or innate immune cell infiltration (leucocytes, B cells, macrophages and dendritic cells) into infected tumors. The degree of immune infiltration and cytokine expression was directly correlated to the number of virus particles. Increased virus replication led to more recruited immune cells and secreted cytokines/chemokines. It was proposed that tumor regression is at least partially mediated through activation of innate immune mechanisms.

In conclusion, the novel EPO-VACVs were shown to significantly increase the number of RBCs, Hb levels, and virus replication in tumors as well as to enhance tumor regression in the A549 tumor xenograft model. Moreover, locally expressed hEPO did not promote tumor angiogenesis, tumor growth, and immune infiltration but was shown to cause enlarged tumoral microvessels which might facilitate virus spreading. It is conceivable that in a possible clinical application anemic cancer patients could benefit from the EPO-VACVs, where they could serve as “wellness pills” to decrease anemic symptoms, while simultaneously destroying tumors.

1. INTRODUCTION

1.1 Overview on cancer

Cancer is a type of diseases characterized by abnormal growth of cells. It is caused by an imbalance between cell proliferation and cell death. If the proliferation is not controlled, it can result in death. Both, internal factors (metabolism, mutations, immune conditions, hormones) and external factors (chemicals, radiation, tobacco, and virus infection) can cause cancer. According to statistics of the World Health Organization in 2008 (Fig. 1.1), cancer is a leading cause of death for 7.6 million people, accounting for 13% of all deaths over the world. Six leading types of deaths are: lung with 1.37 million people, stomach with 736,000 people, liver with 695,000 people, colorectal with 608,000 people, breast with 458,000 people and cervical cancer with 275,000 people [1]. In 2012, there are 577,190 Americans expected to die of cancer, over 1,500 people a day. Cancer becomes the second leading killer after heart disease, accounting for nearly 1 of every 4 deaths [2].

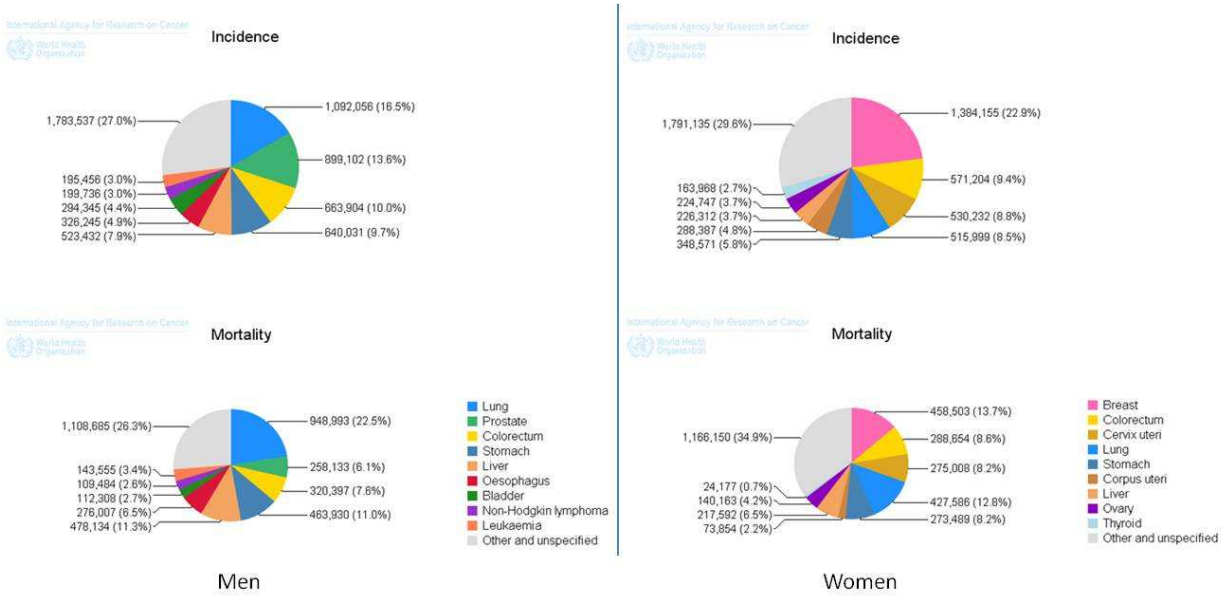

Fig. 1.1 Proportion of frequent cancers in the world in men and women, the WHO [1].

1.2 Lung cancer carcinoma

As an estimate, there are about 226,160 new cases of lung cancer to be expected in 2012, accounting for about 14% of all diagnosed cancers in the US. This type of cancer is increasing with aged-modality rate and accounts for more deaths than any other type of cancer in both men and women (28% of all cancer deaths) [2]. There are many reasons that can be causes of lung cancer but cigarette smoking is one of the most important risk factor. Exposure to other factors such as radioactive compounds, organic chemicals, air pollution or genetic susceptibility can play a contributing role in lung cancer development. Non-small lung cancer is the most common type, accounting for 85% of all lung cancers while small lung cancers account for about 14%. Currently, surgery, radiation therapy, chemotherapy, and targeted therapies such as erlotinib (Tarceva), crizotinib (Xalkori) and bevacizumab (Avastin) or combination therapies are being used for lung cancer treatments.

The conventional clinical methods still have limitations in both diagnosis and therapies such as non-specificity, side effects and almost fail to treat the disease once the cancer cells have spread to other organs (metastasis). The overall survival rate is low (16% for 5 years). The number would be higher if the disease was detected at an earlier stage, when the tumors are still localized (52% survival for 5 years). However, only 15% cases are diagnosed at early stage [2]. For that reason, it is vital to find out novel therapeutic strategies in which tumors can be earlier detected, feasibly controlled (localization and metastasis), and which are less invasive as well as more tumor specific. Oncolytic virotherapy is one of such approaches which are being in development.

1.3. Vaccinia virus

1.3.1 An overview on vaccinia virus

Vaccinia virus (VACV) is an enveloped virus belonging to the poxvirus family with widely susceptible animal hosts [3]. It has preserved the name vaccinia since Edward Jenner's time when it was first reported as an isolated material from a milkmaid to vaccinate against the smallpox disease in 1796. At that time it was known as cowpox virus. In the 1930s the cowpox vaccine used in the 20th century

for smallpox vaccination was determined to be a distinct virus, named vaccinia. VACV belongs to the same genus as variola virus does, the virus causing smallpox pandemics, which had been spread out over the world from the 17th to mid-20th century with an estimated deaths of about 300-500 million people. In 1980, after the long vaccination campaign using attenuated VACV [4], the WHO certified the eradication of smallpox disease in humans [5]. For that reason, the viral structure and biology have been intensively investigated. Nowadays, despite not being used as a vaccine, VACVs are still interesting tools for transcription machinery studies or protein interactions [6]. Moreover, with long-historical safety profile in humans as a vaccine, broad natural tumor tropism [7-8] and many other biological properties, VACVs are considered potential candidates for oncolytic viral therapies [9-10].

The first vaccinia genome sequenced was that from the vaccinia virus Copenhagen strain. The open reading frames (ORF) were determined based on its HindIII restriction map. VACV is a large (191,636 kbp) double-stranded DNA-containing virus with a complex enveloped membrane [11]. The virus replicates entirely in the cytoplasm of infected cells; thus, it encodes all of the enzymes and proteins necessary to express the DNA genome.

1.3.2 Vaccinia virus molecular biology

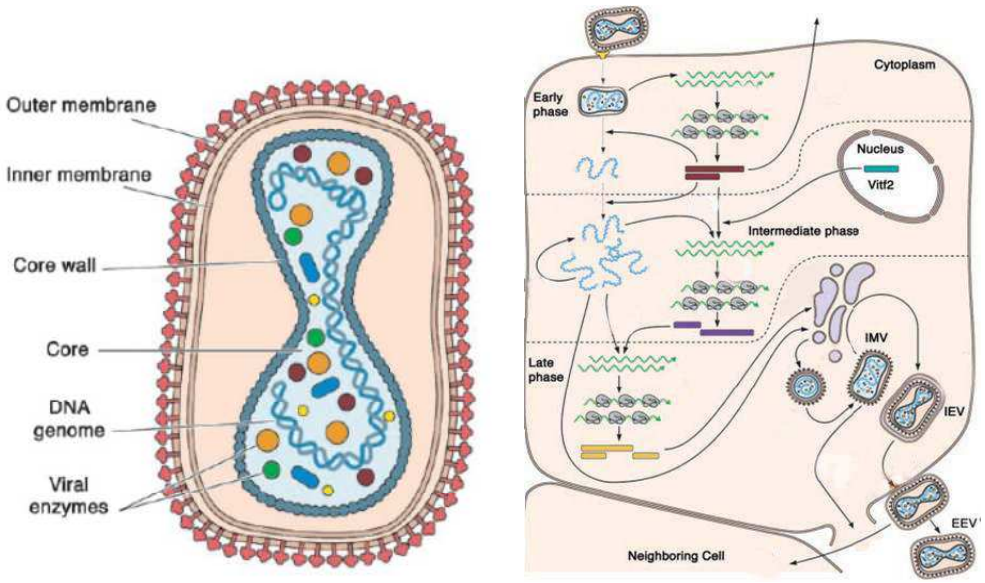

Fig. 1.2 The overview on vaccinia virus structure and replication cycle. (A) Virion structure includes 1 - 3 membranes and a core containing a double-stranded DNA,

enzymes, and factors for the initial replication of virus in host cells. (B) The life cycle is entirely restricted to the cytoplasm and occurs in three phases: early, intermediate and late, accompanied by different forms of virions [12]. Mature vaccinia virions exist in four forms which differ in the number of surrounding membranes and the location of viral particles. Intracellular mature virus (IMV) is the first assembled and simplest infectious form of virus with one membrane, which is retained inside of infected cells following virus maturation. Intracellular enveloped virus (IEV) is essentially IMV with two additional surrounding membranes which are derived from the Golgi apparatus or endosomal cisternae [13]. Cell-associated enveloped virus (CEV) is derived from IEV after outer the IEV membrane fused with the plasma membrane. CEV remains attached to the outer surface of cells. Extracellular enveloped virus (EEV) is a CEV which has been released from the cell surface. Therefore, EEV is mainly responsible for the spread of virus during infection [14].

The initial step for virus entry is the attachment of the virus to the cell plasma membrane. The detailed mechanism of action is still not well understood. It can occur via direct fusion at plasma membranes or low pH-dependent endosomal pathways [15]. Three viral membrane proteins: H3L [16] D8 [17] and A27 [18], were showen to be involved in the attachment of virus to glycoaminoglycans (GAGs) at the cell surface. But virus can also use GAG independent pathways to enter the cell [19]. Soon after the entry, the core is released from virions and the virus uses packaged materials to start an early phase transcription, followed by intermediate and late phases as illustrated in Fig. 1.2. The life cycle of virus happens entirely in the cytoplasm of host cells, hence it will not integrate to the host structural genome. Viral proteins which are necessary for functions of certain replication phases will be synthesized at different stages of the infectious cycle. Gene expression during VACV infection occurs in a tightly regulated temporal cascade featuring sequential synthesis of early, intermediate and late gene classes which are distinguished by special transcriptional promoters and its enclosed factors.

About half of VACV genes belong to the early class [20]. The VACV early class mRNA appears within minutes and reaches a peak at about 100 min after virus entry into cells [21]. Viral mRNAs are synthesized inside the core and are extruded outside its surface by packaged initial materials along with DNA genome which is necessary for early transcription and translation [22]. They include early transcription factors such as 80 kDa and 72 kDa proteins encoded by *A7L* and *B6L,* correspondingly [23]

which bind to promoters with assistance of RNA polymerase to activate the transcription processes [24-26]. Subsequently, the synthesis of early proteins is synthesized. This includes proteins required for core wall uncoating reactions, and viral DNA replicational and transcriptional factors to activate intermediate genes.

Early viral DNA released from the core is a template for intermediate gene transcription which is then used for translation into transcription factors for intermediate gene transcriptions. The intermediate genes are believed to be few in number and encode materials to initiate the late gene transcriptions and translations [27]. The late gene expression becomes detectable about 140 min after infection [21], and mainly encodes for viral structures, virion enzymes as well as essential proteins such as early initial proteins which must be incorporated into virus particles during assembly. Once all necessary materials are synthesized, the assembly process is initiated to first form immature virions. These mature virus particles with a brick shape are called IMVs. IMVs acquire a second membrane from Golgi apparatus to form double-membrane IEVs. In a next step, IEVs are release to the outside of the infected cell. They may contain one more layer of cell plasma membrane named EEV or CEV (if it is still retained on cell plasma membrane). While there is no evidence for the participation of host proteins in early phase of virus infection, the situation is different in intermediate and late phases. Virus appears to borrow host cell proteins for mRNA synthesis [27-28]. Soon after infection, VACVs develop multiple mechanisms to interfere with the host gene expression, such as inhibition of host mRNA synthesis [29] as well as induction of actin and tubulin mRNA degradation. Eventually, after 2-4 hours, host translation is drastically impaired in order to temporally maximize the expression of viral genetic information [30-31].

1.3.3 Vaccinia virus as an oncolytic agent

There are numerous inherited biological properties that make VACV suitable for development as an oncolytic agent. As a member of the poxvirus family, VACV has been reported to have a broad host range in which the virus can use multiple host entrance mechanisms [16, 19, 32]. VACV is one of the safest viruses which has been intensively studied concerning molecular biology and pathogenesis, as a result

of being used as a vaccine for eradiation of smallpox disease in human. Besides, it owns natural tumor tropism which enable it to selectively infect, replicate in and destroy tumor cells while leave the harmless to normal cells [7, 33]. VACV owns a large double DNA genome (~200 kbp) encoding almost all needed enzymes and factors for virus replication in the cytoplasm, and therefore physically independence on host-genome modification. In addition, this virus is able to carry multiple large transgenes, up to 25 kbp which allows a variety of genes to be added and engineered without remarkably affecting viral replication [34]. Recently, many genetically engineered VACVs were generated based on wild-type VACV backbones [10, 35-36]. These new generations showed significantly improved tumor selectivity and efficacy both in cell cultures and animal studies of various cancer cell types. Some potential candidates are tested in different tumor models in clinical trials (reviewed in [9]).

1.3.3.1 First generation of oncolytic VACVs

The term “oncolytic virus” means that a virus is able to selectively infect, replicate within and eventually destroy cancer cells once a number of viral particles are well accumulated. These properties derive from either inherence or genetic engineering. The first generation of oncolytic VACVs mostly exploit natural tumor tropisms to target cancer cells. In 1922, VACVs was used to infect and inhibit the growth of many kinds of tumors in rabbits, mice, and rats. Concomitantly, at the same year, Salmon and Baix tried to use the virus for treatment of breast carcinoma in human [37]. However, no tumor regression outcome was reported. Years later, more virus strains were explored. They showed a potential therapeutic spectrum in different cancer cells such as leukemia 9471, sarcoma, human cervix carcinoma or in combination with x-ray [9]. VACVs displayed the ability to preferentially replicate in tumor cells. However, non-specific effects such as high virus replication in normal organs or high toxicity are the limitations of first generation oncolytic VACVs [35].

1.3.3.2 Second generation of oncolytic VACVs

In order to improve tumor specificity, the 2nd generation VACVs were genetically manipulated to inactivate some critical genes necessary for virus replication in

normal cells but dispensable in cancer cells. Thymidine kinase (TK), a 19 kDa vaccinia virus protein [38], is a key function enzyme for DNA replication by making nucleotide pools. A hallmark of cancer cells is unlimitedly dividing, therefore, abundant nucleotide pools in tumors can serve as the sources for viral DNA replication and thereby propagation. Deletion of TK tremendously attenuates virus virulence in normal tissues, up to 7000-fold lower in lung, 3000-fold lower in liver, and 250-fold lower in ovaries 4 days after intraperitoneal (i.p.) injection of virus while the virus is still strongly active in tumors [39], resulting in an increase in the survival rate [40]. VACV also expresses vaccinia growth factor (VGF) that binds to epidermal growth factor receptor (EGFR) to promote cell proliferation through Ras signaling pathway [41], creating material sources (ATP, nucleotide pools) for virus replication. Therefore, the deletion of both TK and VGF can result in a higher therapeutic index in cancer cells with an activated Ras pathway than either mutant with single deletion [31, 42]. Vaccinia hemagglutinin (HA) has a specific affinity with membrane structure proteins which is believed to work as a bridge for virus binding [43]. A complete tumor regression was achieved when Zhang *et al*. used GLV-1h68, a replication-competent derivative of the vaccinia LIVP strain carrying a triple gene inactivation of the HA, TK and F14.5L loci, to treat breast carcinoma xenografts while poor or no replication of virus was detected in normal tissues compared to wild-type strains [35]. It has been known that oncolytic viruses induce many adaptation processes in infected cells which are similar to the hallmarks of malignant cells, including anti-apoptosis [44], induction of interferon [45] and immune evasion. This means that cancer cells are already suitable for viral replication. Therefore their deletions result in viral strains that are attenuated for replication in normal tissue but not in tumors [10]. Beside the deletion of virulence genes, the insertion of biomarker genes such as fluorescent proteins (green fluorescent protein (GFP) [33, 46], red fluorescent protein (RFP), luminescent proteins (luciferase-GFP fusion protein [47]) or product converting enzymes (β-galactosidase, β-glucuronidase [48]) make it feasible for real time visualization and quantifying virus actions in cancerous tissues. Due to their advantages, we can understand why almost vaccinia constructs carrying live biomarkers were applicable [35, 39, 45, 47].

1.3.3.3 Third generation of oncolytic VACVs

Third generation oncolytic VACVs were equipped with more powerful "tools" to specifically target and destroy tumor cells. Recently, Chen and Szalay published a detailed review on those strategies [9].

Briefly, vaccinia viruses can express transgenic **immunostimulatory cytokines** such as interleukins (IL-2, IL-6, IL-12), interferons (IFN-γ, IFN-β) and alpha tumor necrosis factor (TNF-alpha). They are important mediators in immune responses against tumors by promoting maturation of immune cells such as B cells, T cells, or monocytes. The expression of some IFNs also has a protective function for normal cells against virus infection but not in cancer cells. It has been shown that the combination of virus with cytokines enhanced tumor selectivity and antitumor effects in many tumor models [45, 49-51]. Lately, JX-495, an engineered vaccinia virus expressing GFP, β-galactosidase and granulocyte-macrophage colony stimulating factor (GM-CSF), showed for the first time expression of their marker genes in tumor tissues of treated patients [52]. However, increased cytokine-associated toxicity has been reported elsewhere, so the control of timing and concentration of administration must be taken into consideration to achieve a successful therapy [53].

Monoclonal antibody therapy is also a strategy that has been described. Multiple mechanisms have been exploited to inhibit tumor growth beside oncolysis. They include induction of apoptosis, alternation of tumor intracellular signaling, and inhibition of growth factor receptors [54]. Tumor-antigen specific monoclonal antibodies use their effects through Fc receptors such as antibody-dependent cell cytotoxicity and complement-dependent cytotoxicity, subsequently activating cell-mediated immune cells such as recruitment of macrophages, monocytes, natural killer cells, or neutrophills by producing cytokines and chemokines [55-56]. Avastin is one of the most successful immunotherapeutic proteins, which has been approved by the US Food and Drug Administration for treatment of metastatic colorectal cancer and most forms of metastatic non-small cell lung cancer. This monoclonal antibody is supposed to inhibit the growing of blood vessels in tumors (angiogenesis) which is a phenomenon characteristic found in most tumors and metastasis. Exploiting the same strategy, Fentzen *el al*. genetically engineered vaccinia viruses expressing anti-vascular endothelial growth factor (VEGF) antibodies (GLAF-1), and

showed significantly enhanced tumor therapeutic efficacy compared to controls via the massive reduction of tumor vascularization [57].

Anti **apoptosis** is a common way used by tumor cells to avoid cell-death programming which all normal cells have to pass through. Apoptotic cells display a number of characteristic features such as DNA fragmentation, chromatin condensation, mitochondrial dysfunction, and plasma membrane alterations ultimately leading to the death of the cells [58]. The human *TP53* gene encodes for the P53 protein which is known as an important protein in cell cycle control and apoptosis. In many organisms P53 plays a critical role in suppressing cancer cells. In most human tumors, P53 is inactivated either by *TP53* mutations or by inactivation of the P53 signal transduction. Therefore restoration of the activity of P53 could be beneficial to inhibit cancer growth. Vaccinia virus expressing wild-type P53 (rVACV-p53) was shown to inhibit tumor growth and induce apoptosis of different human and rat glioma cell lines [59] or in combination with radiotherapy [60].

In recent years, various **tumor antigens** (tumor-associated or tumor-specific antigens) have been discovered. They are the attractive targets for specific immunotherapy. Due to the ability of cancer cells to escape the recognition and destruction by the host immune system, a strategy in which tumor antigens is expressed by oncolytic viruses will exert synergic action of both, direct tumor destruction and activation of immune cells. Attenuated VACV expressing oncofetal antigen (5T4), a 72 kDa glycoprotein displayed on cell membrane of various cancer cell types, including ovarian, colorectal, and intestinal, but limited expression in normal tissues, showed significant tumor reduction compared with mice subjected with controls in models of colorectal and melanoma tumors [61]. Some other virus-expressing tumor-specific antigens were also shown to increase therapeutic benefit such as 47-LDA-Fcγ [62], and the prostate-specific antigen (PSA) [63]. Moreover, virus itself or debris from lysed tumor cells is able to initiate immune responses. Immune response to viral infection is a double-edged sword for virus therapy. On the one hand, it can eliminate viral particles and therefore decrease anti-tumor efficacy. But on the other hand, the local infiltration of immune cells help recognize and attack tumor cells [64]. GLV-1h68 treated various cancer cell types (breast [35], pancreatic [65], prostate [66], canine carcinoma [67], squamous carcinoma [68]), which showed massive infiltration of immune cells with cytokine and chemokine productions in

tumors in parallel with virus replication, and eventually led to inhibition of tumor growth.

Prodrug-converting enzyme-encoding viruses help overcome the limitations of conventional chemotherapy. With conventional chemotherapy, drugs are unspecifically delivered to the whole body in their active forms and therefore side effects are major concerns in chemotherapy. When inactive (non-toxic) forms of a drug (pro-drug) are combined with virus-mediated expression of pro-drug converting enzymes, the drug will only be activated inside the tumor where the needed enzyme is provided by the virus-infected cells and side toxicity is minimized. VACV carrying cytosine deaminase (CD) showed virus-specific targeting in liver metastasis after virus administration in both immunocompetent and athymic nude mice models. Following treatment with 5-fluorocytosine (5-FC) which was then activated by virus-expressing CD led to remarkable tumor response with cured rate up to 30% of animals with established liver metastasis [69].

1.3.3.4 Combination therapies

Combination with radiotherapy

The principle of interaction between oncolysis and radiation is not well understood. However, it appeared to have a synergistic function in enhancement of radiation-mediated virus replication and virus-mediated tumor sensitizing, as many positive antitumor effects of this combination therapy which have been documented in various preclinical models [70]. Lately, using U-87 glioma xenografts (subcutaneous and orthotopic) pre-treated with radiation showed preferential virus replication in tumor and correlated with tumor regression and survival rate when compared to individual therapies [71]. In another study, the combination between a VACV and radiation resulted in enhanced cancer cell death, reduction of caspase activity, and eventually improved long-term tumor regression [72], or lower tumor incidence and tumor progression on C6 glioma tumor model when combined VACV expressing P53 protein [73].

Combination with chemotherapy

Chemotherapy is a conventional therapeutic option to treat cancer by preventing cancer cells from rapidly dividing. The effectiveness is one of the most important

advantages of chemotherapy over other cancer treatments. Chemotherapeutic drugs will reduce the possibility of cancer spreading. But on the other hand, this is a main reason for some commonly known side effects. Because drugs are subjected to the whole body, cells which rapid multiply such as hair cells, bone marrow or reproductive cells will also be killed by the drugs. Consequently, chemotherapy is associated with high levels of cytotoxicity. Meanwhile, oncolytic virotherapy has a higher tumor specificity due to the virus itself or/and body immune barriers [74]. The synergistic actions therefore are thought to be beneficial in combination of oncolytic virus and chemotherapy, since the mechanism of action of those two therapies are quite different [75]. In preclinical modes, enhanced tumor therapeutic effects have been reported elsewhere. In human and rat glioma models, EGFP-expressing vaccinia virus (vvDD-EGFP) combined with rapamycin or cyclophosphamide promoted virus replication in tumors and further prolonged animal survival rates [76]. Another VACV, GLV-1h68, caused enhanced tumor regression in a pancreatic tumor model in combination with cisplatin or gemcitabine [65]. One derivative of GLV-1h68, GLV-1h90-encoded hyper-IL6, reduced chemotherapy-associated side effects of mitomycin C in a prostate model, and significantly improved anti tumor efficacy [51].
Although numerous encouraging results from cell culture and *in vivo* studies have been shown, the transfer from preclinical to clinical settings is still faced with many limitations. This fact could be explained by the complex interactions between virus and tumor microenvironment or virus and the host immune response [74]. During evolution, the human body has developed many barrier defenses against virus infections. Especially for VACV in this case, which has been used as a vaccine in the smallpox eradication campaign with an estimated hundred million people who still have some degree of immunity to VACV. This has imposed a significant barrier to achieve maximum therapeutic efficacy of oncolytic viruses.

1.4 Erythropoietin

1.4.1 An overview

Erythropoietin (EPO) is an obligatory growth factor (hormone) in many mammalians by promoting the formation of red blood cells. In the body, EPO is produced mainly in the kidneys, and subsequently circulated to the bone marrow where it activates the

proliferation and differentiation of erythroid progenitors. During the last two decades, recombinant human erythropoietin protein (rhEPO) has become the most successful drugs produced by recombinant DNA technology. Millions of people worldwide have benefited from research on erythropoietin. Epoetin alfa (EPO-α), a rhEPO trade mark from Amgen, has been widely used to correct anemia. Fatigue, weakness, and shortness of breath are common symptoms seen in anemic patients due to the lack of oxygen transportation to the target tissues. In many types of cancer, tumor hypoxia is associated with poor prognosis and chemo- or radio-therapy resistance. Besides, rhEPO is an effective way to reduce the risks in blood transfusion. rhEPO was approved by the FDA in 1989 for chronic renal failure and related-blood loss and for cancer-related anemia in 1993. For that reason, patients with chronic kidney decease, anemic HIV infection, hemalotogic disorders, cancer-related anemia, and surgical blood loss benefit most from rhEPO.

Table 1.1: Milestones in studying of erythropoietin (modified from [77-78])

1882	Bert describes the first time the relationship between increase of red blood cells in people living in high attitudes and consequently increased blood O_2 capacity.
1906	Carnot *et al*. report a humoral hormone responsible for red blood cell production which then is known as erythropoietin (hEPO).
1940s	Researchers give evidence for increase of immature red blood cells (reticulocytes) when exposed to hypoxic plasma factor.
1950	Reissman *et al*. show on parabiotic rats that the induction of erythroid hyperplasia in bone marrow and production of reticulocytes increases in both parabiotic rats when only one partner is exposed to hypoxic condition.
1953	Erslev *et at*. confirm the increase of reticulocytes and hematocrit in rabbits which were subjected with plasma from anemic donor animals.
1957	Jacobson *et al*. find that erythropoietin is mainly produced in the kidneys.
1972 1974	Zanjani *at al*. show that the liver is the main site for EPO production in the fetus. However, Fried finds small amounts of EPO still synthesized in the liver after birth.
1977	Miyake *et al*. purify hEPO from the urine of anemic patients.

1985	Two independent research groups led by Lin and Jacobs successful clone and express the human erythropoietin gene in Chinese hamster ovaries and green monkey kidney cells, respectively.
1986	Eschbach and colleagues first use rhEPO to correct the anemia of chronic renal disease.
1989	The FDA approved the administration of rhEPO for the treatment anemia of chronic renal failure.
1993	The FDA approves the administration of rhEPO for cancer-related anemia.

1.4.2 Structure of erythropoietin

EPO is a glycoprotein hormone belonging to the class I cytokine family. The human *EPO* gene locates in chromosome 7, which is about 2.2 kb, encoding for 192 amino acids that include a 27 amino acid signal peptide and 165 core amino acids linked with 4 carbohydrate side chains (account for 40% of the molecular mass) which are the critical structures for the halflife of this protein *in vivo*. Its molecular mass is 30.4 kDa [79]. The polypeptide has a tertiary folding structure of the as a bundle of globular forms with 4 alpha helices [80]. Three of four carbohydrate side chains, N-linked oligosaccharides at asparagines 24, 38 and 83, are important for protein stabilization and activity. However, the O-linked oligosaccharide at serine 126 appears to lack of functional importance [81]. The mature hEPO has a half-life of about 8 hours in blood circulation.

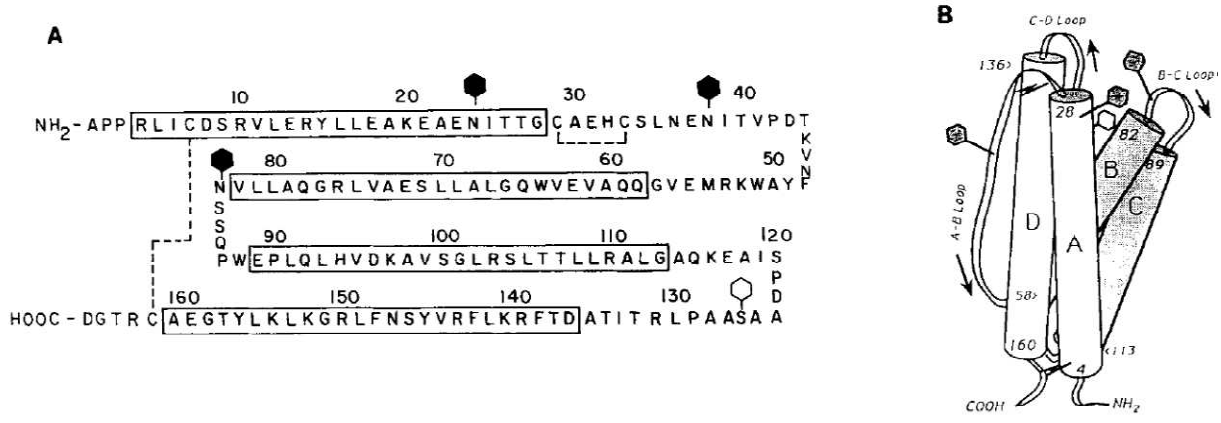

Fig. 1.3 Amino acid sequence (A) and predicted tertiary structure (B) of human EPO. (A) Primary sequence of EPO contains 165 amino acids, including 3 N-linked and 1 O-linked glycosylations. The site of O-glycosylation is represented by an open hexagon; sites of N-glycosylations are represented by filled hexagons. Rectangles show the predicted α-helical

sequences. Dashed lines indicate disulfide bonds. (B) The predicted tertiary structure of human EPO is based on folded, antiparallel arrangements of α-helices. Glycosylation sites are designated as in (A). α-helices are labeled A through D in order of the N-terminus to the C-terminus with intervening loops shown with an arrow directed toward the C-terminus [82].

Recombinant human erythropoietin

In 1985, the human *EPO* gene was independently cloned by two research groups within a few weeks of each other [83-84]. The hEPO primary structure consists of 166 amino acids, however, there are some debates regarding the existence of arginine 166 (R166) in mature form. Although, by using peptide mapping and fast atom bombardment mass spectrometry, Recny and his colleagues did not see the existence of R166 in recombinant human protein purified from Chinese hamster ovary (CHO) cells [85], Lai *et al*. demonstrated the presence of R166 in human urinary EPO by protein sequencing determination [86]. It is possible that the presence or absence of R166 depends on the cells in which it was produced or the loss just happened during EPO circulation [87].

Human urinary EPO and rhEPO are identical in primary and secondary structures. However, there are minor quantitative differences in O-linked and N-linked glycan composition which make some of them distinguishable under isoelectric focusing. The species, the tissues where protein is produced, or the ways of protein purification will result in different isoelectric patterns which is majorly due to post-translational modification [88]. There are more than six different rhEPO forms produced in the world but only available in certain country markets [87]. Three commonly used variants which were approved by the FDA are EPO-α and EPO-β (recombinant form) and darbepoetin-α (synthetic form). They all share similar primary protein sequences, but differ in carbohydrate side chains. In contrast to recombinant forms (EPO-α and EPO-β), which have 3 N-linked carbohydrate chains with maximum 14 sialic acids, darbopoetin-α has 5 N-linked carbohydrate side chains and contains up to 22 sialic acids. Those differences can be an explanation for the greater half-life (~25 hours) and stronger *in vivo* bioactivity of darbopoetin-α compared to recombinant ones [89]. Isoelectric patterns from human urine have about 10 isoforms, with *pI(s)* ranging from 3.77 to 4.77, while recombinant human EPO-α and EPO-β consist of 6 and 7 isoforms (pI: 4.42 - 5.11), respectively [90].

Both EPO-α and EPO-β showed very similar isoform pattern, although EPO-β has an extra basic band due to more sialic acids in carbohydrate chains [88]. The migration patterns of rhEPO and Darbepoetin-α differ greatly (Fig. 1.4). Darbepoetin-α appeared in the basic area (anode), while rhEPO appeared in the acidic area (cathode) [91].

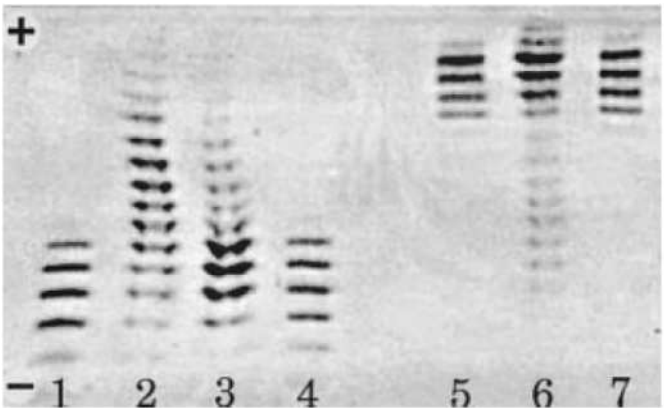

Fig. 1.4 Isoforms of rhEPO, darbepoetin-α, the extractions from urine of healthy and treated individuals with rhEPO and darbepoetin-α. Lanes 1 and 4 are rhEPO; lane 2 is endogenous hEPO from a healthy individual; lanes 5 and 7 are darbepoetin-α; lanes 3 and 6 are from patients treated with rhEPO and darbepoetin-α, respectively [91].

Structure-activity relationships

Conserved regions of the EPO structure from 6 mammals representing 5 different orders were tested by a series of scanning deletion mutations (Table 1.2). Boissel *et al*. found that in helix A, when arginine 14 was replaced by alanine, EPO's biological activity was dramatically reduced, whereas replacement with glutamine reduced its bioactivity to undetectable levels. In a similar manner, mutating arginine 103 to alanine in the helix C resulted in complete lack of biological activity without effects of conformational change of this protein [92] Alanine substitutions of serine 104 and leucine 108 reduced bioactivity to 35% and 47% compared to wide type activity. In contrast, alanine substitutions at three nearby sites in helix D of arginine 143, serine 146 and asparagine 147 resulted in mutants with increased bioactivity [93].

Table 1.2 Bioactivity of EPO by alanine substitutions.

Helix	Mutein	Specific bioactivity		
		UT7	HCD	Spleen
		% wild type human Epo		
A	S9A	148 ± 35; [3/3]	123 ± 13; [3/3]	
A	R10A	91; [1/1]	123; [1/1]	
A	E13A	111, 74; [2/2]	80, 99; [2/2]	
A	R14A	58, 56; [2/2]	2, 30; [2/2]	18, 24; [2/2]
A	R14L	91 ± 8; [4/6]	86 ± 15; [4/6]	67, 111; [2/2]
A	R14E	11 ± 6 [3/5]	12 ± 1; [5/3]	17, 17; [2/2]
A	L17A	110; [1/1]	95; [1/1]	
A	E18A	70 ± 17; [3/3]	100, 90; [2/2]	
A	K20A	252 ± 81; [4/4]	103 ± 21; [4/4]	
A	E21A	99, 69; [2/2]	50; [1/1]	
A-B	C29Y/C33Y	75; [1/1]	42; [1/1]	
A-B	K45A	110, 101; [2/2]	100, 100; [2/2]	
A-B	F48S	146, 110; [2/2]	100, 61; [2/2]	
A-B	Y49S	150 ± 7; [3/3]	146, 138; [2/2]	
A-B	A50S	128, 92; [2/2]	140, 37; [2/2]	
A-B	W51S	101, 78; [2/2]	89 ± 7; [3/3]	
A-B	K52S	99, 90; [2/2]	99, 88; [2/2]	
B	Q59A	156, 125; [1/2]	130, 134; [1/2]	
B	E62A	101, 85; [2/2]	63, 78; [2/2]	82, 111; [2/2]
B	W64A	102, 112; [2/2]	87, 143; [2/2]	90, 107; [2/2]
B	Q65A	96; [1/1]	140; [1/1]	99; [1/1]
B	G66A	130; [1/1]	103; [1/1]	85; [1/1]
B	L69A	94; [1/1]	84; [1/1]	
B	S71A	64; [1/1]	130; [1/1]	85; [1/1]
B	E72A	NS		
B	A73G	242 ± 25; [2/3]	104; [1/1]	
B	R76A	109; [1/1]	138; [1/1]	
C	Q92A	112; [1/1]	98, 95; [2/2]	113, 91; [2/2]
C	L93A	123, 126; [2/2]	127, 95; [2/2]	
C	H94A	NS		
C	D96A	NS		
C	K97A	84 ± 9; [2/4]	77 ± 27; [2/3]	94; [1/1]
C	S100A	98, 85; [2/2]	131; [1/1]	104; [1/1]
C	G101A	166 ± 52; [3/3]	146 ± 26; [3/4]	73, 152; [2/2]
C	R103A	3 ± 3; [3/5]	7 ± 1; [2/3]	6; [1/1]
C	S104A	114 ± 28; [2/4]	35 ± 17; [2/3]	
C	T106A	120; [1/1]	108; [1/1]	
C-D	L108A	158 ± 41; [2/4]	48 ± 6; [2/4]	12, 52; [2/2]
D	T132A	120, 104; [1/1]	98, 108; [1,1]	
D	D136A	108, 114; [2/2]	88 ± 20; [3/3]	
D	R139A	171, 91; [2/2]	120, 109; [2/2]	90, 131; [1/2]
D	K140A	189 ± 30; [3/3]	110 ± 19; [3/3]	
D	R143A	276 ± 85; [3/3]	150 ± 27; [3/3]	
D	S146A	198, 269; [1/2]	58, 110; [1/2]	
D	N147A	457 ± 185; [3/6]	115 ± 22; [5/6]	
D	R150A	181 ± 94; [3/4]	92 ± 28; [3/4]	28, 64; [1/2]
D	G151A	11 ± 4; [2/3]	6 ± 2; [2/3]	
D	K152A	89, 73; [1/2]	46, 20; [1/2]	16, 35; [1/2]
3′D	L153A	95; [1/1]	83; [1/1]	46; [1/2]
3′D	K154A	175 ± 60; [3/4]	185 ± 84; [3/5]	82, 157; [1/2]
3′D	L155A	95, 128; [2/2]	115; [1/1]	40, 98; [2/2]
3′D	Y156A	105; [1/1]	65 ± 12; [3/3]	
3′D	T157A	86, 104; [2/2]	89, 91; [2/2]	102, 104; [2/2]
3′D	G158A	84, 109; [2/2]	94, 89; [2/2]	77, 139; [2/2]
3′D	E159A	89, 97; [2/2]	101 ± 10; [2/3]	33, 96; [2/2]

The three bioassays were conducted on human UT7 cell line, murine HCD57 cell line, and primary mouse spleen erythroid cell line. 3 right columns show specific bioactivity of each mutant, expressed as a percentage of wild type human EPO bioactivity. The letters in the column on the left designate predicted helices (A, B, C, and D) or inter helical loops (A-B, C-D). The numbers within the brackets indicate the number of separate COS cell transfections over (/) the number of separate bioassays that were performed. NS, not secreted from COS 7 cells [93].

1.4.3 Mechanism of action of erythropoietin

The liver is a major site for production of EPO during the fetal stage. Even though after birth, the kidney's renal cortex takes over as a principle site of EPO production. In adults, minor EPO mRNA amounts are found in the brain, spleen, lung, and testis. However, the mechanism of action of EPO seems to be different in erythropoiesis. In the brain, for instance, EPO exerts neutrotropic and neuroprotective effects to protect neuronal cells from damaging under stress conditions [94]. Tissue hypoxia is the main stimulus for EPO production. In normal, healthy persons with intact renal function, EPO plasma can exponentially raise up to 10.000 U/l compared to about 15 U/l at normal levels. EPO production is not only a reaction to decreasing of haematocrit but also to decreasing arterial pO_2 or increasing blood O_2 affinity [95]. The principle responsible the clearance of EPO from the circulation is not completely understood. However, glycosylation of EPO appears to be a critical factor for *in vivo* function as well as protein clearance. EPO clearance has been stated to take place in the liver, kidneys, and bone marrow [87].

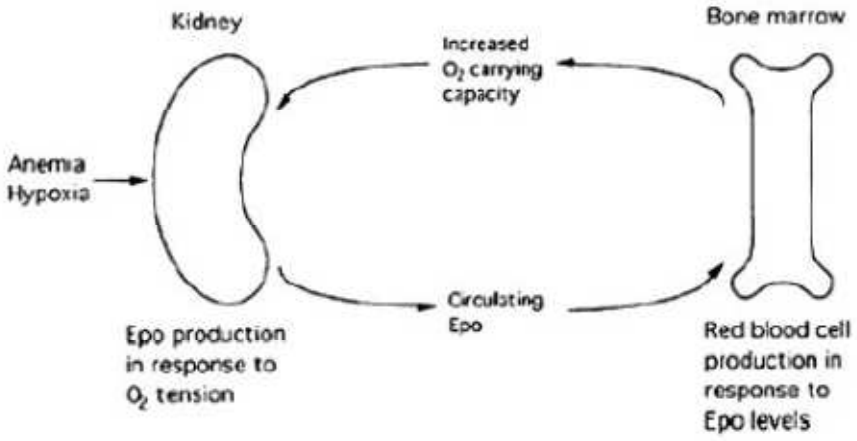

Fig. 1.5 The relationship of anemia and erythropitein production [96]. EPO is produced in the kidney in response to the oxygen tension of the blood. EPO then circulates to the bone marrow where it stimulates the proliferation and differentiation of red blood cell progenitors, leading to more red blood cells and increased oxygen-carrying capacity.

Erythrocytic progenitors in the bone marrow are the principle target of EPO. Here, EPO will bind to EPO receptors (EPOR) present on the surface of progenitor cells to trigger the signaling cascade. Normally, a small amount of EPO will activate a certain amount of cells which eventually mature to red blood cells. The remaining progenitor cells which are not activated will undergo programmed cell death (apoptosis). In order to become a mature red blood cell, erythrocytic progenitor cells have to pass through a series of developmental steps which are distinguished by morphological, functional and antigenic characteristics. Passing through each step, cells will have less proliferative potential than in the preceding step but will result in two daughter cells and therefore a doubled number of cells [82]. The primitive EPO-responsive progenitor is referred to as a burst-forming unit-erythroid (BFU-E) that needs EPO as both, a mitogen and survival factor. The direct progenitor in the lineage is the colony-forming unit-erythroid (CFU-E) which seems to need EPO just for survival and expresses abundant level of GATA-1, an important transcription factor for erythrocytic development [95]. CFU-E cells give rise to proerythroblasts, the first morphologically recognizable erythroid cell in the bone marrow. They continue to differentiate via basophilic erythroblasts, polychromatophilic erythroblasts, orthochromatic erythroblasts, and then reticulocytes before becoming circulating red blood cells [97].

Signal transduction of EPO

Signal transduction of EPO shares the similar principle with other type I cytokine family such as granulocyte colony stimulating factor (G-CSF), thrombopoietin (TPO), IL-1, IL-2, IL-3, etc. which bind to homodimer receptors associated with tyrosine kinase JAK2 (Janus kinase 2). EPOR is a single-transmembrane receptor that is expressed on several forms in erythrocytic progenitor cells. Human EPOR comprises of 225 amino acids on the extracellular side, 22 amino acids in the transmembrane region and 236 amino acids on the cytoplasmic side with a predicted molecular mass of about 56 kDa [87]. The ligand-induced conformational change results in the activation of several kinases and in tyrosine-phosphorylation of the EPOR. When phosphorylated, the eight tyrosine residues of the EPOR cytoplasmic portion function as docking sites for different SH2-containing proteins to initiate multiple signal transduction pathways that include the JaK2/STAT5, Grb2/Sos1/Ras/Raf-1/MEK/MAP kinase, PI-3 kinase/Akt/GSK-3 and PKC pathways. Among these signaling pathways, the JaK2-STAT5 pathway is the most dominant. As soon as being activated by JaK2, STATs dimerize and translocate to the nucleus where they bind to consensus sequences present in the promoter sequences to activate transcription (as represented in Fig. 1.6) [87, 97-98].

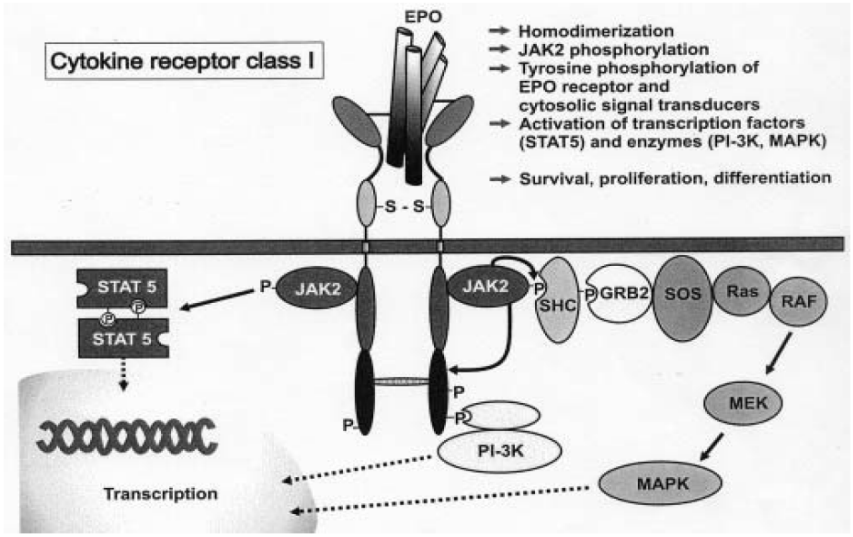

Fig. 1.6 A schematic representation of EPO signaling cascade [95].

1.4.4 Erythropoietin therapy in cancer anemia

1.4.4.1 Cancer-associated anemia

Anemia is a condition in which the body does not have enough healthy red blood cells. Anemia is a common complication associated with cancer or cancer therapy and is a debilitating factor affecting the quality of life of many cancer patients. About 50% of cancer patients with solid tumor show symptomes of anemia at the time of cancer diagnosis [99]. The prevalence also depends on the cancer staging, types of cancer and therapeutic uses as well. Advanced cancers are usually associated with lower hemoglobin levels compared to early-stage cancers. Many factors can contribute to the anemia in cancer patients. Besides, direct factors such as hemolysis, tumor bleeding, deficiency in iron, vitamin B12 or folic acid, or the production of inflammatory cytokines and chemokines which are results of immune activation at the tumor site, can cause anemia. Especially, the release of interleukin-1 (IL-1), interferon-gamma (IFN-gamma) and tumor-necrosis factor alpha (TNF-alpha) can strongly disrupt erythropoiesis in the bone marrow. Moreover, cytotoxic macrophage activation can shorten up red blood cell half-life and decrease iron utilization, an important component of red blood cells. In others, the damage of endothelial vasculature by embolism or activation of coagulation by the tumor could lead to impaire red blood cell numbers [97].

The direct effects of myelosuppression from patients receiving radiotherapy or chemotherapy have been documented for EPO resistance as well as reduced endogenous EPO production in cancer patients. Cisplatin, a common chemotherapeutic agent for lung or ovarian cancer, has been shown to be especially associated with reduced production of EPO [100]. The direct effects of myelosuppressive-based chemotherapy or radiotherapy on the marrow could be the most prevalent cancer-related anemic factor. For instant, grade 1 and 2 anemia (hemoglobin level: 8-10 g/dL) could affect up to 60% cancer patients after receiving platinum-based chemotherapy. Grade 3 (hemoglobin level: 6.5-7.9 g/dL) anemia can rise up to 74% in elderly patients with non-Hodgkin lymphomatic malignancy after treatment with cyclophosphamide, doxorubicin, vincristine and prednisolone combination [101].

Another aspect of cancer-related anemia is caused by the cancer itself. For various types of cancer, anemia is related with poor prognosis, some of them has been reported as cervical carcinoma, prostate, head and neck and lymphoma [102]. This is due to the abnormal development of blood vessels and the fast proliferation of cancer cells, which is well characterized in most solid tumors [103].

1.4.4.2 Benefit of EPO as erythropoiesis

Anemia has negative effects on health-related quality of life (QOL) with common symptoms as fatigue, nausea, headache or depression. EPO has been shown to improve QOL by correction of anemia [104]. Before the erythropoiesis stimulating agent (ESA) was available, blood transfusions were the only effective way for treatment of cancer-related anemia. But transfusion contains many risks for recipients in long or short term treatment such as contagious disease, immune-related reactions, allergic reaction, febrile reaction, lung injury or iron overload [105]. Today, the safety of blood transfusion has tremendously improved by the support of modern screening techniques and knowledge. However, blood transfusions still carry risks, including infection with unknown prions, viruses, bacteria, parasites or cause immunological reactions [97, 106]. It has been demonstrated that EPO treatment reduced risks of blood transfusion and improve QOL in a variety of clinical and meta-analysis models [99, 107-109]. Correction of hemoglobin loss, reduction in fatigue, improvement of productivity and reduction in direct health care costs are benefits that have been reported by cancer patients treated with ESA supporting [99, 106].

Resistance of chemo- and radio-therapies has been reported in tumor hypoxia [110]. Tumor hypoxia does not necessarily indicate tissue anemia. But recent studies have shown the adverse relationship between therapeutic response and hemoglobin levels in cervical, head and neck and breast cancers [97]. Many clinical trials of small cell lung, head and neck, bone and ovarian cancers have demonstrated benefits of using rhEPO in the chemotherapy regime in correcting anemia and improving QOL [87]. In a randomized, double-blind, placebo-controlled trial in 375 patients with cancer and anemia receiving non-platinum based-chemotherapy, rhEPO seemed to improve overall survival to 17 months compared to 11 months at placebo group even though statistical significance was not achieved [107]. Correction of anemia by rhEPO enhanced the anti-tumor effects of radiotherapy [111]. The reason might be

explained by the increased oxygen delivery to the tumor cells, since radiation cytotoxicity is enhanced with tumor oxygenation. This indication was supported in some preclinical models. First, rhEPO administration raised tumor oxygenation [112] and then increased radio-sensitivity resulting in delayed tumor growth [113]. These data suggests that rhEPO might have an important adjuvant function in cancer treatment. US$4.3 billion is an impressive number (an annual rhEPO' profit in 2002) which showed the most successful recombinant product for therapeutic purpose up to date [97].

1.4.5 EPO functions beyond erythopoiesis

The principal function of EPO is to regulate red blood cell formation via its specific receptor (EPOR). Recently, however, emerging evidence showed tissue-protective functions of EPO in neurological, cardiovascular diseases, wound healing responses or endothelial induction. Furthermore, some researchers also figured out the immune modulation or immune attraction of this protein [94].

Tissue protective function

EPO plays an important role during normal brain development where it associates with apoptosis and differentiation of neuronal precursors. In the condition of distress such as ischemic and inflammation, EPO and/or EPOR were found strongly up-regulated in hippocampal and cortical neurons and seemed to act as a part of the endogenous neuroprotective system [114]. Using EPOR knock-out, Yu and colleagues showed the increase of apoptosis and significant decrease of neuronal progenitor cells in an embryonic mouse model [115]. Administered at a high-dose, EPO has been shown to have neuroprotective functions, including conditions like hypoxia-ischemia, hemorrhage or stroke [116-117]. Although the precise mechanisms of EPO actions in the central nervous system (CNS) have not been fully defined, it is thought to act via a signaling pathway dependent on the activation of AKT (protein kinase B), upregulation of BCL-XL (B-cell lymphoma-extra large) and inhibition of caspase activity [118]. A variety of neuroprotective effects which was depended on the species, age, tissue and dosing interval, but normally ranging from 1000 to 30,000 Unit/kg, were administered. Those doses were quite high compared to amounts that have been used for anemia treatments (≤ 500 Unit/kg) [119].

Potential protective effects of EPO were also observed in the heart [120] or liver [121]. The administration of rhEPO (5000 Unit/kg) 7 days before coronary ischemia-reperfusion reduced 50% myocadiocyte loss in a rat model. Similarly, the reduction of liver injury was observed in rats when rhEPO was administered 5 minutes before ischemia.

Angiogenesis

*The effect of exogenous EPO on angiogenesis is still a contradictory issue. At a dose o*f 2000 Unit/kg administered thrice per week, no evidences were observed for tumor proliferative, growth and angiogenenic effects in mouse colon carcinomas, rat mammary adenocarcinomas, human colon carcinomas, and human head and neck tumorous models, even though all cell lines expressed EPOR [122]. However, several studies suggested EPO might promote endothelial proliferation or migration of endothelial progenitor cells from the bone marrow [94]. Ribatti *et al.* showed the presence of pro-angiogenenic phenotypes such as stimulation of Janus Kinase-2 (JAK-2) phosphorylation, matrix metalloproteinase-2 (MMP-2) production and cell proliferation in endothelial cell line (EA.hy926) [123]. In another study, Monestiroli *et al*. reported the increase of circulating endothelial progenitor cells in lymphoma-bearing immunodeficient mice *[124].*

Immune modulation

*Som*e recent findings suggest that EPO has a function as a immunomodulator [125-127]. EPOR have been found in various cells other than erythroid progenitors such as polymorphonuclear leukocytes, megakaryocytes, endothelial, myocardial and neural cells [128-130] suggesting that EPO has other biological functions beyond erythropoiesis and involving both, cell-mediated and humoral immune responses. In murine multiple myeloma (MM) models [126], rhEPO-treated mice showed higher levels of endogenous polyclonal immunoglobulins, compared to those in untreated groups. 6 weeks after tumor challenge, sera from mice treated with rhEPO for the previous 2 weeks displayed higher levels of endogenous κ light chains and γ2a heavy chains. It was also demonstrated that rhEPO augments B cells in both, mice treated with rhEPO and hEPO-transplanted mice compared to controls by increasing IgG1 antibody leves by immunization with the well-characterized hapten determinant, DNP (2,4-dinitrophenyl) or increasing IgG2a levels when immunized with HBsAg. A

clinical trial with rhEPO has demonstrated the elevation of T cell populations in sera [131]. But up to now no EPOR was found on activated or proliferating T cells. Therefore, it is possible that the effects of rhEPO observed in T cells are indirect, or mediated by other cell types that do express EPOR. However, Pruitchi *et al.* showed that rhEPO has a direct effect on dendritic cells (DCs) where they found EPOR expression and the increase of peripheral blood DCs or monocyte-derived DCs after treatment with EPO [127].

By using murine myeloma models (MOPC-315-IgAl2 and 5T33 MM-IgG2b), daily treatment of MOPC-315 tumor bearing mice with rhEPO for several weeks induced complete tumor regression in 30–60% of mice. Interestingly, all regressive mice that were re-challenged with tumor cells rejected tumor growth [132].

1.4.6 Safety concerns of using rhEPO

Some recent studies alarmed about the negative effects of rhEPO in the treatment of anemia-related cancers. The double-blind, randomized, placebo-controlled trials were performed with head and neck cancer (first line radiotherapy) [133] and metastatic breast cancer (first line chemotherapy) patients [134]. Although there was a correlation between rhEPO and Hb levels, yet rational survival in patients receiving rhEPO was lower than in patients receiving placebos. In a head and neck study [133], Epoetin beta was given at a dose of 300 U/kg, three times per week. According to Henke *el at*. the observed lower survival in Epoetin beta compared with placebo group may derive from hemorrhage, thrombosis and pulmonary embolism (Epoetin beta 11% versus placebo 5%) or cardiac disorders (Epoetin beta 5.5% versus placebo 3%). The rate of locoregional tumor progression was also higher in patients receiving Epoetin beta, with an RR of 1.69 (95% CI 1.16–2.47, P = 0.007). In a metastatic breast cancer study [134], Epoetin alfa was given at a dose of 40,000 units once a week. Significant differences in survival were found in the placebo group (70%) and in the Epoetin alfa (76%) group for 12 months (p=0.01). Both, thrombovascular events and disease progressive were higher in Epoetin alfa treated group. However, there were some methodological limitations in both studies, such as that an imbalance in patient randomization could not be excluded, the baseline and target hemoglobin were already high and may have contributed to the

thrombovascular events [97]. In addition, in the head and neck study, the patients of stage III and IV underwent surgery combined with radiation, and even nowadays some causes of death still remain unclear, in spite of intensive re-evaluation [99].
As mentioned above, these clinical studies were imperfectly designed. However, EPO might have cancer promoting functions that were supported by several preclinical models. One of thatis anti-apoptosis [135] by acting on expressed EPOR of some cancer cell lines [136-137], subsequently activating EPO signaling cascades and eventually promoting target gene transcription [138-140]. The solid tumors are known to be highly hypoxic, hence increasing Hb with rhEPO can improve tumor oxygenation [112], resulting in a preferable environment for tumor growth [99]. But these findings and the hypothesis based on it are still a struggling issue, with the arguments focusing on the expression and function of EPOR on cancer cells. In other point of view, low evidences were found in 1083 solid tumor samples examined for EPOR transcription [141]. Swift *el et*. tested EPOR expression in 209 human cancer cell lines, some highly expressed EPOR, but none of them activated downtream signaling cascades such as STAT5, AKT, ERK, or S6RP when exposed to rhEPO [142]. Other clinical trials documented no differences in tumor control with erythropoietin treatment. Moreover, EPO treatement significant improved disease-free survival for 4 years compared with the control group ($P < 0.001$) (reference in [99]).

*Bas*ed on our current available knowledge, the use of recombinant erythropoietin in cancer patients should be put under careful considerations. EPO could be used to increase Hb level to reduce the need of blood transfusions in patients with Hb levels below 10 g/dL but target levels should not exceed 12 g/dL [99]. Concomittantly, there is a need to carry out larger, well-designed clinical trials in multiple types of cancers that might result in tremendous benefits for the future application of EPO in oncology [106]. In parallel, mechanism of action of EPO in cancer needs to be better elucidated [87].

2. MATERIALS AND METHODS

2.1 Materials

2.1.1 Equipments

Equipment	Manufacturer
Anesthetic devices	VetEquip
Autoradiography films	Amersham
Bio Doc-It system	UVP
Biological safety cabinet, class II	Thermo electron Corporation
Blotting paper 3MM	Whatman
Cell counting chamber	VWR
Cell culture dishes (24,12,6-well)	Corning Inc.
Cell culturing flasks	Corning Inc.
Cell scraper	Corning Inc
Centrifuge Centra CL2	Thermo scientific
Centrifuge Micro CL21	Thermo scientific
Centrifuge Sorvall RC 6 Plus	Thermo scientific
Circulation chiller RTE-111	Neslabs
CO2 incubator HERA cell 150	Thermo electron corporation
CO2/O2 incubator	Sanyo
Confocal microscopy MZ 16 FA stereo	Leice
Cryo-tube 2ml	Nalgene

Cuvettes	Eppendorf
Digital caliper	VWR
Digital dry bath incubator	Boekel scientific
EDTA tube	DB
Electrical repeated pipette	Eppendorf
Electrophorstic vertical system	Hoefer DALT
ELISA plate	Costar
Embedding Mold Tissue-Tek	IMEB Inc.
Ettan IPGphor	Amersham
Falcon tube (15,50 ml)	DB
Film cassette	Fisher scientific
Film developer AGFA CP1000	Superior Radiographics
Fluorescence Microscope IX71	Olympus
Heater	VWR
Imaging system	Carestream
Incubator shaker	New brunswick scientific
Insulin syringe-100 29G1/2	DB
Inversed microscope CK30	Olympus
IPG strips	Bio-Rad
IPG strips	Amersham
Laminar fume hoot	Air master systems
MagNA beads	Roche
MagNA Lyser	Roche
Mastercycler personal	Eppendorf
Micro-Hematocrit Capillary Tubes	Global scientific

Microplate reader SpectraMax MS	Molecular divices
Microtube easy open cap 1.5ml	Saarstedt
Mini-electrophoresis system	Bio-Rad
Multi Casting chamber	Bio-Rad
Multichannal pipette	Eppendorf
Nitrocellulose	Sigma
Nitrocellulose membrane	Fisher scientific
Orbital shaking	VWR
pH meter Accumet AR15	Fisher scientific
Pipet aid	Drummond
Pipet tips	VWR
Pipettes	Eppendorf
Power supply Power Pac	Bio-Rad
PROTEAN IEF System	Bio-Rad
PROTEAN plus dodeca cell	Bio-Rad
PVDF membrane	Invitrogen
Realtime PCR	A&B applied system
Repeated pipette	Eppendorf
Rocking platform	VWR
Scalper	Sklar instruments
Sectioning machine leica RM 2125	IMEB Inc.
Semi-Dry Blot apparatus	Peqlab
Slide warmer	Barnstaed labline
Sonifier 450	Branson
Spectrophotometer (Biomate3)	Thermo scientific

Stirrer	VWR
Surgeon scissors	E.A Beck
Tweezers	E.A Beck
Vertical 96-well thermal cycler	A&B applied system
Vortex VX100	Labnet
Water bath	Fisher scientific
Weight	VWR
Xcell II Blot Module	Invitrogen

2.1.2 Reagents

Name	**Manufacturer**
1x PBS	Cellgro
3-(4,5-Dimethylthiazol-2-yl)-2,5-diphenyltetrazolium bromide	Sigma
5-brommo-4chloro-3-indolyl D-glucuronide (X-GlcA)	Sigma
Acetic acid	VWR
Acetol	Sigma
Acrylamide / Bisacrylamide	Bio-Rad
Agarose	Roth
Agarose Low Melt	Fisher scientific
Ammonium persulfate (APS)	Merck
Amonium sulfate	Fisher scientific
Benzonase	Merck
Bovine Serum Albumine (BSA)	Omega scientific
Bromophenol blue	Sigma

Carboxymethylcellulose (CMC)	Sigma
CHAPs	Bio-Rad
Coelenterazin	Sigma
Coomassie Brilliant Blue G-250	Fisher scientific
Crystal Violet	Sigma
Diaminoethanetetraacetic acid (EDTA)	Fisher scientific
Dimethyl sulfoxide (DMSO)	Sigma
Dithiothreitol (DTT)	Bio-Rad
D-luciferin	Goldbio com
DMEM medium	Cellgro
dNTP-Mix	Fermentas
Ethanol (p.a.)	VWR
Ethidium bromide	Sigma
Fetal Bovine Serum (FBS)	Mediatech
Formaldehyde (37%)	EMD
Formamide	Fisher diagnostics
Glacial acetic acid	Fisher scientific
Glycerol	Fisher scientific
Glycine	Bio-Rad
Hydrogen Peroxide	Sigma
Iodoacetamide (IAA)	Bio-Rad
Isoflurane	VetEquip
Isopropanol	VWR
Luminol	Amersham
Methanol	Sigma

N´, N´, N´, N´-Tetramethylethylenediamine (TEMED)	Fluka
o-nitrophenyl-β-D-galactoside (ONPG)	Sigma
p-Coumaric acid	Sigma
Penicillin / Streptomycin	Mediatech
Phosphoric acid	Fisher scientific
Ponceau S	Sigma
Powdered milk	DB
Prestained protein marker	Bio-Rad
Procrit (epoetin anfa)	Amgen
Protease inhibitors mix Complete Mini	Roche
RPMI medium 1640	Cellgro
RPMI 1640 without phenol red	Cellgro
Sodium azid	Sigma
Sodium carbonate	Merck
Sodium chloride (NaCl)	Fisher scientific
Sodium dodecyl sulfate (SDS)	Fisher scientific
Sodium hydroxide	Merck
ß-Mercaptoethanol	Sigma
Taq DNA polymerase	Fermentas
Thiourea	Amresco
Trichloroacetic Acid	BDH
Tris-Base	Fisher scientific
Tris-HCl	Fisher scientific
Triton X-100	Sigma
Trypan blue	Cellgro

Trypsin-EDTA	Cellgro
Tween 20	Bio-Rad
Urea	Boehringer
β-Galactosidase	Sigma
Restriction enzymes	Neblabs
Opti-MEM reduced-serum medium	Invitrogen

2.1.3 Kits

Name	**Manufacturer**
Absolute QPCR Cyber green mix	Thermoscientific
Absolute™ QPCR SYBR® Green Mix	Thermo fisher
AccuPrime™ *Pfx* SuperMix	Invitrogen
DC™ Protein Assay	Bio-rad
DNA Clean & Concentrator™-5 - Uncapped Columns	Zymo research
DNA-free™ Kit	Ambion
ECL plus western blotting detection	GE healthcare
hEPO Elisa kit	Stem cell technologies
Hypoxyprobe-1 Plus Kit	Hypoxyprobe
ImmPACT DAB diluent and chromogen	Vector
Opti-4CN Substrate Kit	Bio-rad
QuantiChromTM Hemoglobin Assay Kit	BioAssay Systems
QuikChange II Site-Directed Mutagenesis Kits	Agilent technologies
Revert Aid™ First Strand cDNA Synthesis Kit	Fermentas
RNeasy Mini Kit	Qiagen
Vectastain ABC kit	Vector

Zero Blunt® TOPO® PCR Cloning Kits	Invitrogen
Zymoclean™ Gel DNA Recovery Kit	Zymo research

2.1.4 Solutions and buffers

Overlay medium

15 g	CMC
1000 ml	DMEM
1%	Pen/Strep
5%	FBS

Crystal violet staining solution

1.3 g	Crystal violet
50 ml	Ethanol
300 ml	Formaldehyde (37%)

Tumor lysis buffer (RBM lysis buffer)

50 mM	Tris-HCl, pH 7.4
2 mM	EDTA
Protein inhibitor coltail (Roche)	

10x Laemmli buffer

440 mM	Tris-Base
2 M	Glycine
1.5%	SDS

ECL Reagent

Sol 1	90 mM p-Coumaric acid
Sol 2	250 mM Luminol
Sol 3	1 M Tris-HCl pH 8,5
0.5 ml	Sol 1
1.0 ml	Sol 2
20 ml	Sol 3
200 ml	dH_2O

Cell lysis buffer (RIPA)

25 mM	Tris HCl pH 7.6
150 mM	NaCl
1%	Triton-X100
1%	Sodium deoxycholate
0.10%	SDS
Protein inhibitor coltail (Roche)	

50x TAE buffer

242 g	Tris-Base
100 ml	0.5 M EDTA (pH 8.0)
57.1 ml	Glacial acetic acid

10x TBE buffer

108 g	Tris Base
55 g	Boric acid
40 ml	0.5 M EDTA (pH 8.0)

Rehydration solution

8 M	Urea
2%	CHAPS
1%	IPG buffer
0.30%	DDT
0.002%	Bromophenol blue

Equilibration buffer

6 M	Urea
30%	Glycerol
4%	SDS
0.002%	Bromophenol

1x Towbin buffer pH 8,3

0,025 M	Tris-base
0,192 M	Glycin
20%	MeOH

Bradford solution

50 mg	Coomassie Blue G250
25 ml	Ethanol 96%
50 ml	Phosphor acid
25 ml	dH_20

5x Loading buffer (SDS-PAGE)

50 mM	Tris (pH 6.8)
2%	SDS
30%	Glycerol
0.04%	Bromphenol blue
8.4 mM	

Fixation solution

50%	Ethanol
10%	Acetic acid

2.1.5 Cell lines and culture media

A549	human lung adenocarcinoma epithelial cell line
CV-1	african green monkey kidney fibroblast
NCI-H1299	human non-small lung carcinoma cell line

A549 cultivation

500 ml	RPMI1640
10%	FBS
5 ml	Antibiotics (Pen/Strep)

CV-1 cultivation

500 ml	DMEM
50 ml	FKS
5 ml	Antibiotics (Pen/Strep)

NCI-H1299 cultivation

500 ml	RPMI1640
10%	FBS
5 ml	Antibiotics (Pen/Strep)

2.1.6 Antibodies

Primary antibody	Origin	Manufacturer
anti-beta actin	mouse	Abcam
anti-beta actin	mouse	Sigma
Anti-HP-Red549	mouse	hpi

anti-beta galactosidase	rabbit	Molecular Probes
anti-GFP	rabbit	Santa Cruz
anti-hEPO	rabbit	Santa Cruz
anti-vaccinia virus	rat	Abcam
Anti-MHC-II	rat	eBioscience

Secondary antibody	**Origin**	**Manufacturer**
anti-sheep, HRP-conjugated	donkey	Santa cruz
Anti-rat, AlexaFluor549	donkey	Jackson I.R.
anti-mouse,HRP-conjugated	goat	Abcam
anti-rabbit, HRP-conjugated	goat	Santa cruz
anti-rat, HRP-conjugated	goat	Sigma
anti-rabbit, HRP-conjugated	goat	Jackson
anti-mouse, HRP-conjugated	goat	Sigma
anti-goat, HRP-conjugated	rabbit	Invitrogen

2.1.7 Oligonucleotides

Name	**Sequence**	**Length**
hEPO1-F	5'-TCA TCT GTG ACA GCC GAG TCC T-3'	80bp
hEPO1-R	5'-TTC AGC ACA GCC CGT CGT GAT ATT-3'	
GAPDH-F	5'-GGT CAC CAG GGC TGC-3'	168bp
GAPDH-R	5'-GCT CCT GGA AGA TGG TGA TGG-3'	
R103A-F	5'-GCC GTC AGT GGC CTT GCC AGC CTC ACC A-3'	Vector
R103A-R	5'-TGG TGA GGC TGG CAA GGC CAC TGA CGG C-3'	

2.1.8 Animal use

5-6 weeks old female athymic nude mice, Hsd: Athymic Nude-Foxn1^{nu}, were purchased from Harlan Laboratories, Inc. Athymic mice are are immunodeficient (T-cell deficient) due to a dysfunctional and rudimental thymus and display a hairless phenotype. These mice are a suitable model for human cancer research because the tumor xenografts will not be rejected by host immune responses while other immune cells such as B cells, macrophages, monocytes, shown normal expression. All mice were cared for and maintained in accordance with animal welfare regulations under an approved protocol by the Institutional Animal Care and Use Committee of Explora Bio labs, Inc (San Diego, CA, USA).

2.1.9 Recombinant vaccinia virus

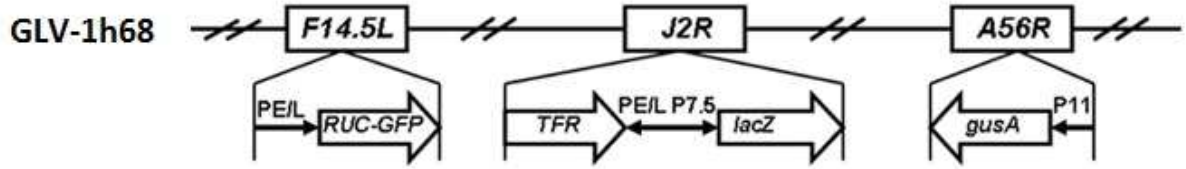

All recombinant vaccinia viruses used in this study are derived from the parental virus, GLV-1h68 [35]. Briefly, GLV-1h68 was derived from the LIVP strain and carries three marker gene cassettes encoding *Renilla* luciferase–*Aequorea* green fluorescent protein fusion, β-galactosidase, and β-glucuronidase inserted into the *F14.5L, J2R* (encoding thymidine kinase) and *A56R* (encoding hemagglutinin) loci of the viral genome under the control of pE/L (synthetic early/late), p7.5 (vaccine early promoter) and p11 (vaccinia late promoter), respectively. This virus can selectively penetrate, replicate in and lyse cancer cells while leave the harmlessness to normal cells. Moreover, the insertions of the marker genes allow for real-time visualization and quantification of the virus action inside the tumors which is tremendously helpful for tumor diagnosis and therapy.

2.2 Methods

2.2.1 Culture of monolayer cells

Culture and passage of the cells

CV-1 cells and cancer cells (A549 and NCI-H1299) were cultured in well plates, dishes, or flasks, depending on the purpose. To get enough cells, the stock cells were normally scaled up in 225T flasks (40 ml medium volume). A proper ratio of stock cells was pipetted into a tissue culture flask containing the respective fresh culture medium (Material). Cells were grown in a humidified 5% CO_2 incubator at 37^0C. To maintain appropriate growth of those cells, they were closely observed and their medium was changed regularly to ensure that the cells were in a good condition. At 80-90% confluence, cells were washed with BSS buffer and treated with 5 ml EDTA-trypsin. After 5 to 8 minutes (cells should become detached), the flask was shaken to completely detach the cells. Then, 10 ml medium containing Mg^{2+} and Ca^{2+} (growth medium with FBS) was added to stop the EDTA-trypsin reaction. Cells were resuspended by being pipetted up and down several times to disrupt the cell clumps. Cell counting was performed by using a hemocytometer under an inverted light microscope. The cells were then ready for passage with a designated ratio into suitable plates, dished, or flasks.

Cell counting

The numbers of cells were determined by using hemocytometer. The hemocytometer is a modified glass slide with two chambers of known area. Each chamber is subdivided into 9 equal 1 mm^2 square parts. The chamber is made of a glass cover slip with a thickness of 0.1 mm. Therefore each part can contain 0.1 mm^3 volume offluid. Each part is further subdivided into 16 smaller grids. For accurate result, the cells on 4 grids (1 line) of each corner part (1, 2, 4 and 5 as in showed picture below) were randomly counted. The total cells counted in 16 squares are the number of cells in 0.1 mm^3 of culture volume ($1x10^{-4}$ mL).

Calculation of cells/mL: $c = n \times V$ ($V = 10^4$)

(c: cells/ml, n: number of cells in 16 counter squares, V: Volume of sample (mL))

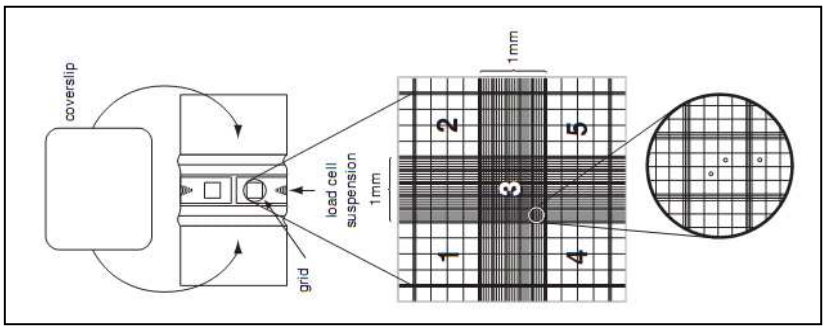

Fig. 2.1 Schematic representation of a Neubauer hemocytometer

Freeze and thaw

Cells can be preserved in liquid nitrogen for long-term storage. Cells were grown with fresh growth medium until 80-90% confluence. 5 x 10^6 – 1 x 10^7 cells were then aliquoted in 900 μl medium-containing labeled cryo-tubes and then 100 μl of DMSO were added. The cyo-tubes were immediately mixed, put into a cold cryobox, and stored at -80°C. On the next day, the cryo-tubes were moved to a liquid nitrogen tank for the long-term storage.

When reused, the preserved cells (-80°C) were thawed in a 37°C water bath with gentle agitation. Thawing should be rapid (approximately 2 minutes). Suspension cells were then transferred to a 15 mL centrifuge tube containing 9.0 mL complete culture medium and centrifuged at 1,500 rpm for 5 min. The supernatant was removed and the cell pellet was suspended with a suitable fresh medium and incubated in a 37°C incubator with 5% CO_2 in air atmosphere.

2.2.2 Virus titration assay

To determine the number of virus particles in the samples, standard plaque forming assay on CV-1 cells was performed. Samples from -80°C were thawed at 37°C (water bath) for 10 min, then sonicated on ice at the maximum level for 40 sec. Serial dilutions (10^{-2} - 10^{-8}) of the samples in infection medium (DMEM with 2% FBS) were prepared in 1.5 ml microcentrifuge tubes. 100% confluence monolayer CV-1 cells in 24-well plates were infected with 0.2 ml virus dilutions in duplicates. Infected cells were maintained in a 5% CO_2 incubator at 37°C for 1 h with gentle agitation for every 20 min. After 1 h infection, 1 mL overlay medium was added to each well. Cells were incubated for 2 days before staining with 0.5 ml crystal violet solution per well for 1

more day at room temperature (RT). After that, crystal violet was washed off with water and plates were dried at RT. The virus titer was determined by counting the formed plaques in those wells and multiplication with the dilution factor. Accurate results are usually obtained from wells containing 20-80 countable plaques.

2.2.3 Virus infection and replication assay

To determine the level of virus infection and replication in each cancer cell lines, the cancer cells were infected with vaccinia virus. Virus replication was then examined at 4, 24, 48, and 96 hpi. 80-90% confluent monolayer cells in 24-well plates were infected with a virus at a designated multiplicity of infection (MOI) for 1 hour with gentle agitation for every 20 min, in a 5% CO_2 incubator at 37°C. After 1 hour of infection, the infection medium was aspirated and replaced with 1 ml fresh growth medium. Infected cells were then incubated in the 5% CO_2 incubator at 37°C until the time points of harvesting.

At 4 h, 24 h, 48 h, and 72 h post infection, both supernatants and cells were collected. Cells were detached from the wells by using 200 μl EDTA-Trypsin for 8 min and then EDTA-trypsin was neutralized by adding 1 ml of culturing medium (harvested from the same well). Samples (cells and supernatant) underwent three cycles of thawing and freezing and then 3 times of sonication at maximum level for 30 sec to release the virus particles into the medium. Standard plaque forming assay on CV-1 cells was performed to determine the virus titers.

2.2.4 Cell viability assay (MTT assay)

The cell viability assay is a method to determine a living cell proportion based on metabolic enzyme activity (NADPH). It is widely used in the testing of drug action, cytotoxic agents and the screening of other biologically active compounds. Among a variety of non-radioactive cell proliferation assays, the MTT assay developed by Mossman [143] is still among one of the most versatile and popular assays. This method is based on the reaction of MTT (3-(4,5-Dimethylthiazol-2-yl)-2,5-diphenyltetrazolium bromide) with NADPH enzyme which is released during the

metabolism activity of living cells, to form an color adduct which is measurable using an absorbance reader.

Cells were seeded in 24-well plates to achieve 80-90% confluence and then infected with VACVs at an MOI of 0.1 or 0.01, respectively, for 1 hour with gentle agitation for every 20 min. Infection medium was replaced with 1 ml of fresh growth medium. The plates were then returned in the 5% CO_2 incubator at 37^{o}C. At 24, 48, 72 and 96 hpi, growth medium was replaced with 500 μl of MTT buffer and incubated for 4 hours before MTT buffer aspiration. The reaction was stopped by adding 0.5 ml stop solution (1N HCl in isopropanol) for 10 min with shaking. The clear yellow solutions (use 0.2 ml for each well) were transferred into flat-bottom 96-well plates and absorbance was measured at 570 nm wavelength. Uninfected cells served as controls and were considered as 100% viable.

2.2.5 Protein isolation

From cell cultures

RIPA lysis buffer supplemented with complete protease inhibitor cocktail was used to isolate total proteins. Cells cultured in 6- or 12-well plates were washed with 1x PBS and a proper amount of lysis buffer (300 μl of lysis buffer for 10^6 cells) was added. Adherent cells were scraped off the wells using sterile cell scrapers, and then transferred to 1.5 ml microcentrifuge tubes. Membranes from cells were disrupted by 2 cycles of sonication for 1 min at 4^{o}C. Supernatants were collected after 10 min of centrifugation at 10,000 rpm. Protein concentration was determined by DC protein assay kit (Bio-rad) or Bradford protein assay. Proteins were kept at -4^{o}C for the whole extraction process.

From in vivo

Tissues were weighted, cut into smaller pieces and transferred to MagnaBead tubes containing cold RBM lysis buffer supplemented with complete protease inhibitor cocktail (0.8 g tissue in 500 μl RBM buffer, tumors in 1 ml RBM buffer). Tissues were homogenized using MagNA lyser (Roche diagnostic) at 6,500 rpm for 30 sec. Sample went through 3 freeze-thaw cycles and 3 rounds of sonification at maximum level for 30 sec at 4°C. The tissue lysates were centrifuged at 10,000 rpm for 10 min

at 4°C. Proteins in supernatants were collected, quantified and stored at -80°C until further use.

2.2.6 Western blotting

Western blotting (immunoblotting) is a commonly used method to detect specific antigens by its polyclonal or monoclonal antibodies. In this study, Western blotting was used to detect virus-mediated expression of GFP, beta-glucoronidase, beta-galactosidase, β-actin and hEPO in infected cell cultures. Twenty (20) μg of total isolated proteins was used for gelelectrophoretic separation on 10% SDS-PAGE gels. Proteins were transferred to nitrocellulose or polyvinylidene difluoride (PVDF) membrane by a semi-dry blotting or liquid blotting system. The transfer process was monitored by staining with Ponceau S solution for 1 min. Stained membranes were subsequently rinsed with dH_2O to remove the staining. Membranes were blocked with 5% milk in PBS-T for 1 h at RT to prevent non-specific binding of antibodies to the surface of the membrane. After blocking, the membranes were incubated either with anti-GFP (1:10,000), -gusA (1:500), -lacZ (1:5,000), -β-actin (1:10,000) or -hEPO (1:500) primary antibodies at 4°C for overnight. The membrane was washed 4 times with PBS-T washing buffer for 15 min. The membrane was next incubated with a secondary antibody conjugated with horseradish peroxidase (HRP) for 1 h at RT. After washing, luminescent or choromogenic substrate was added onto membrane to visualize the HRP activity. Signals released were either detected on autoradiograph film or directly on the membrane.

2.2.7 Real-time quantitative polymerase chain reaction (Q-PCR)

This method was used to quantify the transcriptional levels of *hEPO* under the control of four different promoters; p7.5, pSE, pSEL and pSL. $1x10^6$ A549 cells were seeded in 6-well plates and incubated at 37°C overnight. Cells were then infected with the EPO-VACVs (GLV-1h210, GLV-1h211, GLV-1h212, GLV-1h213) at an MOI of 5 in duplicates. At 2, 4, 6, and 8 hpi, cells were washed with 1x PBS, harvested with the sterile cell scrapers, and transferred into microfuge tubes. Tubes were immediately snap-frozen in liquid nitrogen and stored at -80°C. Total RNA from the

cells was isolated using the RNeasy kit (Qiagen), following the manufacturer's instructions. DNA was digested by DNase I (Ambion). The concentration of isolated RNA was measured by using an absorbance reader at 260 nm. 1 μg total RNA was used to synthesize single strand cDNA (Fermentas). One (1) μl of cDNA (1:10 dilution) was used as a template for PCR amplification of 80 bp long *hEPO* fragments with specific designed primer pair (EPO1-F and EPO1-R). The reaction was carried out in Cyber green mix solution (Thermo scientific) in a total of 25μl reaction mixture. Thermo-cycles consisted of 15 min for enzyme activation at 95^{o}C, 15 sec for denaturation at 95^{o}C, 30 sec for annealing at 62^{o}C, 30 sec for extension at 72^{o}C. The procedure was repeated for 28 cycles. PCR products were performed melting curves from 55^{o}C to 90^{o}C to analyze the product specificity. GAPDH, a fragment with 168 bp in length, was used as a reference gene for normalization. All samples were tested in duplicate.

For quantification of mRNA products by qPCR, fluorescent dye SYBR Green I that sensitively binds to dsDNA was used. This dye was added to the PCR reaction mixture. Therefore, the more dsDNA product is formed in the PCR tube, the higher the detected signal from DNA-bound fluorescent dyes. The results were analyzed based on equations established by Pfaff [144]. This analysis method results in relative differences of the target genes over the control gene under normalization to the reference gene (GAPDH). The transcriptional levels of *hEPO* at 2, 4, 6 and 8 hpi (targets) are under the control of different promoters; p7.5, pSE, pSEL, or pSL were compared to a chosen control [p7.5 (GLV-1h210), at 2 hpi] with an assumption that PCR efficiency of all test genes were 100% (product formation after n PCR cycles were 2^{n}). The Ct threshold value in this study was set at 0.025. Based on Ct value, relative fold differences were calculated as following this formula (http://pathmicro.med.sc.edu/pcr/realtime-home.htm)

Fold difference = $2^{(\Delta\text{target}-\Delta\text{control})}$

[Δtarget = Ct (target) - Ct (reference); Δcontrol = Ct (control) - Ct (reference)]

2.2.8 Enzyme-Linked Immunosorbent Assay (ELISA)

This method was used to detect and quantify the presence of hEPO protein in cell cultures and tumors after treatment with the EPO-VACVs. In culture, A549 cells (80-90% confluence) were mock-infected or infected either with different EPO-VAVs, or GLV-1h68 at an MOI of 10 in triplicate. At 2, 6, 12, and 24 hpi, supernatants were harvested for the ELISA test. To quantify hEPO expression in virus-treated tumor-bearing animals, protein samples (from tumors and sera) from 4-5 mice per group after 14 days of treatment with EPO-VACVs, GLV-1h68 or untreated controls were used. The representative samples were diluted and pre-screened to assure that diluted samples were located inside the detectable range. The dilution factors at different time points were determined as 20, 40, 100, 100 (2 hpi); 200, 200, 1000, 1000 (6 hpi); 300, 300, 5000, 5000 (12 hpi); and 500, 500, 10000, 10000 (24 hpi) from supernatants of cells infected with GLV-1h210, -1h211, -1h212, and -1h213, respectively. The similar orders for the sera were 200, 300, 5000, 5000 and for the tumors were 1000, 1000, 20000, 20000.

A "sandwich" ELISA, based on the binding of two monoclonal antibodies, was used. These antibodies bind to 2 non-overlapping epitopes on EPO's polypeptides. The testing procedure is summarized in the following three steps:

Firstly, test samples and standards were added in the anti-hEPO-coated 96-well plates (first antibody), followed by incubation with a biotinylated anti-hEPO antibody (second antibody). The plates were sealed and incubated at RT for 1 h on a shaker. hEPO was captured by 2 monoclonal antibodies at that time. The unbounded antibodies were washed away using washing buffer.
Secondly, the well plates were incubated with streptavidin conjugated to horseradish peroxidase (HRP) for 15 min on the shaker. The HRP-conjugated streptavidin binds to the immobilized biotinylated anti-EPO antibody during the incubation. The unbound reagents were then washed away using washing buffer.

In the last step, chromogenic substrate Tetramethylbenzidine (TMB) was added to the wells and oxidized by the immobilized peroxidase yielding in a blue-colored reaction product. The reaction was stopped with 0.5 N sulphuric acid, which converts the blue product into yellow. The color intensity was proportional to the amount of hEPO present in each well and was determined using a spectrophotometer at an

absorbance wavelength of 450 nm. The hEPO concentrations of the test samples were determined by comparison with established hEPO concentration from the standards. The detailed protocol can be referenced from a manufacturer instruction (Stemcell technologies #01630).

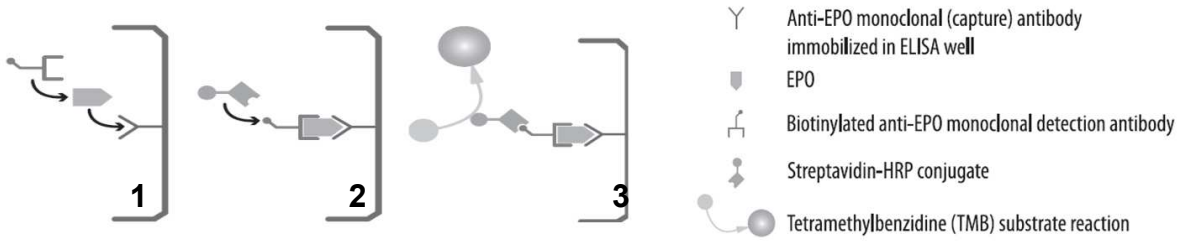

Fig. 2.2 The schematic diagram of demonstration for three steps of hEPO ELISA test

2.2.9 Detection of hEPO isoforms

hEPO exists in different isoforms due to posttranslational modification. These isoforms are important in determining of protein secretion, clearance and bioactivity *in vivo*. The isoform expression patterns depend on species, tissues and protein isolation methods. Isoform patterns of hEPO in A549 cells, supernatants, tumors and sera of tumor-bearing mice after treatment with EPO-VACV (GLV-1h212) were analyzed by 2D-gel electrophoresis [145].

100-150 μg protein samples from infected cells (MOI 0.1, 48 hpi), infected tumors (2 x 10^6 pfu/mouse, 14 dpi), sera (2 x 10^6 pfu/mouse, 14 dpi) and 200 U Epoetin alfa (Amgen) were purified using by precipitation with 15% TCA (trichloroacetic acid). Supernatants harvested from infected cells (MOI of 0.1, 48 hpi) were desalted and concentrated using 10 kDa utra-0.5 ml centrifugal filters (Millipore). Protein samples were solubilized in 130 μl rehydration buffer for 1 hour at RT and passively loaded on 7 cm IPG strips, pH 4-7 (Bio-rad) for 16 hours at RT (on sealed tray). The isoelectric focusing (first dimension) was performed on a PROTEAN IEF system (Bio-rad) with a preset linear program for 7 cm strip, 50 μA/ IPG strip:

Length of strip: 7 cm	Ramping mode	Voltage (V)	Duration
Step 1	Linear	250	15 min
Step 2	Linear	4000	2 hour
Step 3	Rapid	4000	10,000 Vhr

Separation in the second dimension: before SDS-PAGE, the strips were equilibrated with DTT equilibration buffer and then with IAA equilibration buffer to apply negative charge and uniform shape to all proteins (15 min for each buffer). The strips were carefully applied on top of 12% Bis-tris-SDS gels and overlaid with 0.5% aragrose (in 1x SDS running buffer with 0.002% bromphenol blue). After 10 min, gels were transferred into a SDS-PAGE chamber filled with 1x SDS running buffer and set at 100 V for 60 min. In the next step, the gels were processed for Western blot detection as described before.

2.2.10 Tumorigenicity and tumor therapy

Tumors were generated by the subcutaneous implantation of A549 cells ($5x10^6$ cells in 100 ml 1x PBS) on the right hind flank of 6-to-8-week-old male nude mice (NCI/Hsd/Athymic Nude-Foxn1nu, Harlan), once tumors reached a volume of about 200 mm^3 (tumor volume was calculated using the following equation: [(height - 5 mm) x width x length]/2), tumor-bearing mice were treated with a single dose of $2x10^6$ pfu/mouse (unless otherwise indicated) of EPO-VACVs, GLV-1h68 or received no treatment. Tumor volume, GFP signal, and animal weight were measured for once a week. Animals were observed daily for any signs of toxicity. At the designated time points, mice were sacrificed and blood, tumors, and tissues (liver, lung, kidney, brain, and spleen) were excised. The samples were used for blood tests, histology, protein isolation, or determination of virus replication.

2.2.11 Hemoglobin test and total blood cell counts

Retro-orbital bleeding

Mice were anesthetized using a combination of isoflurane and oxygen. An EDTA-coated blood capillary tubewas inserted into the lateral canthus. The capillary tube is rotated into the orbital cavity (sinus) at an angle of 30° until the capillary touched the end of the cavity and blood flew in the capillary tube. The tube is then slightly pulled backwards for the blood to enter the tube (~50 μl). The bleeding of the mouse was stopped by directly pressing a Q-tip (cotton) at the site of bleeding for 5 seconds. Collected blood from the capillary tube was transferred into 1.5 ml microcentrifuger tubes or EDTA-coated tubes.

Hemoglobin test

*QuantiChr*om hemoglobin assay (BioAssay Systems) was performed for hemoglobin quantification. The assay is based on an improved Triton/NaOH method, in which the hemoglobin is converted into a uniformly colored end product. Color intensity measured at 400 nm reflects the hemoglobin concentration in the samples. Whole blood was diluted 1:100 in a total volume of 500 μl dH_2O. 50 μl of diluted samples or the calibrators were pipetted into a 96-well assay plate. Then, 200 μl dH_2O was added into the wells containing blanks and calibrators, while 200 μl reagent was added into the sample wells. The plate was incubated for 5 min at RT and was measured at 400 nm. Hemoglobin levels were determined using this formula:

$$\mathrm{Hb(mg/dL)} = \frac{\mathrm{OD(sample)-OD(blank)}}{\mathrm{OD(calibrator)-OD(blank)}} \mathrm{x100\ x\ n}$$ (n: dilution factor)

Total blood cell count (CBC)

100 μl of whole blood was taken r.o. in the morning (9-11 AM) 14 days post virus injection using EDTA-coated capillary tubes and transferred to EDTA-coated tubes (Microvette). Samples were kept on ice and tested by Explora Biolabs (San Diego, CA, USA) within 2 hours from time of blood collection. Numbers of red blood cells, neutrophils, monocytes, white blood cells, platelets and proportion of each type were determined.

2.2.12 Cytokine and chemokine profiling

In order to evaluate cytokines and chemokines expression in tumors after 14 days of treatment with a single dose of 2 x 10^6 pfu/mouse of EPO-VACVs and GLV-1h68, 58 cytokine and chemokine antigens were analyzed using antibody-linked beads (Myriad RBM). Four animals in each group were sacrificed at 14 dpi. Tumors were excised, homogenized in RBM lysis buffer (50mM Tris-HCL with 2mM EDTA, pH 7.4) and supplemented with complete protease inhibitor cocktail (Roche). All protein samples in each group were normalized (based on protein concentration) and pooled. Samples combined from each group were then analyzed for 58 mouse immune-related protein antigens by magnetic beads as described in the previous section.

2.2.13 Immunohistological staining

Immunohistological staining is a method to visualize the presence and location of antigens in tissue sections. This method is not quantification sensitive but allows for observation of antigen detection in the intact tissues. In this study, two types of sectioning, paraffin- and agarose-embedded sections, were used to stain for VACV, hEPO, MHC-II, CD31, hypoxyprobe or H&E (hematocylin and eosin stain).

Paraffin-embedded sectioning

After excision, tumors were immediately cut into smaller pieces (< 3 mm in thickness), restrained in embedding cassettes and fixed with 10% formalin overnight at RT on a rocking platform. Tumors were then rehydrated step-wise with 0.9% NaCl, 30% Ethanol in 0.9% NaCl, 50% Ethanol in 0.9% NaCl, 70% Ethanol in H2O, 90% Ethanol in H2O, and 100% Ethanol (2x), for 1 hour with gentle agitation. The rehydrated tumors were embedded using melted paraffin at 58^{o}C. Subsequent to paraffin infiltration, the tumors were placed into embedding molds and overlaid with melted paraffin for embedding. Blocks were cooled down at RT and are then ready for sectioning. Sections of 5 µm thickness were cut using a Leica RM2125 microtome, and then mounted on the glass slides in adjacent orders.

For antibody staining, the slides were deparaffinized with xylene and ethanol, and the antigens were retrieved with citrate buffer (pH6). Endogenous peroxidase activity

which can cause high background signals was inhibited using 3% H_2O_2. Slides were then blocked with normal goat serum to reduce the cross reaction of endogenous globulins in the tissues, and incubated with rabbit polyclonal anti-VACV antibody (1:1,000, Abcam). After rinsing with PBS to wash off the antibodies, Slides were incubated with secondary goat-anti-rabbit IgGs conjugated with HRP (Vector Laboratories). The detection was performed with Vectorstain Elite ABC reagent and Vector ImmPact DAB Peroxidase substrate (Vector Laboratories). Sections were counterstained with hematoxylin.

For hEPO staining, primary polyclonal rabbit-anti-hEPO (1:200, Santa Cruz) and secondary goat-anti-rabbit IgGs conjugated with HRP (Vector Laboratories) were used as a primary and secondary antibodies, respectively.

H&E (Hematoxylin and Eosin, Vector laboratiories) is one of the most common histological stainings. This staining gives a structural overview of the tissue and can be used to distinguish normal, pathological or degeneratively changed tissues. The slides were stained with hematoxylin solution for nuclei eosin for cytoplasm, collagen, keratin and erythrocytes.

Agarose-embedded sectioning

For hypoxia staining (HP-Red594), 2 hours before sacrificing the animals, 60 mg/kg of pimonidazole was intraperitoneally (i.p.) injected into all mice. This chemical forms adducts with thiol containing tissue proteins under hypoxic condition (pO_2 < 10 mm Hg). After harvesting, tumors were snap-frozen in liquid nitrogen and stored at -80^{o}C. Tumors were fixed with 4% paraformaldehyde (FDA) in PBS for 15 hours at 4^{o}C, shaking, and washed 5 times with 1x PBS for 30 min. Tumors were cut in half and embedded in warm (70^{o}C) 5% low melt agarose in 6-well plates, and then cooled down to form hardened blocks. The blocks were cut into 100-μm-sections using the Vibratome (Leica).

Sections were incubated with 200 µl permeabilization buffer (0.2% Triton-X 100, 5% FBS in 1 x PBS), and subsequently incubated with a primary antibody cocktail for 15 hours at 4^{o}C, shaking.

- HP-Red549 for hypoxia (1:200, mouse monoclonal antibody conjugated to Dylight549 fluorophore, Hypoxyprobe)
- CD31 for blood vessel (1:200, rat monoclonal anti-mouse CD31, BD)

- MHC-II for innate immune cells (1:500, rat monoclonal anti-mouse MHC-II, eBioscience)

After washing away the unbound primary antibodies, CD31- and MHC-II-stained sections were incubated with secondary donkey anti-rat conjugated AlexaFluor594 antibodies (1:500, Jackson ImmunoResearch) for 1 hour at RT. Sections were then embedded onto microscope slides with Mowiol 4-88 (Roth # 0713) and stored at 4^{o}C. The fluorescent intensity was visualized and measured under an inverse fluorescent microscope (Leica).

2.2.14 Measurement of fluorescent intensity

Five tumors from each treatment group (GLV-1h210, GLV-1h209, GLV-1h68 or untreated controls) at 14 dpi were used. Fluorescent intensity in sections stained for CD31 (15 sections, 3 sections for each tumor), hypoxia (HP-Red549, 15 sections, 3 sections for each tumor) and MHC-II (5 sections, 1 section for 1 tumor) were measured using ImageJ software based on brightness-related pixels (with intensity ranging from 0 to 255) on the captured pictures in average 1 square inch (1 in^2). The picture areas (12.7 x 9.51 mm) covered almost tumor-area sections. All pictures were captured with identical settings. In ImageJ, the whole picture was applied with the horizontal and vertical lines dividing the picture into 12 grids of 1 square inch (1 field). Fields which were mainly covering the tumor section were used to quantify signal intensity (usually 5-11 fields for each section, with median of 8 fields). Individual values for each counted field was averaged and represents the signal intensity of one section. (Fig. 2.3).

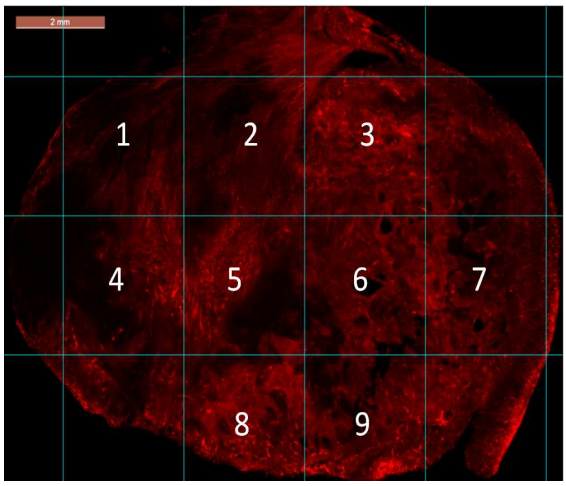

Fig. 2.3 A representative picture demonstrating vessel intensity measurement. The fluorescent intensity of this section was calculated by averaging the single values of the 9 indicated fields.

2.2.15 Measurements of vessel density and vessel diameter

30 fields for each group (2 fields for 1 section, 3 sections for 1 tumor, and 5 tumors for each group) of GLV-1h210, GLV-1h209, GLV-1h68 and untreated controls stained for CD31 were used for measurement of vessel density and vessel diameter. On the fluorescent microscope, images were adjusted (exposure time, gain, gamma) to get the best visualization. The magnification was fixed for all captured pictures with dimension of 1.91 x 1.43 mm. In ImageJ, pictures of sections were overlayed with 5 horizontal lines. All blood vessels that intersected with the lines were counted for blood vessel density and measured for blood vessel diameters.

2.2.16 Statistical analysis

A two-tail student's t test was used for analysis of statistically significant differences between treatment groups. Differences in survival rates were analyzed using log-rank test. P values of < 0.05 were considered as significant differences.

3. RESULTS

3.1 Characterization of recombinant vaccinia viruses expressing hEPO in cell culture

3.1.1 Construction of hEPO-encoding recombinant VAVCs

Four different hEPO-encoding recombinant vaccinia viruses (EPO-VACVs) were derived from the genetically modified and attenuated VACV GLV-1h68 [35]. This parental virus contains a *Renilla* luciferase–*Aequorea* – green fluorescent protein (Ruc-GFP) fusion gene, *lacZ* (encoding β-galactosidase), and *gusA* (encoding β-glucuronidase) inserted into the *F14.5L*, *J2R*, and *A56R* loci of the LIVP (Lister strain, Institute of Viral Preparation, Russia) viral genome, respectively. In hEPO-encoding recombinant vaccinia viruses, the β-galactosidase expression cassette was replaced with the hEPO expression cassettes in which the *hEPO* cDNA is under the control of 4 different VACV promoters: natural vaccinia early (p7.5), synthetic early (pSE), synthetic early/late (pSEL), and synthetic late (pSL), resulting in the vaccinia virus strains GLV-1h210, GLV-1h211, GLV-1h212 and GLV-1h213, respectively (Fig. 3.1).

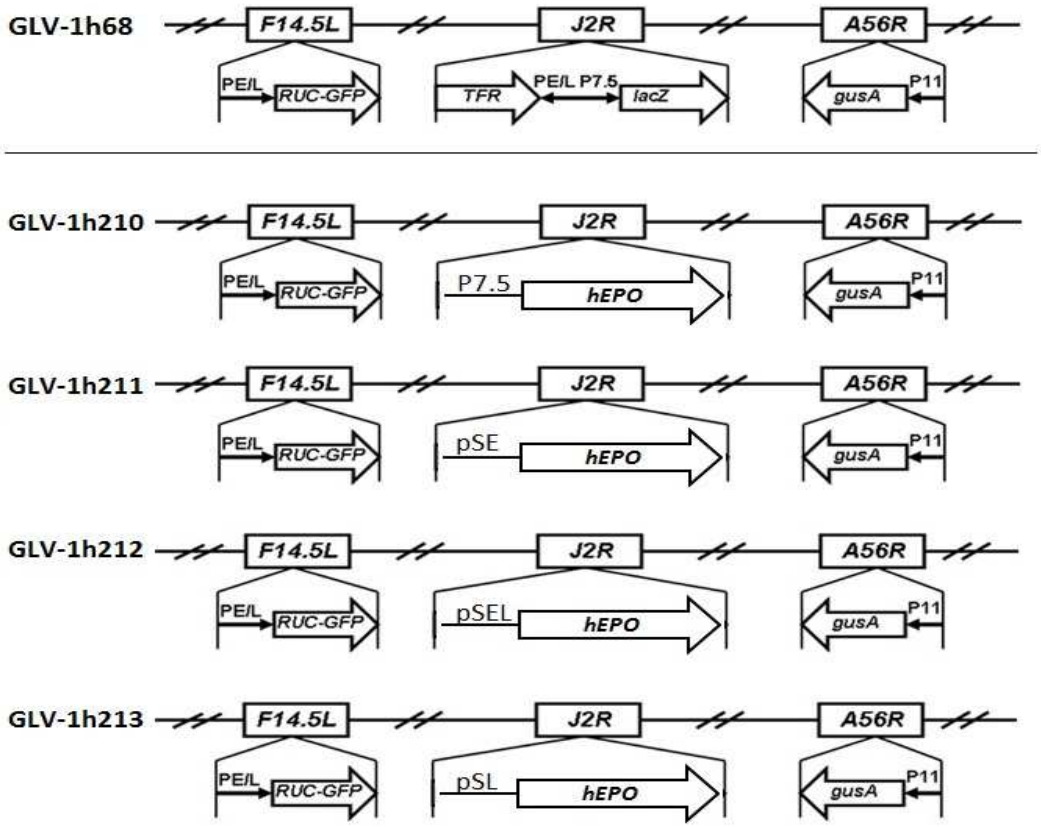

Fig. 3.1 Schematic representation of EPO-VACV constructs. The β-galactosidase expression cassette from the parental virus GLV-1h68 was replaced via homologous recombination at the *J2R* locus with the *hEPO* expression cassettes in which the *hEPO* cDNA is under the control of four different VACV promoters: natural vaccinia early (p7.5), synthetic early (pSE), synthetic early late (pSEL) and synthetic late (pSL). All viruses contain *ruc-gfp* (controlled by pSEL) and *gusA* (controlled by vaccinia later promoter, p11) at the F14.5L and *A56R* loci, respectively. GLV-1h68 carries *lacZ* (controlled by p7.5) and *rft* (human transferrin receptor controlled by pSEL in a reverse orientation).

3.1.2 Detection of Ruc-GFP, *lacZ* and *gusA* expression by western blotting

All EPO-VACVs were constructed to express Ruc-GFP, β-glucuronidase, and hEPO which was replaced for β-galactosidase in the parental virus GLV-1h68. To confirm that the replacement of *gusA* by *hEPO* does not affect the expression of other marker genes, A549 cells infected with either EPO-VACVs or GLV-1h68 were examined at 6, 12, 24 and 48 hours post infection by Western blot for the gene product expression of these marker genes using anti-β-galactosidase, -GFP and -β-glucuronidase antibodies (Fig. 3.2).

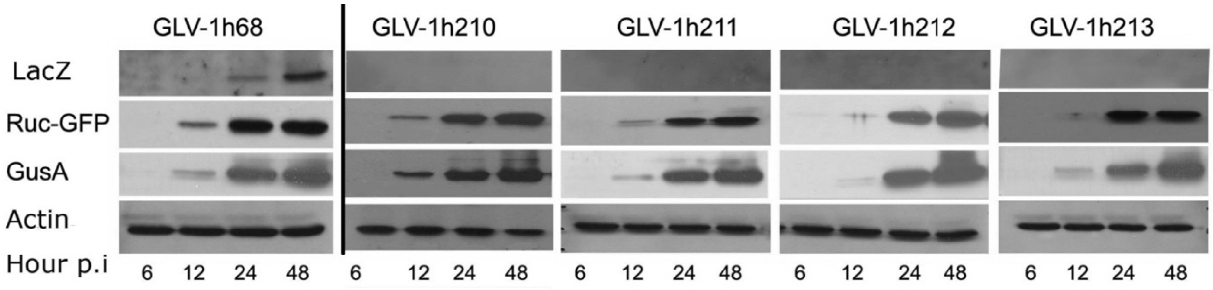

Fig. 3.2 Detection of β-galactosidase, Ruc-GFP, β-glucoronidase in cell culture by Western blot. Cells infected with GLV-1h210, -1h211, -1h212 and -1h213 (MOI=0.1) were harvested at 6, 12, 24 and 48 hpi. Cells were lysed in RIPA lysis buffer. Twenty (20) μg of protein was loaded on each lane and separated on a 10% SDS-PAGE before transfer onto 0.45 μm nitrocellulose membranes. Membranes were incubated with specific antibodies against β-galactosidase, β-glucoronidase, and GFP conjugated with HRP. Signals were then detected on autograph films with enhanced chemiluminescence (ECL). Human β-actin was loaded as an internal control.

The expression levels of Ruc-GFP and β-glucoronidase were comparable in all viruses and seemed independent from the insertion of hEPO in GLV-1h210, -1h211, -1h212 and -1h213. Signals can be clearly detected at 12 hpi and increased in late time points in all EPO-VACVs as well as in GLV-1h68. Little differences in protein expression of marker genes between 24 and 48 hpi indicated that most cancer cells were infected by viruses at 24 hpi with an MOI of 0.1.

The replacement of *lacZ* in EPO-VACVs was successfully shown. In cells infected with the parental virus GLV-1h68, β-galactosidase signal was visibly detected at 24 hpi whereas no signals came from the EPO-VACVs infected cells. However, the signal of β-galactosidase expression showed up later and weaker than Ruc-GFP or β-glucuronidase. That could be due to either less sensitivity of anti-β-galactosidase antibody or lower protein expression level caused by the weaker promoter p7.5 compared with pSEL and p11 promoters.

3.1.3 Detection of Ruc-GFP expression via fluorescent microscopy

A faster and simpler way to visualize virus replication is to use Ruc-GFP fusion protein via fluorescent microscopy. For better comparison, two different cell lines were used: human non-small cell lung carcinoma (A549) and human small lung carcinoma (NCI-H1299) cell lines. Confluent cell monolayers in 24-well plates were mock-infected or infected with EPO-VACVs and GLV-1h68 at an MOI of 0.1. One hour after infection, infection medium was replaced with fresh growth medium and cells were maintained in a 5% CO2 incubator at 37^{o}C. Pictures were captured at 24, 48, 72 and 96 hpi (Fig. 3.3).

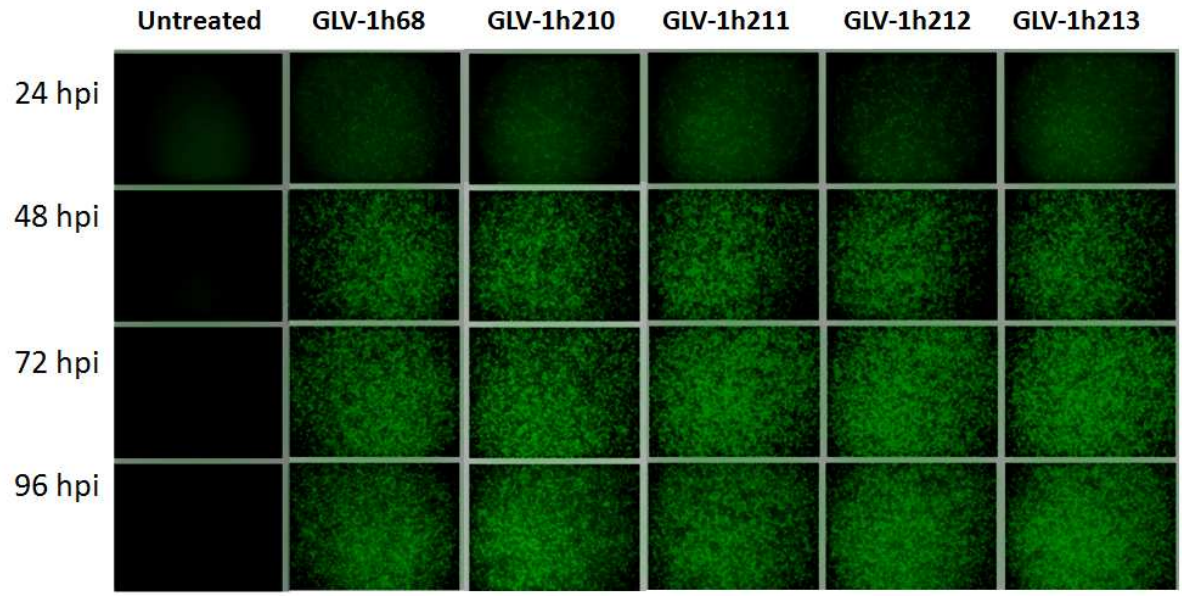

Fig. 3.3a GFP expression in A549 cells infected with EPO-VACVs or GLV-1h68. A549 cells were infected with the indicated viruses at an MOI of 0.1. The pictures were captured at 24, 48, 72, and 96 hpi by using a Leica MZ16 FA fluorescence stereomicroscope at 50x magnification.

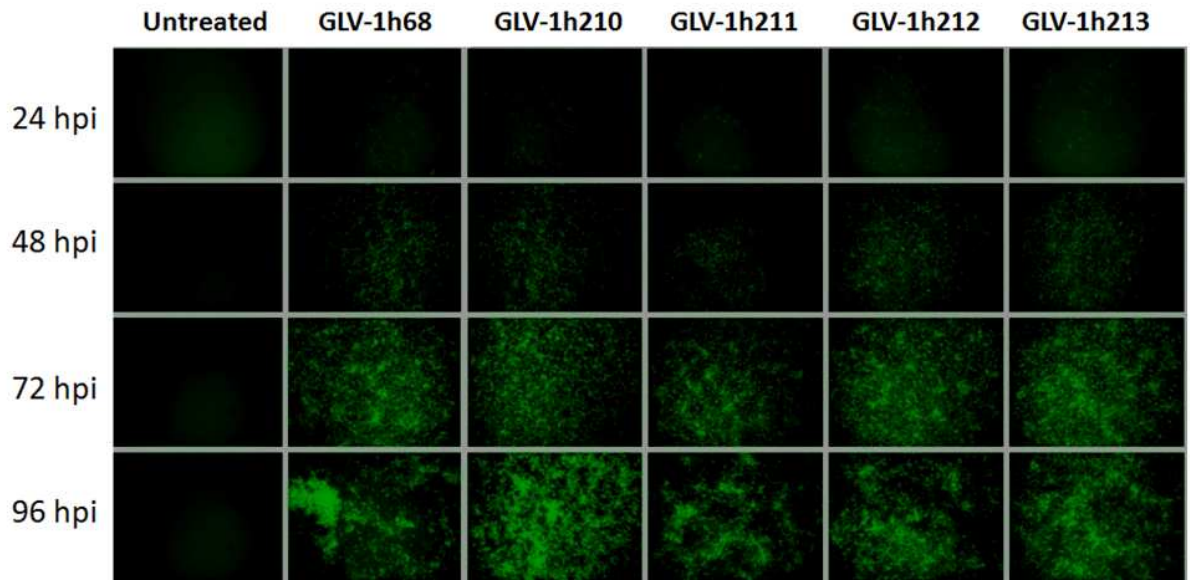

Fig. 3.3b GFP expression in NCI-H1299 cells infected with EPO-VACVs or GLV-1h68. NCI-H1299 cells were infected with the indicated viruses at an MOI of 0.1. The pictures were captured at 24, 48, 72, and 96 hpi by using a Leica MZ16 FA fluorescence stereomicroscope at 50x magnification.

Signal intensity from A549-infected cells was much stronger than that from NCI-H1299 infected cells at everyobserved time point. Infection patterns also differed between the two tested cell lines. A549 cells seemed to be equally infected, whereas HCI-H1299 cells were not. No visible differences in signal intensity among all viruses were observed. At 96 hpi almost all cells were infected and detached from the wells, demonstrating the ability of the viruses to infect, replicate, and lyse in both tested cell lines.

3.1.4 Detection of hEPO expression by western blotting

To confirm the successful expression of the transgene *hEPO* in EPO-VACVs, proteins from infected A549 cells were used to detect hEPO by a specific antibody. Shown in Fig. 3.4 is a Western blot analysis of hEPO expression at different time points after virus infection. At 3 hpi, a slight signal was seen only in GLV-1h212. At 7 and 21 hpi, strong signals were detected in GLV-1h212 and GLV-1h213 with a molecular mass of about 34 kDa but not in GLV-210 or GLV-1h211. Possibly, the expression of hEPO in GLV-210 or GLV-1h211 was not strong enough to be

detected in 20 μg of extracted protein. No signal was detected in lanes loaded with protein from GLV-1h68- or mock-infected cells.

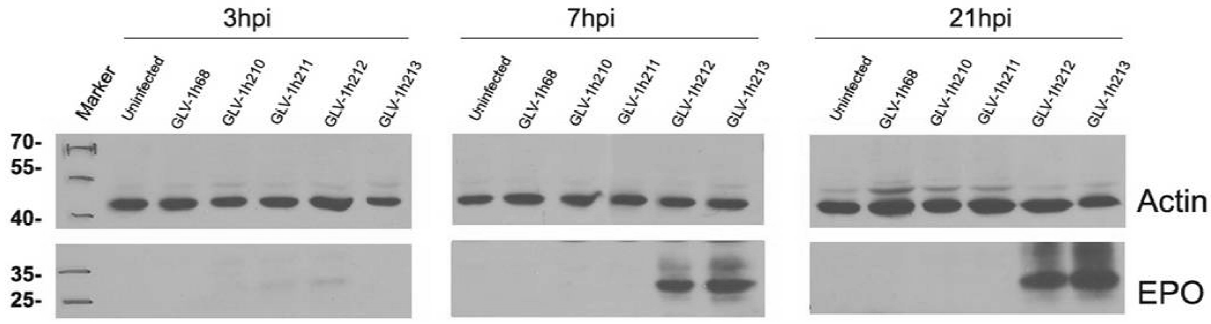

Fig. 3.4 Detection of hEPO expression in infected A549 cells. Cells were seeded in 12-well plates, then either mock-infected or infected with each EPO-VACVs or GLV-1h68 at an MOI of 5. At 3, 7 and 21 hpi, cells were harvested and proteins were extracted using RIPA lysis buffer plus protease inhibitor cocktail. 20 μg of protein were loaded on 10% SDS-PAGE gels. hEPO was detected using an anti-hEPO antibody. Human β-actin was loaded as an internal control for all samples.

3.1.5 Transcription of *hEPO* in cells infected with different EPO-VACVs

Four EPO-VACVs, GLV-1h210, -1h211, -1h212, and GLV-1h213 carry hEPO under the control of 4 different promoters; p7.5, pSE, pSEL and pSL, respectively. To determine relative transcriptional strength of these promoters, quantitative real-time polymerase chain reaction assay (Q-PCR) of *hEPO* gene by specific designed primers was performed.

A549 cells were mock-infected or infected with GLV-1h68 or each EPO-VACVs at an MOI of 10. Cells were harvested after 2, 4, 6 and 8 hours post infection. Isolated mRNA was converted into cDNA which was then used as a template for amplification of the 5'-end 80 bp portion of the *hEPO* gene. At 2 hpi, the transcription of *hEPO* was detected in GLV-1h210 (used as control with level of 1), GLV-1h211 and GLV-1h212, but not in GLV-1h213 (pSL) in which the transcription did not start yet. *hEPO* transcription in GLV-1h211 (pSE) showed the strongest activity which was 1.4-fold higher compared to in GLV-1h210, whereas it was only 0.7-fold in GLV-1h212 (pSEL). At 4 hpi, the transcription of hEPO in GLV-1h213 was detectable but at a

very low level (0.1 fold). The highest levels at this time point were observed in GLV-1h212-infected cells (2.5 fold) followed by GLV-1h210 and GLV-1h211. The transcription seemed to be fully activated from 6 hpi onwards when levels of transcription among promoters consistently increased. The promoter strength increased from p7.5 (GLV-1h210), to pSE (GLV-1h211), pSEL (GLV-1h212) and pSL (GLV-1h213) with the estimated ratio of 1:2:10:15, respectively (Fig. 3.5).

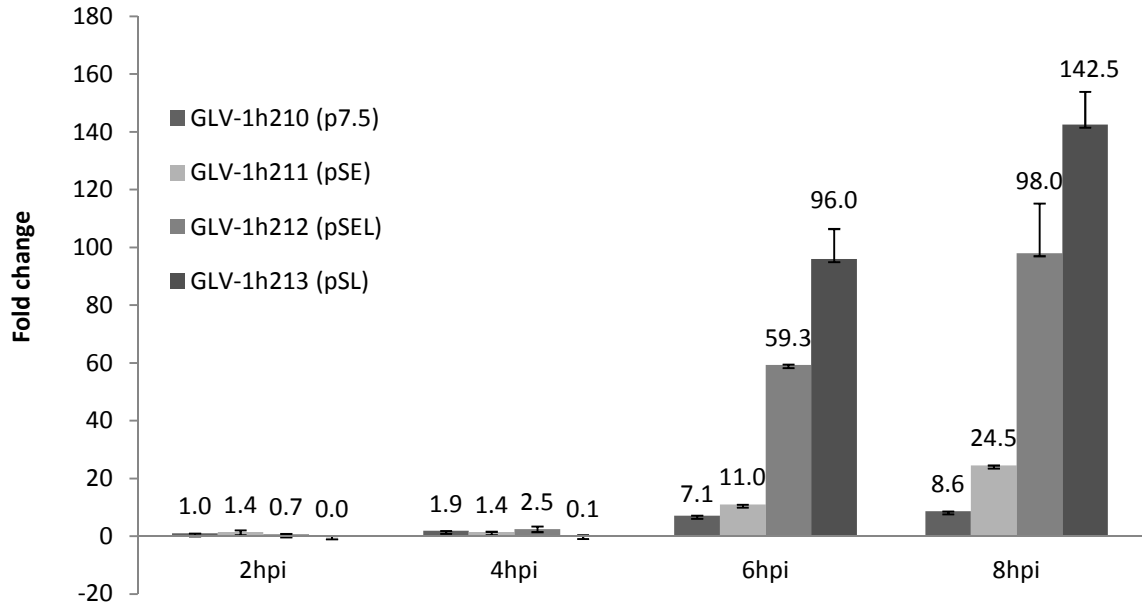

Fig. 3.5 Relative promoter strength of p7.5, pSE, pSEL, pSL in controlling *hEPO* transcription. A549 cells were infected with each EPO-VACVs at an MOI of 10. At 2, 4, 6, and 8 hpi, cells were harvested, and total mRNA was isolated. 1 μg of RNA was converted to cDNA which was then used as template for amplification of the *hEPO* mRNA. By qPCR, the transcription of *hEPO* gene using specific primers was analyzed. The numbers on each column show fold differences in transcription level of promoters at time points compared to the p7.5 promoter (GLV-1h210) at 2 hpi. The transcription level of p7.5 at 2 hpi was considered as 1. Two wells in each virus were harvested and tested in duplicate. Data is presented as averaged values with standard deviations (SD).

3.1.6 Quantification of hEPO expression by ELISA

To evaluate the correlation of transcription and translation of hEPO controlled by different promoters, hEPO expression after infection with different EPO-VACVs (MOI

of 10) was measured by ELISA. This is a sensitive method based on 2 distinct monoclonal anti-hEPO antibodies; one was coated on the 96-well plates and another one was added after the antigen (hEPO in samples) was already linked to the first antibody. The sensitivity was enhanced by streptavidin conjugated with horseradish peroxidase (HRP) which then converted the tetramethylbenzidine (TMB) substrate to a colored product which could be measured by absorption spectrophotometry at 450 nm. The hEPO concentration in test samples can be inferred based on absorbance values of known standard hEPO concentrations.

Consistent with transcriptional data at 2 hpi, no hEPO protein was detected in GLV-1h213 (pSL). Interestingly, in GLV-1h212 (pSEL)-infected cells, however, not showing the highest level in the transcription, protein amounts of EPO were the highest, followed by GLV-1h211 (pSE) and GLV-1h210 (p7.5). The translation at 6 hpi remained the strongest expression level for GLV-1h212. Although showing the highest transcription levels at 6 hpi, the translated hEPO protein levels in GLV-1h213-infected cells were lower than in GLV-1h212 at this time point. The translation in all viruses from 12 to 24 hpi was stable with an estimated consistent expression ratio of 1:2:20:20 from GLV-1h210 to GLV-1h211, GLV-1h212 and GLV-1h213, respectively.

A constant ratio of 2 was found between GLV-1h211 and GLV-1h210 in all tested time points of translation closely reflectingtheir relative transcription levels, indicating a direct relationship between transcription and translation of the two early promoters (p7.5 and pSE). While no tight correlation of transcription and translation in pSEL and pSL promoters was shown at the early time points (2-6 hpi), (Fig. 3.6).

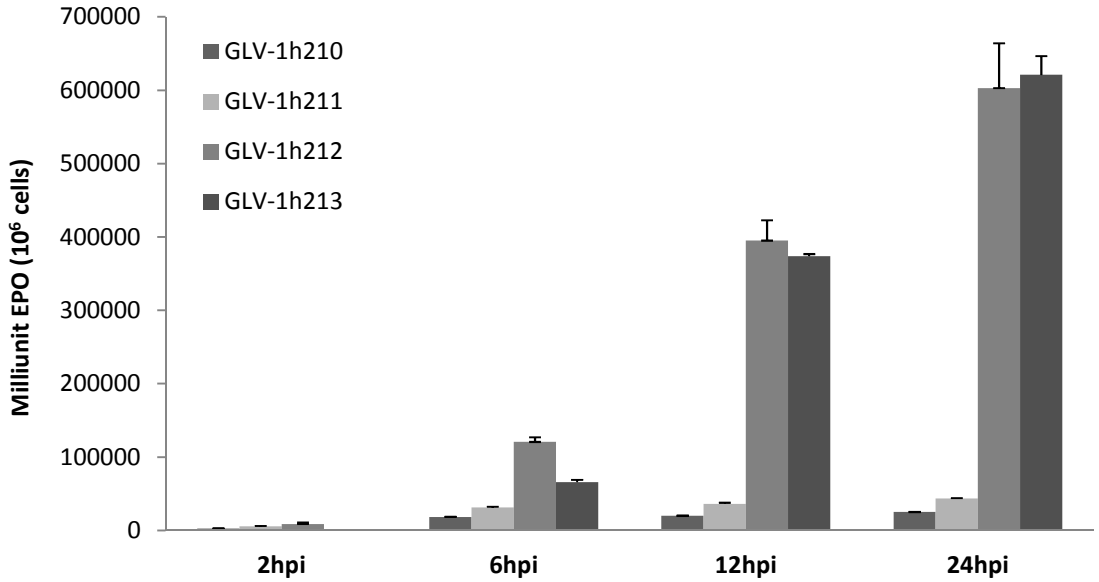

Fig. 3.6 Concentration of secreted hEPO in the supernatant of A549 cells infected with different EPO-VACVs. Cells were infected with each EPO-VACV at an MOI of 10. Supernatants were collected at 2, 6, 12 and 24 hpi. Secreted hEPO in supernatant was quantified by ELISA. Three individual samples were collected and tested in duplicate. Data was presented as average values with SD.

3.1.7 Replication of EPO-VACVs and GLV-1h68 in A549 and NCI-H1299

To evaluate the replication efficiency of different VACVs expressing of hEPO in A549 and NCI-H1299 cells, 80-90% confluent cells were infected with EPO-VACVs or GLV-1h68 at an MOI of 0.1. All viruses were able to replicate well in both cell lines. The replication was more than 100-fold stronger in A549 than in NCI-H1299 at 24, 48 and 72 hpi. In A549, all EPO-VAVCs shared similar replication efficiency and were slightly stronger than GLV-1h68 at 24 and 48 hpi, but GLV-1h68 titers caught up at 72 hpi.

In NCI-H1299, the replication efficiency of EPO-VACVs seemed opposite to the promoter strengths, stronger promoter delayed the replication of viruses which were descendent in order of GLV-1h213 (pSL), -1h212 (pSEL), -1h211 (pSE), and -1h210 (p7.5). GLV-1h68 had a replication curve similar to GLV-1h212, except at 48 hpi. However, 72 hpi all tested viruses showed similar replication levels, again indicating efficient replication in A549 and HCI-H1299 cell lines (Fig. 3.7).

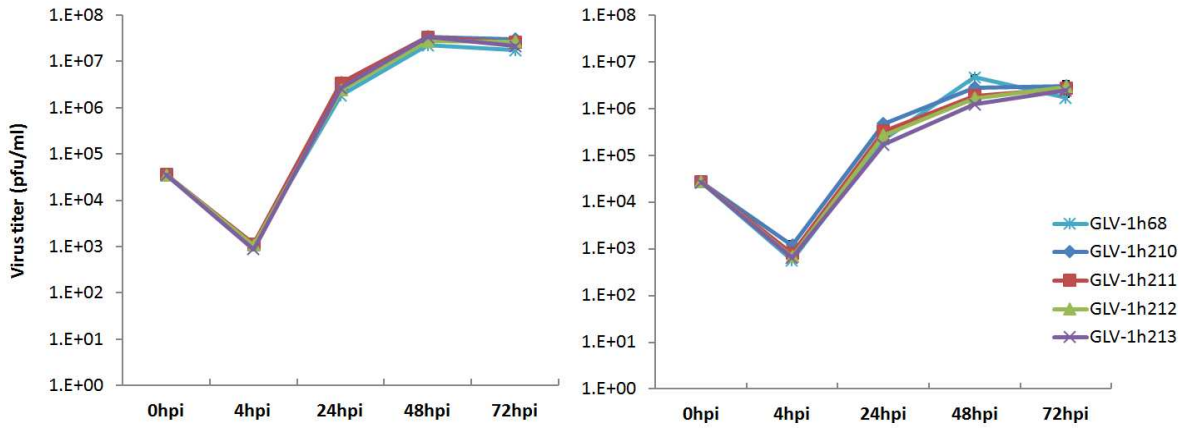

Fig. 3.7 Replication of EPO-VACVs and GLV-1h68 in A549 (left) and in NCI-H1299 (right). Cells were seeded in 24-well plates and then infected with the indicated virus using an MOI of 0.1. At 4, 24, 48 and 72 hpi cells and supernatant in each well were collected. Samples underwent 3 freeze-thaw cycles and sonification to release viral particles into the medium. Standard plaque assay on CV-1 cells was performed for all samples. Averaged values with standard deviations of three independent samples are shown.

3.1.8 Cytotoxicity of EPO-VACVs and GLV-1h68 in A549 and NCI-H1299

To see whether the expression of hEPO would affect the oncolytic activity of VACVs in cell culture, monolayers of A549 cells were infected with either EPO-VACVs or GLV-1h68 at an MOI of 0.1. As shown in Fig. 3.8, the survival in A549 cells was almost identical for all tested viruses. Cell death was observed from as early as 24 hpi. The amount of living cells drastically declined from 24 to 48 hpi. At 96 hpi, more than 95% of all cancer cells had been killed.

In NCI-H1299, a replication-dependent cytotoxic efficiency was seen among the tested viruses. At 24 hpi, the viability of virus-infected cells remained equal or slightly increased compared to uninfected controls, either with EPO-VACVs or GLV-1h68. At 96 hpi, about 84% ± 2.14 cells were killed with GLV-1h210 while only 61% ± 2.44 with GLV-1h211 and GLV-1h68, or 52% ± 5.85 with GLV-1h212 and 41% ± 2.45 with GLV-1h213 were killed, respectively. The differences in replication and cytotoxicity indicated that the VACVs showed more efficient replicating and killing in A549 than in NCI-H1299 cells.

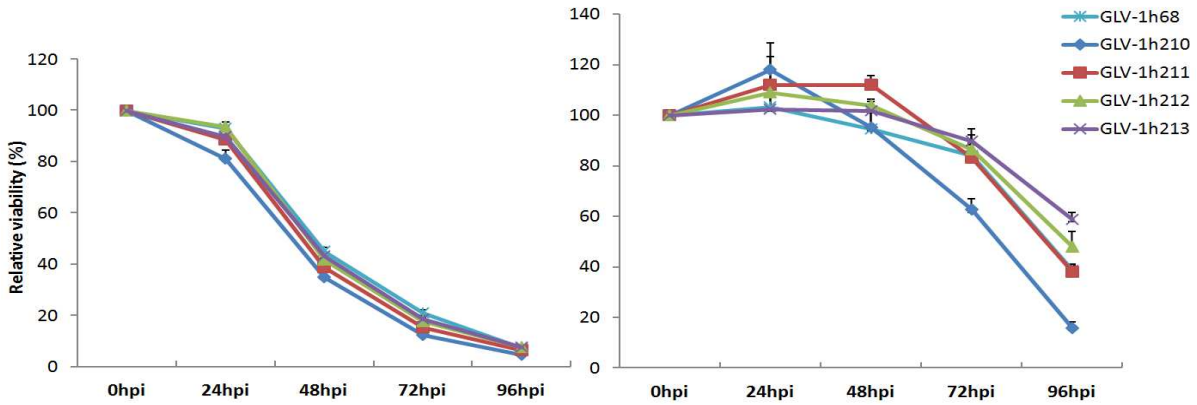

Fig. 3.8 Viability of A549 (left) and NCI-H1299 (right) after infection with EPO-VACVs and GLV-1h68. Cells were seeded in 24-well plates and then infected with indicated viruses at an MOI of 0.1. Cell viability was analyzed every day for 4 days using 3-(4,5-dimethylthiazol-2-yl)-2,5-diphenyltetrazoliumbromide (MTT). Values are shown as percentages of respective uninfected controls which are considered as 100% viability.

3.1.9 Effect of hEPO on oncolytic potential in hypoxia and normaxia

To assess the effect of exogenous rhEPO on virus replication and cytotoxicity in normaxic and hypoxic conditions, A549 cells infected with GLV-1h210, GLV-1h68 or GLV-1h68 in presence of hEPO were harvested at 4, 24, 48, 72 and 96 hpi. Before infection, 10 units/ml of rhEPO (Epoetin alfa) was added and maintained in media of combination treatments. Notably, hypoxia reduced virus replication (Fig. 3.9, left) and slowed down the killing ability of all tested viruses (Fig 3.9, right). While, rhEPO had no effects on virus replication and killing ability at any time points in both hypoxia and normaxia. In detail, the replication was 7-fold (24 hpi), 7-fold (48 hpi) and 4-fold (72 hpi) lower when comparing mean values of virus titers between normaxia and hypoxia. In each condition (hypoxia or normaxia), GLV-1h210, GLV-1h68 or GLV-1h68 combined with rhEPO showed similar replication activity. At the same time point, higher virus titers reflected stronger cell killing ability in normaxia and lower virus titers reflected weaker cell killing ability in hypoxia.

To further assess how hypoxia affects the virus gene expression, selected marker genes (*gfp* and *gusA* which were inserted in the viral genome) were analyzed by using fluorescent microscopy or gusA-activated fluorogenic substrate (4-MUG). A549 cells infected with GLV-1h210 and GLV-1h68 at MOIs of 1 and 0.01 at 48 hpi

showed highest enzyme activity in normaxia compared to hypoxia or adapted hypoxia at both MOIs ($p < 0.01$ or 0.001). Meanwhile, no difference was found between hypoxia and adapted hypoxia, except for GLV-1h68 at an MOI of 1. The difference between normaxia and hypoxia or adapted hypoxia could be visualized by fluorescent microscopy (Fig. 3.10).

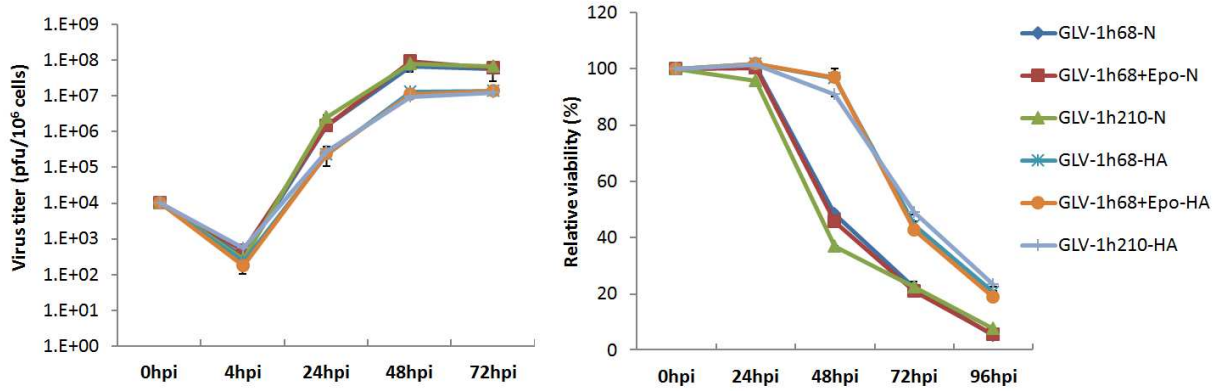

Fig. 3.9 Replication and cytotoxicity of GLV-1h210, GLV-1h68 and GLV-1h68 combined with rhEPO in A549 cells under normaxia or hypoxia condition [normaxia (N): 20% O_2 and hypoxia-adapted (HA) at 2% O_2]. Hypoxia-adapted cells were cultured in a 2% O_2, 5% CO_2 incubator at 37°C and remained for 4 passages (in 225-T flasks). Normal and hypoxia-adapted cells were seeded in 24-well plates and then infected with indicated viruses at an MOI of 0.01. At 4, 24, 48 and 72 hpi cells and supernatant in each well were collected. Virus titers were measured by standard plaque assay on CV-1 cells (left). An identical set of cells was prepared and infected with the same viruses as in the replication assay. At 24, 48, 72 and 96 hpi, cell viability was measured using MTT assay (right). Averaged values with standard deviations of three independent samples are shown.

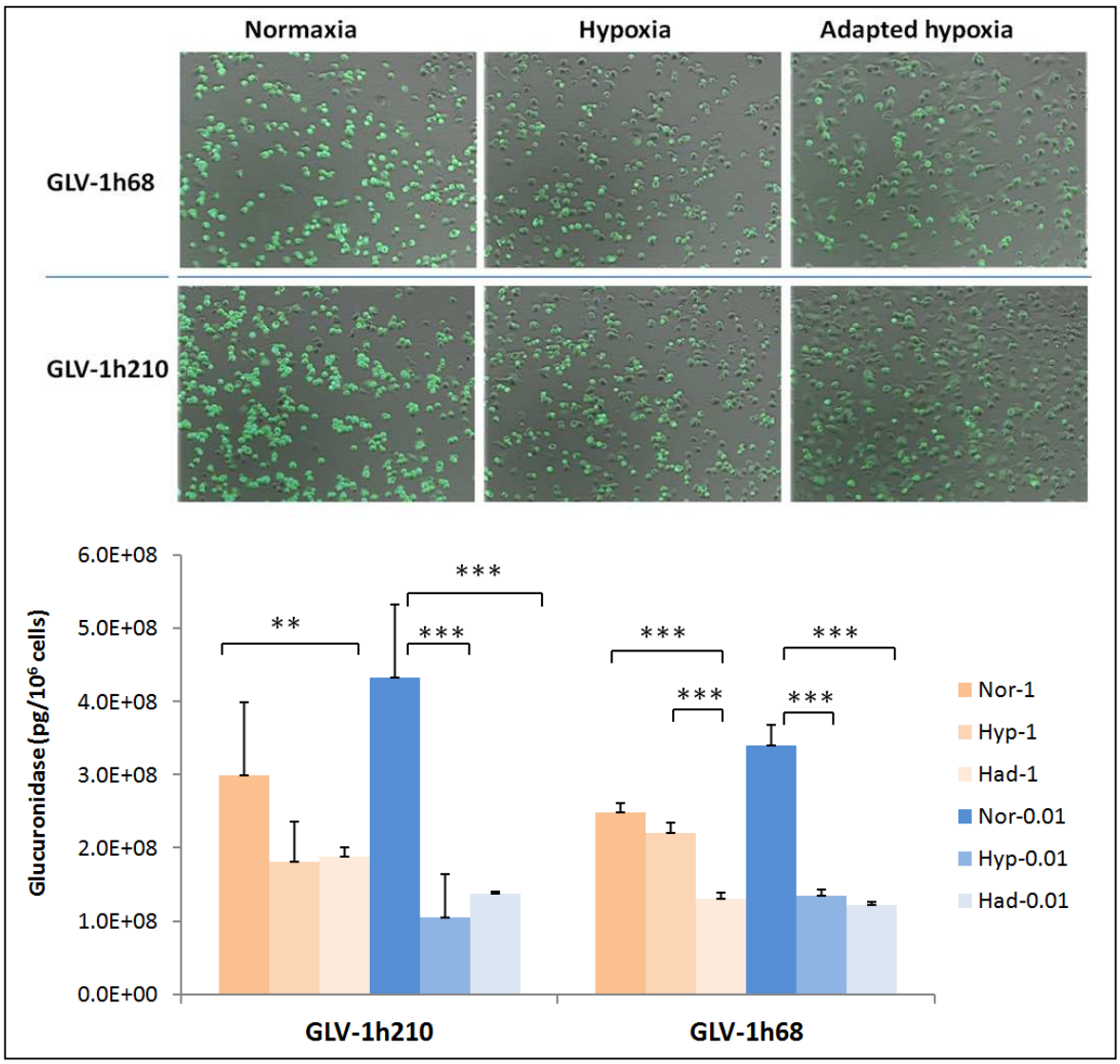

Fig. 3.10 GFP and β-glucuronidase expression after infection with GLV-1h210 or GLV-1h68 in normaxic, hypoxic or hypoxia-adapted environments. A549 cells (adapted or normal) were infected with each virus at MOIs of 1 and 0.01. Infected cells were maintained in normaxia (20% O_2) or hypoxia (2% O_2) and visualized at different time points. The representative GFP pictures were captured under a fluorescent microscope at 24 hpi (MOI 1) and overlaid with their bright field captures. At 48 hpi, 3 infected wells for each virus infection were frozen and thawed to break up the cell membranes. Samples were added with a fluorogenic probe substrate (4-MUG) for 1 hour at 37°C in duplicate, and then measured for fluorescent intensity. The asterisks indicate statistically significant differences in fluorescent intensity of gusA after GLV-1h68- and GLV-1h209-infected A549 cells in normaxic, hypoxic or adapted hypoxic conditions.

3.2 Therapy of A549 xenografts with EPO-VACVs

3.2.1 EPO-VACVs enhance tumor regression

To evaluate the therapeutic ability of EPO-VACVs compared to GLV-1h68 in human lung cancer *in vivo*, 7-8 athymic nude mice in each group were implanted with $5x10^6$ A549 cells in the right hind flank in 100 µl 1x PBS. 100% of all implanted mice generated visible tumors 1-2 weeks after implantation. After about 3 weeks, when the tumor volume reached ~ 150-200 mm^3, a single dose of $2x10^6$ pfu/mouse of each virus was systemically delivered (r.o.). At the same time, rhEPO (Epoetin alfa) was subcutaneously (s.c.) delivered to mice either alone or in combination with GLV-1h68 for 9 consecutive day (d1-d9) at a dose of 500 U/kg.

As shown in Fig. 3.11 (left), three EPO-VACVs exhibited greater tumor regression compared to GLV-1h68, and inhibition of tumor growth occurred a week earlier than in the mice of GLV-1h68 group. In EPO-VACV groups, tumors started shrinking from day 14 post virus injection (dpi) while tumor shrinkage in GLV-1h68-treated animals appeared at day 21. Significant differences in the tumor volumes were observed as early as 21 dpi and remained until day 42 post injection in the mice of the GLV-1h211 treatment group, while statistical significance in the GLV-1h212 treatment group was just observed after 35 days of virus treatment. No statistically significant differences in the tumor volumes were found among tumors treated with the three EPO-VACVs (GLV-1h211, -1h212, -1h213), even though during the first 14 days tumors in GLV-1h211-treated group had a higher tumor volume, and from there on tumor regression started catching up with the two other EPO-VACVs. In the untreated control group, tumors kept continuously growing.

In another study (Fig. 3.11, right), rhEPO treatment did not result in any differences in tumor growth volume when compared to untreated controls. Animals of both groups had to be sacrificed at day 35 post treatment due to excessive tumor burden. In another scenario, GLV-1h68 alone and combinational treatment of GLV-1h68 and rhEPO also did not show statistical differences between each other. As in the previous observations, GLV-1h211 inhibited tumor growth significantly better when compared to GLV-1h68, starting from day 21 post injection. While treatment with GLV-1h210, expressing lowest amounts of hEPO among all EPO-VACVs, resulted in significant lower tumor volumes compared to treatment with GLV-1h68. Observed

anti-tumoral effects were slightly impaired compared to GLV-1h211-treated mice, but no significant differences between GLV-1h210 and GLV-1h211 were found.

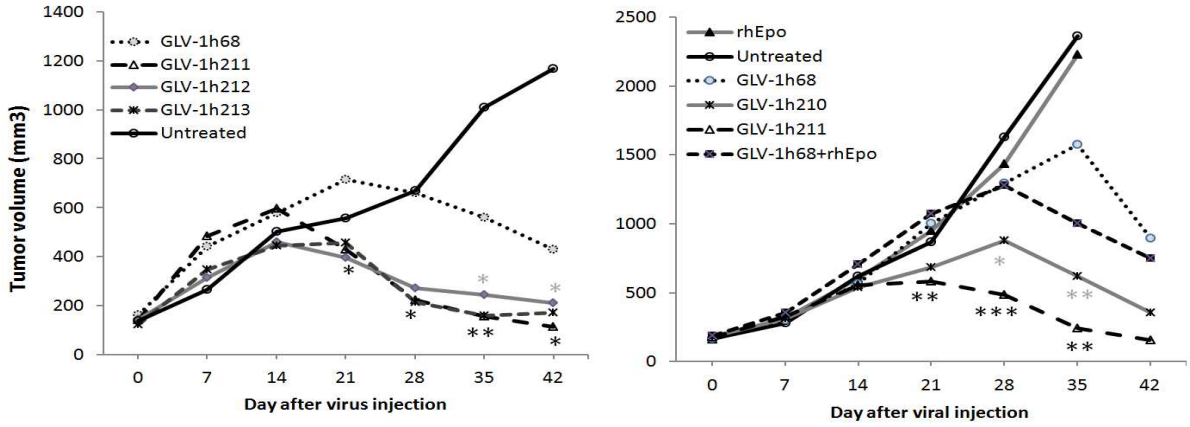

Fig. 3.11 Tumor regression after treatment with GLV-1h211, -1h212, -1h213, and -1h68 (left); GLV-1h210, -1h211, -1h68, hEPO, and hEPO in combination with GLV-1h68 (right). 5-6 week-old-male athymic nude mice were implanted with $5x10^6$ A549 cells in the right hind flank. About 3 weeks later, tumor-bearing mice were retro-obitally (r.o.) injected with single dose of $2x10^6$ pfu/mouse for each virus. Concomitantly, 500 U/kg of rhEPO was subcutaneously (s.c) injected in rhEPO or rhEPO in combination with GLV-1h68 group for 9 consecutive days. Tumor volumes were measured once a week. Data is shown as median values of 7-8 mice in each group. Significant differences were analyzed between GLV-1h68 and other virus-treated groups. (left) Black asterisks (*) indicate statistically significant differences compared to GLV-1h211, light asterisks (*) indicate significant differences compared to GLV-1h212. (right) Black asterisks (*) indicate significant difference compared to GLV-1h211 and light asterisk (*) indicate significant difference compared to GLV-1h210. * $P < 0.05$, ** $P < 0.01$, *** $P < 0.001$.

3.2.2 Increase of hemoglobin caused by virus-mediated expression of hEPO

To evaluate the functionality of hEPO after administration, blood samples from all mice were collected at 9 days or 14 days after virus treatment to measure hemoglobin levels. All groups treated with EPO-VACVs or rhEPO showed a significant increase in hemoglobin levels compared to untreated controls or the GLV-1h68-treated group ($p < 0.001$). Untreated controls and the GLV-1h68-treated group showed hemoglobin levels ranging from 14 to 16 g/dL whereas rhEPO alone, rhEPO

combined with GLV-1h68 or EPO-VACVs groups showed increased Hb values up to 18 - 20 g/dL either 9 dpi or 14 dpi. No significant differences among EPO-VACVs were found. These results confirm the successful administration of hEPO as well as VACVs-mediated expression of hEPO (Fig. 3.12).

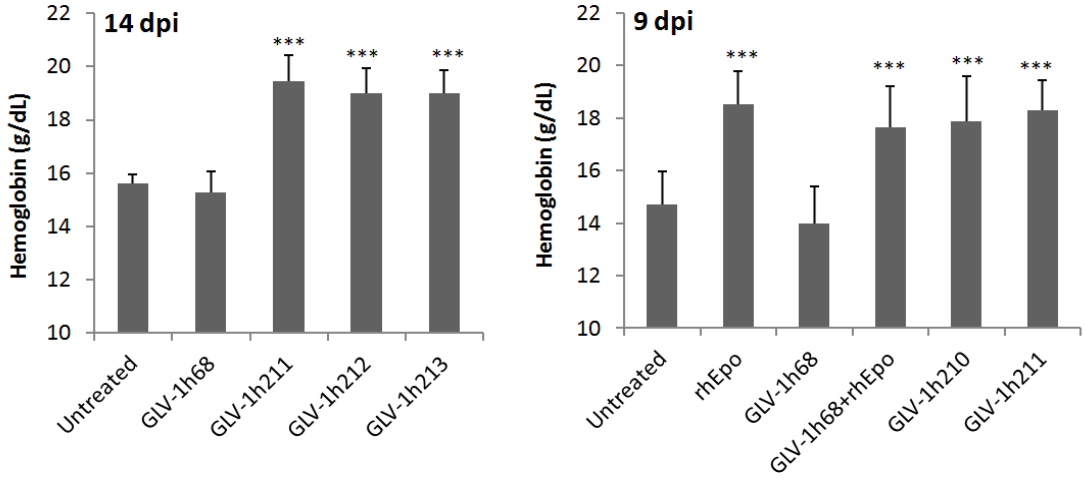

Fig. 3.12 The increase of hemoglobin levels in mice after treatment with EPO-VACVs or rhEPO. Five (5) μl of whole blood were taken from the retro orbital cavity using EDTA-coated capillaries and were immediately tested for hemoglobin by colorimetric detection assay. Shown are averaged hemoglobin levels of 8 – 10 mice plus SD for each group. Statistically significant differences were analyzed between untreated controls and all other groups. *** $P < 0.001$.

3.1.2 Enhanced EPO-VACVs replication in tumors

In order to study whether higher tumor regression in EPO-VACVs-treated tumor-bearing mice is related to virus replication, four (4) mice from each group treated with either EPO-VACVs or GLV-1h68 were sacrificed at 14 dpi. Homogenized tumors were used to perform plaque forming assays on CV-1 cells and results were plotted in Fig. 3.13. All four EPO-VACV groups exhibited higher virus titers in tumors compared to the GLV-1h68 group (3.46 - 3.98 folds). Differences were statistically significant ($p < 0.01$), excepted for GLV-1h212 ($p = 0.051$). Differences in viral titers were observed to be up to 7.56-fold ($p < 0.05$) increased between the GLV-1h211 and GLV-1h68 treatment groups (Fig. 3.13, right). Similar to tumor regression, the obtained virus titers in GLV-1h68 and GLV-1h68 plus rhEPO-treated animals were

similar. These results indicate the positive correlation between virus titer and tumor regression.

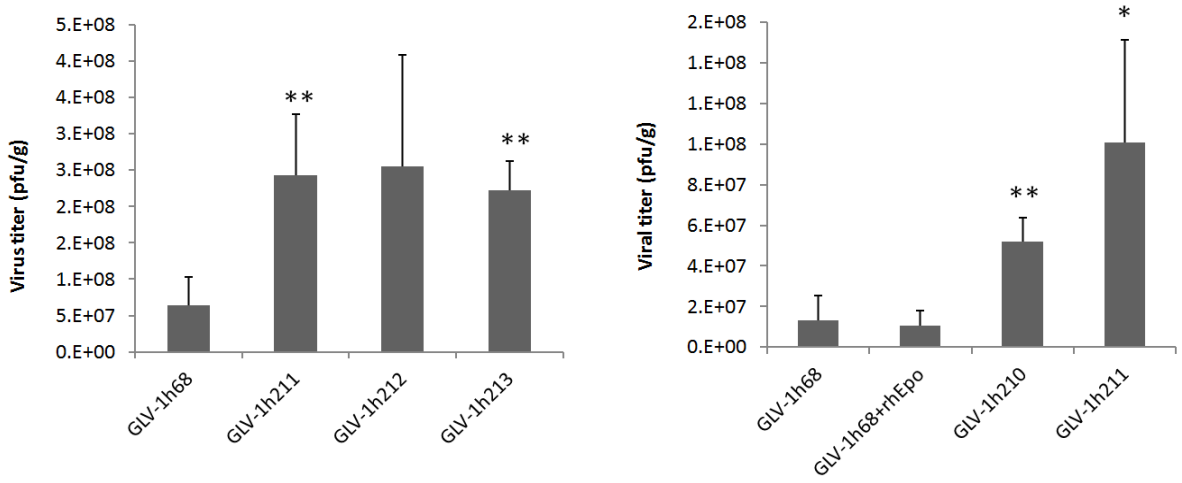

Fig. 3.13 Virus replication in A549 tumors after administration of VACV strains. Tumor-bearing mice were injected r.o. with a dose of $2x10^6$ pfu/mouse of each virus. Fourteen (14) days post virus treatment, tumors from 4 mice in each group were excised. Tumors were homogenized and underwent 3 freeze-thaw to release the viruses from the cells. Virus titers were determined by standard plaque assays on CV-1 cells. Averaged values with standard deviations of 4 individual samples are shown. Significant differences were analyzed between GLV-1h68 and other virus treated groups. * $P < 0.05$, ** $P < 0.01$.

3.2.3 Effects of treatment with EPO-VACVs on organ weights

To assess the effects of virus treatment on animal tissues, brain, liver, spleen, kidney, lung and heart were excised at 14 dpi. Organs were observed, weighted and compared to untreated controls. Brain, liver, kidney, lung or heart from virus-treated groups did not show any differences in weight or visible abnormal signs when compared to untreated controls. However, significant spleen enlargement was found in all EPO-VACV-treated groups when compared with GLV-1h68 (0.197 ± 0.062) and untreated groups (0.165 ± 0.07). The hEPO expression under the control of strong promoter resulted in large spleen weights, in the increasing order of GLV-1h210 (0.475 ± 0.026), GLV-1h211 (0.505 ± 0.104), GLV-1h212 (0.638 ± 0.056), and GLV-1h213 (0.649 ± 0.185), respectively, but significant statistical differences were not

found. No difference in spleen weight was observed between GLV-1h68 and untreated control groups (Fig. 3.14a).

In addition, the effects of exogenous rhEPO alone or in combination with GLV-1h68 were also evaluated. Similar to previous observations, no difference between GLV-1h68 and untreated control were seen. However, spleen enlargement was found in rhEPO alone ($p < 0.01$), or rhEPO combined with GLV-1h68 ($p < 0.01$) when compared to untreated control group at day 7 after virus injection (Fig 3.14b).

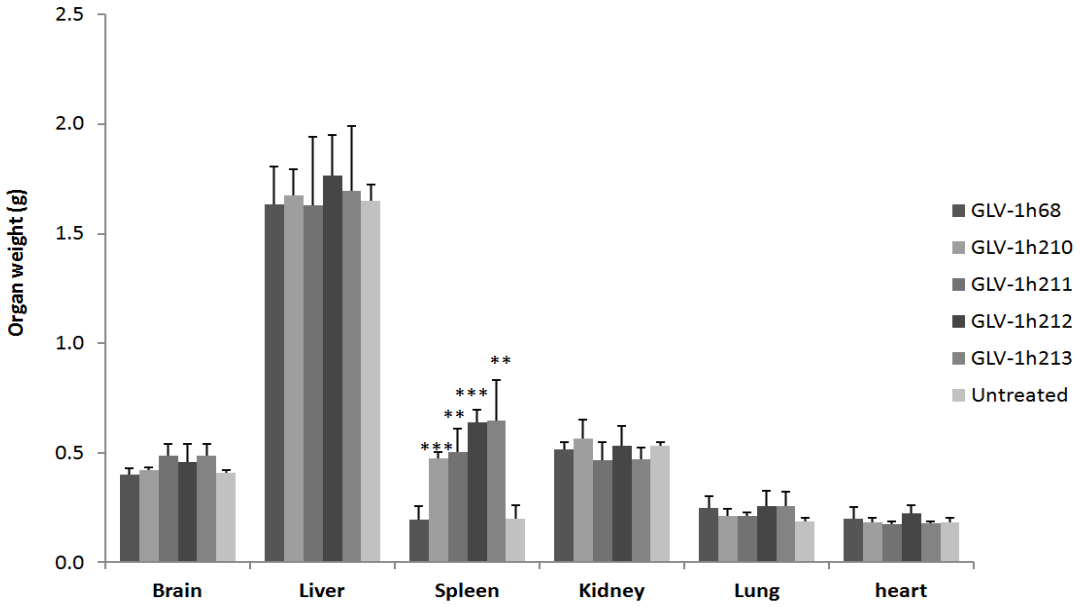

Fig. 3.14a Effects of virus treatment on organ weights. A549 tumor-bearing mice were injected r.o. with a dose of $2x10^6$ pfu/mouse of each virus. 14 days post virus injection, brain, liver, spleen, kidney, lung and heart of 4 mice of each group were excised and weighted. Data is shown as the averaged values with SD. Significant differences were found between all EPO-VACV strains and untreated group (or GLV-1h68). ** $P < 0.01$, *** $P < 0.001$.

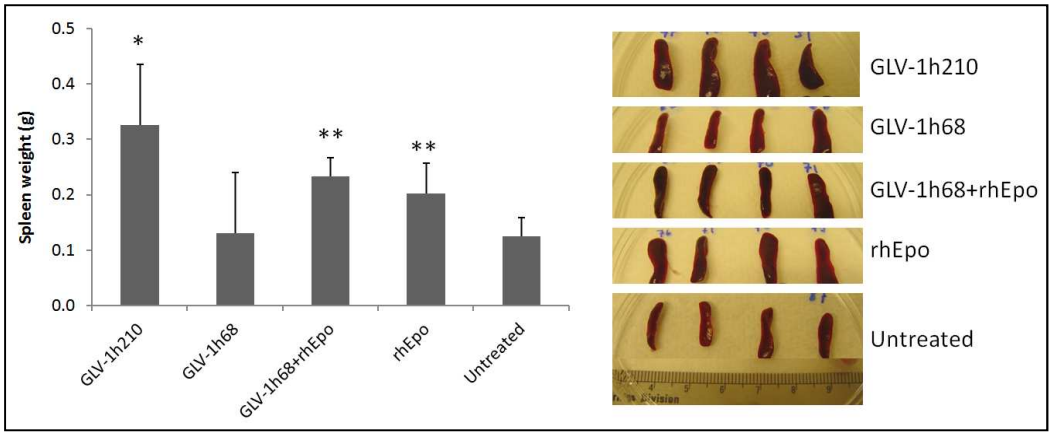

Fig. 3.14b Spleen enlargements 7 days after treatment with rhEPO, rhEPO in combination with GLV-1h68, or GLV-1h210. A549 tumor-bearing mice were injected r.o. with a dose of $2x10^6$ pfu/mouse of each virus. At the same time 500 U/kg of rhEPO (epoetin alfa) was given s.c. alone or in combination with GLV-1h68 (once a day). Shown are the averaged values of 4 animals with SD. * $P < 0.05$, ** $P < 0.01$.

3.2.4 Virus distribution in organs

To further assess possible side effects of virus treatment, blood and main organs from mice excised at 14 dpi, were used for virus titration. Table 3.1 shows the numbers of plaque forming units per gram of organs or per ml blood. Virus particles were found in lungs of all virus-treated groups ranging from 0 to 897 particles. In some virus-treated groups, virus particles were also found in spleen, heart and kidney. A few virus particles were detected in the blood of GLV-1h210- or in the brain of GLV-1h211-treated mice. No virus particles were detected in the livers of all virus-treated groups. The numbers of virus particles found in the organs were much lower than that in tumors (Fig. 3.13). For example, in GLV-1h68, it was $3.28x10^5$-fold and in GLV-1h211 was $1.24x10^6$-fold lower in the lungs compared to that in tumors at 14 dpi. There were no major differences in virus distribution in organs among all viruses. Virus titers appeared not to depend on the expression of hEPO.

Table 3.1 Virus distribution in organs after treatment with VACV strains

	GLV-1h68		GLV-1h210		GLV-1h211		GLV-1h212		GLV-1h213	
Organ	**Average**	**STDEV**	**Average**	**STDEV**	**Average**	**STDEV**	**Average**	**STDEV**	**Average**	**STDEV**
Lung	196	392	199	238	454	615	302	455	448	897
Spleen	1040	774	25	50	191	199	n.d	n.d	70	141
Heart	n.d	n.d	n.d	n.d	243	244	37	73	194	387
Kidney	26	52	388	709	n.d	n.d	103	205	24	48
Testes	45	91	NT	NT	n.d	n.d	101	202	n.d	n.d
Brain	n.d	n.d	n.d	n.d	29	58	n.d	n.d	n.d	n.d
Liver	n.d	n.d	n.d	n.d	n.d	n.d	n.d	n.d	n.d	n.d
Blood*	n.d	n.d	125	50	n.d	n.d	n.d	n.d	n.d	n.d

Organs from tumor-bearing mice treated with following VACVs; GLV-1h210, -1h211, -1h212, -1h213 and -1h68, were excised at 14 day post virus injection. Tissues were homogenized, freezed/thawed (3 times) and viral particles were determined by standard plaque assays on CV-1 cells. Data is presented as averaged values of 4 individual samples per gram tissue with SD. (*) pfu/ml.

3.2.5 Animal toxicity after treatment with different VACVs

To study viral toxicity, the net body weight and animal mortality were measured and observed every week from the day of virus injection to the day of termination (91 days post injection). When A549 tumors reached a volume of about 200 mm^3, a single dose of $2x10^6$ pfu/mouse was administered r.o. to the animals of the virus-treated groups. As shown in Fig. 3.15, EPO-VACVs exihibited higher toxicity than GLV-1h68. Especially, after GLV-1h211 treatments, 90 dpi all animals had lost weight and died, or had to be killed due to animal-care requirements. GLV-1h212 and GLV-1h213-treated animals showed 42% (3/7) survival. In another study (Fig. 3.15a, right), the combination of rhEPO and GLV-1h68 appeared to have higher toxicity than GLV-1h68 alone. GLV-1h210, in which the Epo gene was under the control of the weakest promoter (p7.5E), showed a great improvement in survival rate compared with other EPO-VACVs and was nearly similar to GLV-1h68 after 90 days with constancy in net-body weight.

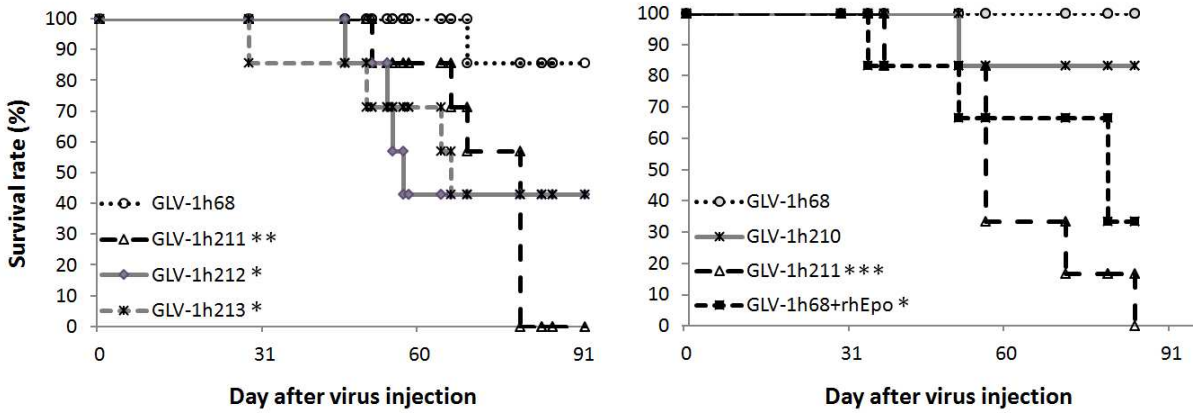

Fig. 3.15a Survival of tumor-bearing mice after treatment with VACV strains. A549 tumor-bearing mice were treated either with indicated viruses, rhEPO or rhEPO in combination with GLV-1h68. Overall survival of all study groups are shown except those for untreated control and rhEPO alone groups which had been killed before the experiment termination due to excessive tumor burden. GLV-1h210-treated animals showed the highest survival rate among all EPO-VACVs-treated groups. Statistically significant differences of animal survival rate were analyzed using log-rank test compared to GLV-1h68-treated group. * P < 0.05, ** P < 0.01, *** P < 0.001.

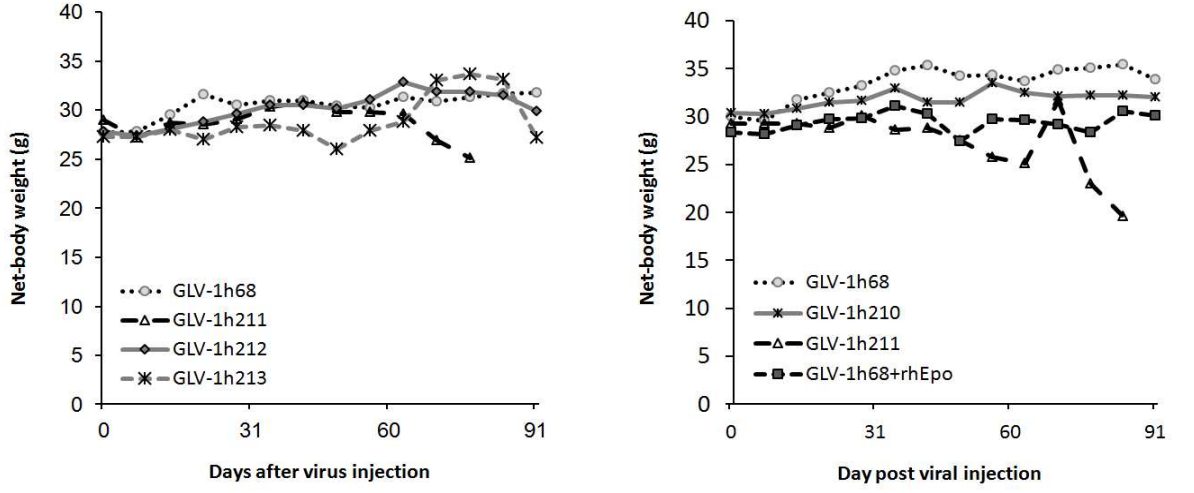

Fig. 3.15b Change in net-body weight after treatment with VACV strains. The animal's weight loss in GLV-1h211 groups from both studies was highly related to low survival rate.

3.3 Functional expression of hEPO in A549 tumor xenografts

3.3.1 Quantification of hEPO expression in tumor and serum

Here, *in vivo* models were studied in depth to analyze hEPO expression levels and its functional effects on animals. The *hEPO* gene is under the control of native vaccinia early (p7.5; GLV-1h210), synthetic early (pSE; GLV-1h211), synthetic early/late (pSEL; GLV-1h212) and synthetic late (pSEL; GLV-1h213) promoters. The strength of the promoters which determined the expression levels of this protein had been examined in culture before. To determine hEPO expression by EPO-VACV-treated mice, a sandwich ELISA method was used. Male athymic nude mice were subcutaneously implanted with $5x10^6$ A549 cells. Three weeks after tumor cell implantation, tumor-bearing mice were injected with $2x10^6$ pfu of EPO-VACVs or GLV-1h68. Tumors and blood were harvested at 14 days post virus injection. Tumors were homogenized in lysis buffer supplemented with a protease inhibitor cocktail. Sera were separated from RBCs by centrifugation at 6,000 rpm for 5 minutes after 4 hours of coagulation at room temperature. A series of test dilutions was made to assure that the sample concentrations fit in the detection range (12.48 – 800 pg/mL). In tumors, the maximum expression levels were detected in GLV-1h212-treated animals (pSEL; 7.02 μg ± 3.15), followed byGLV-1h213-treated animals (pSL; 5.8 μg ± 0.75), GLV-1h211-treated animals (pSE; 0.33 μg ± 0.11) and GLV-1h210-treated animals (p7.5; 0.14 μg ± 0.06). Those expression levels were directly correlated to cell culture observations at 12 hpi (Fig 3.6). For instance, fold differences in hEPO expression compared to GLV-1h210 were 1.82, 19.96, 18.89 (cell culture) and 2.39, 50.68, 41.91 (*in vivo*) for GLV-1h211, -1h212 and -1h213, respectively. However, it was noted that part of the hEPO expression in tumors which had been secreted outside of the tumor environment should be taken into account. In sera, the levels of hEPO detected were closely reflected by the expression strength in tumors. Highest hEPO levels were detected in GLV-1h212 (0.72 μg ± 0.32) and GLV-1h213 treatement groups (0.71 μg ± 0.18), while the order was reversed in GLV-1h210 (0.05 μg ± 0.02) and GLV-1h211 (0.03 μg ± 0.02) treatment group. This difference might derive from the variance in uptake and clearance of hEPO by individual animals. No hEPO was detected in GLV-1h68 or untreated control samples (Fig. 3.16).

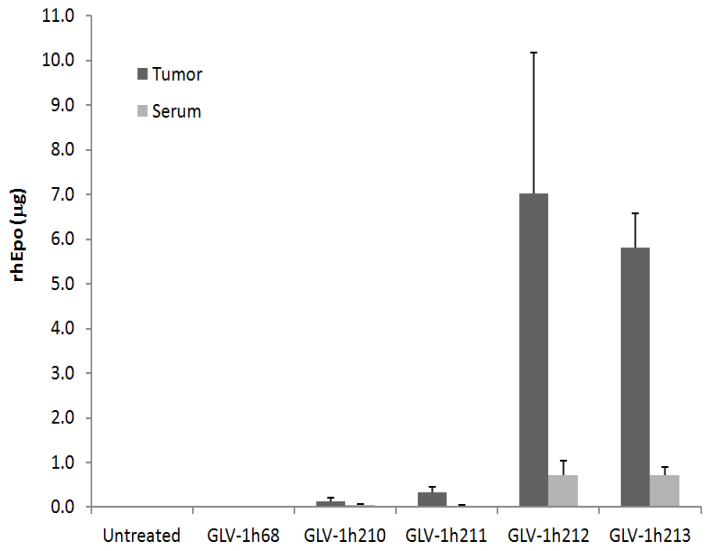

Fig. 3.16 The assessment of hEPO expression in tumors and sera of mice treated with VACV strains. A549 tumor-bearing mice were injected r.o. with a dose of $2x10^6$ pfu/mouse of each virus. Tumors and sera were harvested at 14 days post virus administration. hEPO concentrations were determined by ELISA. Averaged values per gram of tumor or per milliliter of serum plus SD are shown (n=4).

3.3.2 Detection of hEPO isoforms

hEPO has four glycosylation sites with 3 N-linked and 1 O-linked oligosaccharides, which are formed during the posttranslational modification process. These oligosaccharides play an important role in bioactivity of hEPO *in vivo* as well as for the clearance of this protein in the circulation. The differences in bioactivity of some commercially available or natural EPO appeared to be due to the differences in glycosylation, especially in the degree of sialyation [146]. The addition or deletion of sialic acid groups from oligosaccharides affects the electrical charge of the protein, resulting in differences in the isoelectric point (isoforms). The species and tissues in which EPO is produced or different ways of protein purification were reported to affect EPO isoforms. Hence, the goal of the following experiments is to determine how many hEPO isoforms can be identified in tumors after EPO-VACV treatment.

A549 tumor-bearing mice were treated with a single dose of $2x10^6$ pfu of GLV-1h212. Tumor lysates and sera were harvested at 14 dpi. Proteins were separated by isoelectric focusing on 7 cm IPG strips, pH 4-7, and then on 10% SDS-PAGE gels. As shown in Fig. 3.17, the isoform pattern of hEPO in tumors was identical to

those found in the tissue-cultured cells and in supernatants. There were about 9 – 10 isoforms detected with *pIs* ranging from 4.2 to 6.4, with a majority of acidic isoforms. In serum, however, only 6, exclusively acidic, isoforms were detected (pI: 4.2 – 4.8). Detected isoforms shared similar *pIs* to rhEPO (Epoetin alfa), however they appeared thinner in terms of horizontal shapes. Interestingly, there was no difference of isoform pattern between supernatant and cells, but a clear difference between tumor and serum. The differences in isoform patterns between tumor and serum might indicate biological modification processes of intra- or extracellular hEPO or of the different half-life of those isoforms during circulation.

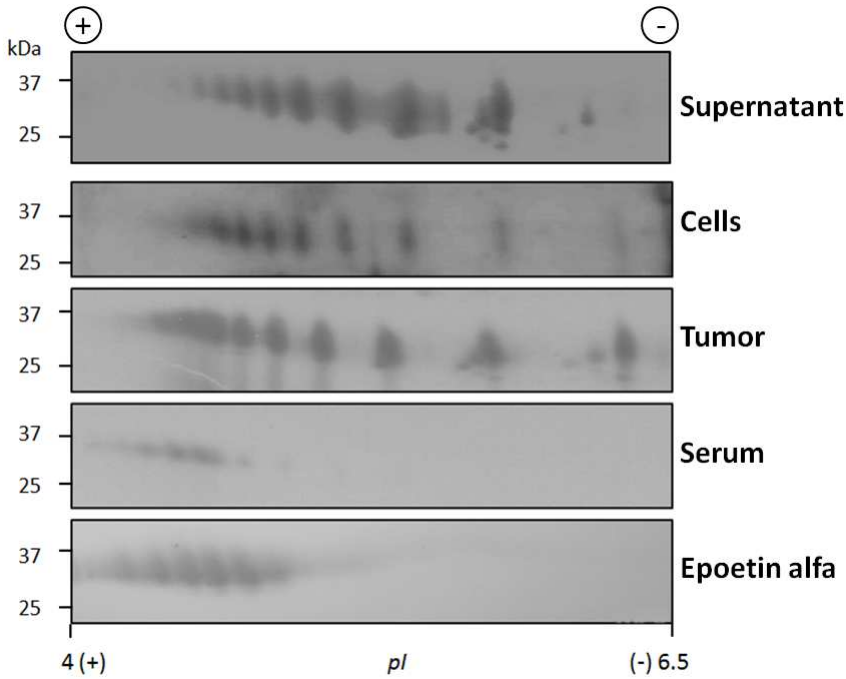

Fig. 3.17 hEPO isoforms of GLV-1h212 were detected in tumor and serum at 14 dpi and compared with isoforms isolated in cells, supernatant and Epoetin alfa. 100 μg supernatant (from virus infected A549 cells at 48 hpi, MOI=0.1), 100 μg cell lysate (from virus infected A549 cells at 48 hpi, MOI=0.1), 100 μg tumor lysate (14 dpi), 150 μg serum, and 200 U Epoetin alfa, were separated on 2-D gels and then detected by Western blot using polyclonal anti-hEPO antibodies.

3.3.3 Effects of EPO-VACV treatment on cell populations of the blood

As shown in section 3.1.2, functional hEPO expression after EPO-VACV treatment was able to increase the Hb levels of treated mice. To further assess how this

protein affects other blood cell populations such as white blood cells, platelets as well as related RBC parameters, blood samples were evaluated at 14 dpi with GLV-1h210, GLV-1h68 and untreated control mice.

The Fig. 3.18a shows an obvious increase in the number of RBCs after GLV-1h210 treatment. The lower-dark portion of RBCs was well separated from the upper-clear portion of serum (A). The levels of Hb in GLV-1h210 treatment groups were significantly higher than in GLV-1h68-treated or untreated controls ($p < 0.001$) (C). Changes in Hb levels were reflected by the increase in the number of RBCs in GLV-1h210-treated ($10.99x10^{12} \pm 0.67x10^{12}$ cells/L) versus GLV-1h68-treated ($8.79x10^{12} \pm 0.96x10^{12}$ cells/L, $p < 0.01$) and untreated control ($9.05x10^{12} \pm 0.03x10^{12}$ cells/L, $p < 0.01$) (B). Furthermore, the increase of Hb levels by hEPO was basically a result of the increase in RBC numbers but not due to the RBC size (D) or the number of Hb contained in RBC (E).

In parallel, the white blood cell (WBC) population was also quantified (Fig. 3.8b, left). Totally, 10.53 ± 2.58 (untreated control), 8.66 ± 3.17 (GLV-1h210) and 7.34 ± 0.91 (GLV-1h68) (x 10^9 cells/L) WBCs in each group at 14 dpi were counted. In detail, lymphocytes (LYM) accounted for 56 - 70% of total WBCs with values of 7.6 ± 2.3, 5.17 ± 2.18, and 5.01 ± 0.36 (x 10^9 cells/L) from untreated control, GLV-1h210 and GLV-1h68 groups, respectively. A similar order for neutrophils (NEU) (2.48 ± 0.75, 3.12 ± 0.68, and 2.18 ± 0.56 (x 10^9 cells/L)) accounted for 24 - 37%, and monocytes (MON) (0.44 ± 0.11, 0.46 ± 0.39, and 0.15 ± 0.14 (x 10^9 cells/L)) accounted for 2 - 5% of total WBCs. The number of LYM was found higher in untreated control than in GLV-1h68 or GLV-1h210-treated groups. In terms of NEU and MON numbers, the highest values were found in GLV-1h210-treated animals. Those differences, however, were not statistically significant. Statistically significant differences were only found between GLV-1h68 and untreated control in the number of MON. The data also suggests that there are high variances in white blood cell population from mouse to mouse.

Furthermore, number of platelets (PLT: Fig. 3.18b, right) or mean platelet size (date not shown) were not affected by GLV-1h210 or GLV-1h68 administration.

These findings suggested that hEPO specifically promotes RBC formation. Nevertheless, hEPO did not affect other blood cell populations such as NEUs,

MONs, LEUs, PLTs as well as ratio, size and concentration of hemoglobin contained in RBCs.

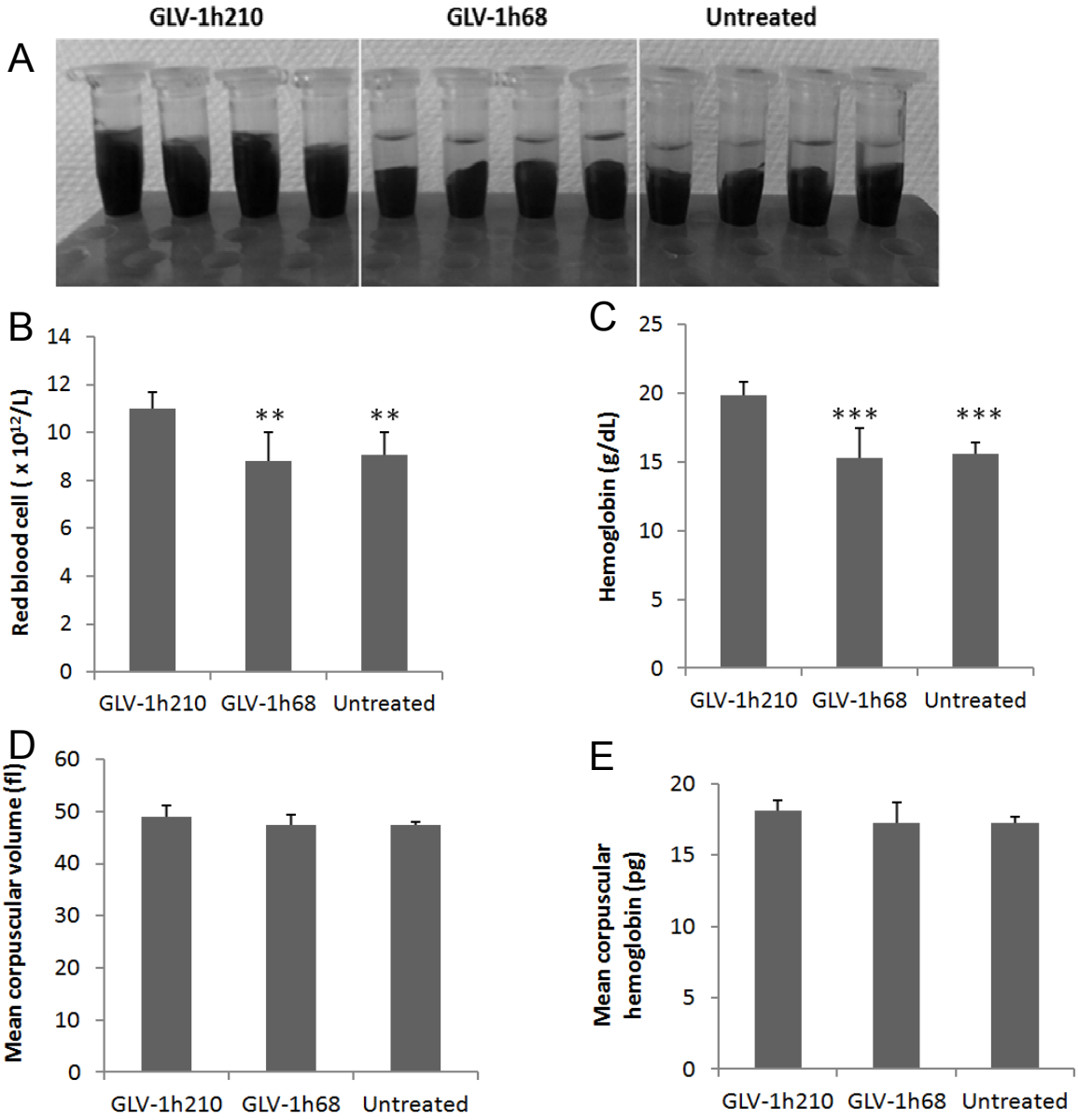

Fig. 3.18a The increase in the number of RBCs after GLV-1h210 administration. 4 male athymic nude mice with a tumor volume of about 200 mm^3 were injected r.o. with a dose of $2x10^6$ pfu of GLV-1h210, GLV-1h68. Fourteen days after the virus injection, mice were euthanasia by CO_2 inhalation and 1 mL of blood from each mouse was drawn by cardiac puncture. Samples were kept at 4°C overnight and centrifuged at 6,000 rpm for 5 minutes to separate sera and RBCs (A). Right after euthanasia, 100 μl of whole blood was immediately used for a complete blood count (CBC). Averaged values with SD of RBCs (B), hemoglobin (C), mean corpuscular volume (D) and mean corpuscular hemoglobin (E) are presented. Significant differences were analyzed for GLV-1h210- and GLV-1h68-treated animals or untreated controls. * $P < 0.01$, ** $P < 0.001$.

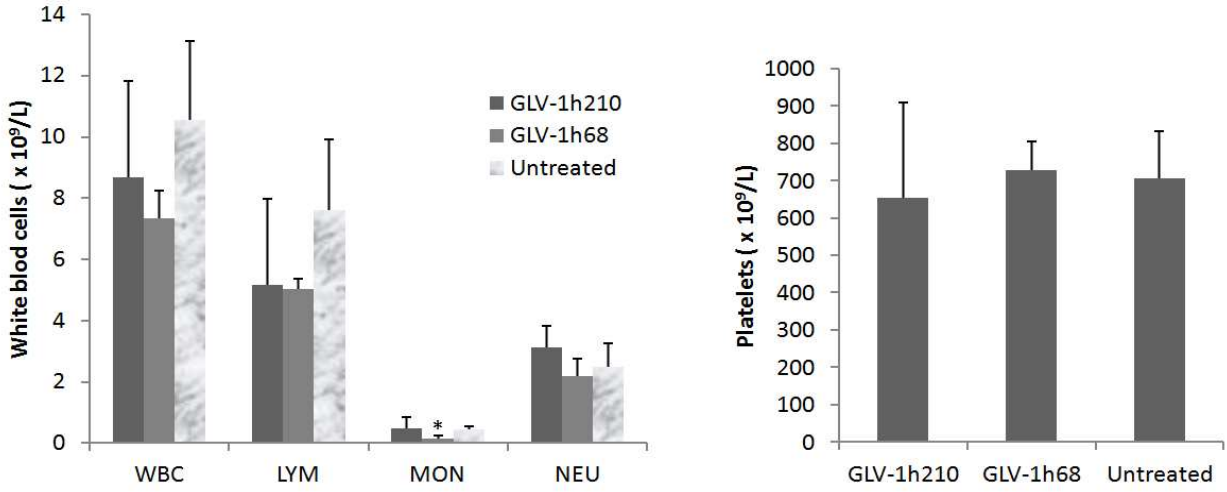

Fig. 3.18b Comparison of the number of white blood cells and platelets in the peripheral blood after treatment with GLV-1h210 and GLV-1h68 at 14 dpi. (left) Avarage white blood cell population: lymphocytes, monocytes and neutrophills. (right) The average numbers of platelets. Significant differences were analyzed between untreated controls and GLV-1h210 or GLV-1h68. * $P < 0.05$.

3.3.4 Assessment of hemoglobin levels during the course of treatment

In order to see how Hb levels (g/dL) change during tumor therapy, time course measurements of Hb levels were performed. In GLV-1h210-treated animals, Hb increased at day 14 with mean value of 20.74 ± 1.33 (versus with 14.32 ± 0.36 at day 0) and reached a maximum at day 40 (22.89 ± 1.08). After this time point, the Hb levels slightly decreased due to the disappearance of virus following complete tumor regression. In these animals, Hb levels returned to baseline (14-16). However, complete regression was not observed in all animals. Hb slightly decreased from 14.97 ± 0.39 and 14.80 ± 0.32 (day 0) to 13.31 ± 0.88 and 13.03 ± 1.04 (day 60) in GLV-1h68-treated or untreated controls, respectively. But Hb was gradually recovered to baseline in GLV-1h68-treated animals at 90 dpi. Mice in untreated control were sacrificed because of tumor burden at 60 dpi (Fig. 3.19, left). In addition, compared to the levels of Hb before treatment, treatment with EPO-VACVs or rhEPO increased the levels of Hb while untreated mice or mice treated with GLV-1h68 showed a decrease in the levels of Hb (Fig. 3.19, right), indicating that treatment with EPO-VACV or rhEPO alleviated cancer-related anemia.

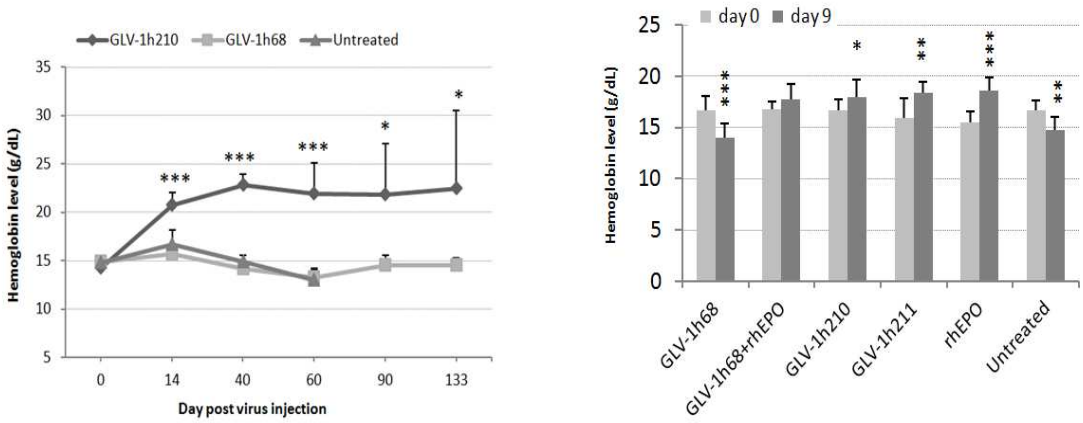

Fig. 3.19 The time course assessment of Hb levels after treatment VACVs. (left) A549 tumor-bearing mice were injected r.o. with with $2x10^6$ pfu of GLV-1h210, GLV-1h68. At day 0, 14, 40, 60, 90 and 133 post virus injection, RBCs of 5 – 8 mice were used for Hb examination. Significant differences were performed between GLV-1h68 and GLV-1h210 groups. (right) Concomitance with virus treatment, 500 U/kg of rhEPO was injected s.c. for 9 consecutive days (day 1-9 post virus injection) into tumor-bearing mice alone or in combination with GLV-1h68. Hemoglobin levels were measured at day 0 and day 9 post virus injection (n=7-10). Averaged values with SD are plotted. Asterisks indicate significant differences, * $P < 0.05$, ** $P < 0.01$, *** $P < 0.001$.

3.3.5 Confirmation of virus-mediated hEPO expression in tumor xenografts

To confirm GLV-1h210-specific expression of hEPO in tumor xenogafts, xenograft tumors were examined by optical and histological imaging. Tumors from mice treated with GLV-1h68, GLV-1h210 or untreated controls were harvested at 28 dpi. Before excision, tumors were optically imaged with for GFP or *Renilla* luciferase expression. Signals were detected in both virus-treated groups (Fig. 3.20). 5-μm- thick paraffin sections were stained for VACV, hEPO and H&E. In tumors from GLV-h210-treated animals, the areas with positive staining (brown) for VACV were also positive for hEPO expression, indicating specific virus replication and expression of hEPO. Meanwhile, VACV-positive tumors were negative for hEPO-staining in GLV-1h68-treated tumors. The specificity of the antibodies was confirmed in untreated control; no positive VACV or hEPO signal was detected. Moreover, most infected areas by either GLV-1h68 or GLV-1h210 at 28 dpi were positive for massive death of tumor

cells, as seen in H&E staining (red). On the other hand, non-virus treatment tumor (control) generally showed viable cancer cells (blue) (Fig. 3.20).

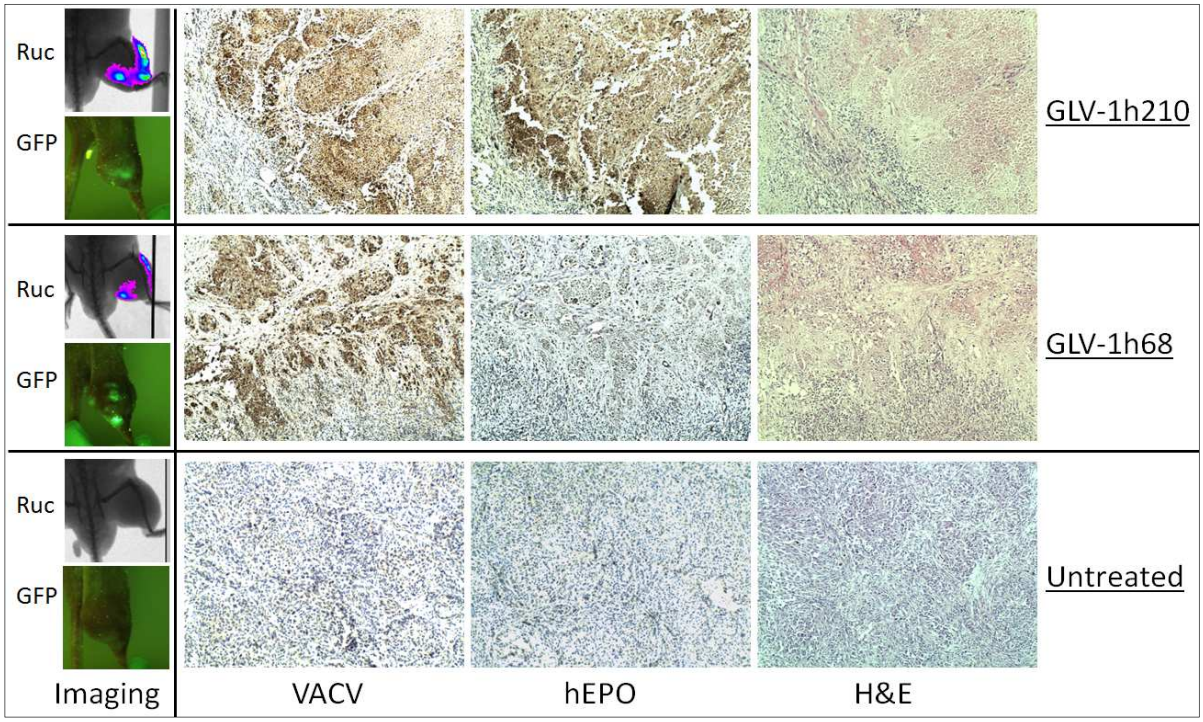

Fig. 3.20 Histological detection of virus-specific hEPO expression in tumor xenografts. Tumor-bearing mice were treated with single dose of $2x10^6$ pfu of GLV-1h210 or GLV-1h68. At 28 dpi, tumors were excised and processed with formalin fixed, paraffin embedded sectioning. Three adjacent 5-μm-sections were stained either with anti-VACV, anti-hEPO antibodies or H&E staining. Hematocylin counterstaining was used for background separation. Pictures were captured at 100x magnification. Left: *Renilla*-luciferase (Ruc) and green fluorescent protein (GFP) expression by virus-infected tumors, which were imaged before tumors were excised.

3.4 Effects of EPO-VACVs treatment on micro tumor environment

3.4.1 Effects of EPO-VACVs treatment on the expression of immune-related antigens in tumors

GLV-1h68 has successfully shown its abilities to inhibit or destroy various types of cancer in cell cultures and tumor xenografts. Along with tumor inhibition or regression, treatment with GLV-1h68 can trigger immune infiltration into the infected tumors [64-65, 67]. Local immune filtration in those tumors was suggested to have

synergistic effects on tumor regression. In addition, hEPO has also been reported as an immune modulator in several preclinical models [126-127]. For these reasons, changes of chemokine and cytokine production as well as the infiltration of different immune cell populations into virus-infected tumors after EPO-VACVs treatment were evaluated and compared with GLV-1h68 treatment.

A549 tumor-bearing mice were treated with $2x10^6$ pfu of GLV-1h211, GLV-1h212 or GLV-1h68. Tumors were harvested at 14 dpi, and then homogenized using magnetic beads in lysis buffer supplemented with protease inhibitor cocktail. Equal amounts of protein from 4 tumors in each group was pooled in 1 representative sample and examined for 58 immune-related antigens. Shown in Table 3.2 are the differences of GLV-1h211 and GLV-1h210 over GLV-1h68 treatment. Twenty-seven out of 58 antigens were differently expressed in GLV-1h211-treated animals. There were 25 antigens up-regulated (ratio > 2) and 2 down-regulated (ratio < 0.5). Eight antigens were up-regulated in GLV-1h210-treated animals and none down-regulated. Interestingly, there was a constantly higher number of immune-related antigens upregulated in GLV-1h211-treated animals compared to the GLV-1h210 treatment group. Compared to GLV-1h68 treatment, IL-11 expression was upregulated only in the GLV-1h210 treatment group, while IL-6 was upregulated higher in GLV-1h210-treated animals (4.05-fold) than in GLV-1h211-treated animals (2.48-fold). Many of the up-regulated chemokines and cytokines, such as MCP-1, IL-1 alpha, IL-2, IL-3, IL-6, IL-7, IL-10, IL-11, IL-18, IFN-gamma, MIP-1, MIP-2, MIP-3, M-CSF, are known to activate monocytes, lymphocytes, neutrophils, and macrophages to trigger inflammatory processes in injury tissues. In parallel, the virus titers (Fig. 3.13, right) and amounts of hEPO expression (Fig. 3.16) in these tumors were also quantified. The results revealed that in concomitance with enhanced immune-related antigen infiltrations, enhanced virus titers and higher hEPO expression were also observed in GLV-1h211-treated animals compared to GLV-1h210-treated animals.

Table 3.2: Comparison of mouse immune-related antigen profiling after treated with VACV strains.

Antigen	**Fold change** (compared to GLV-1h68)		**Classification**
	1h210/1h68	**1h211/**1h68	
Monocyte Chemotactic Protein 1 (MCP-1)	**4.05**	**5.93**	Proinflammatory cytokine
Interleukin-18 (IL-18)	**4.11**	**5.57**	Proinflammatory cytokine
CD40 (CD40)	**3.16**	**5.28**	Proinflammatory cytokine
Eotaxin	**3.35**	**4.60**	Inflammatory chemokine
Interleukin-3 (IL-3)	**2.07**	**4.12**	Proinflammatory cytokine
Granulocyte Chemotactic Protein-2 Mouse (GCP-2 Mouse)	**2.62**	**3.18**	CXC chemokine
Macrophage Inflammatory Protein-2 (MIP-2)	1.82	**3.01**	Proinflammatory cytokine
Tissue Inhibitor of Metalloproteinases 1 Mouse (TIMP-1 Mouse)	1.93	**2.62**	Tissue inhibitor
Macrophage Colony-Stimulating Factor-1 (M-CSF-1)	1.53	**2.62**	Proinflammatory cytokine
Matrix Metalloproteinase-9 (MMP-9)	1.54	**2.58**	Proinflammatory cytokine
Interleukin-7 (IL-7)	1.69	**2.57**	Proinflammatory cytokine
Interleukin-6 (IL-6)	**4.05**	**2.48**	Proinflammatory cytokine
Interferon gamma (IFN-gamma)	1.26	**2.48**	Proinflammatory cytokine
Interleukin-10 (IL-10)	1.36	**2.46**	Anti-inflammatory cytokine
Macrophage Inflammatory Protein-1 beta (MIP-1 beta)	1.51	**2.43**	Proinflammatory cytokine
Interferon gamma Induced Protein 10 (IP-10)	1.95	**2.35**	IFN-gamma induced CXC chemokine
Interleukin-2 (IL-2)	1.22	**2.32**	Anti-inflammatory cytokine
Lymphotactin	1.34	**2.30**	Proinflammatory chemokine
Thrombopoietin (TPO)	0.93	**2.24**	Megakaryocyte growth factor
Macrophage Inflammatory Protein-1 alpha (MIP-1 alpha)	1.07	**2.17**	Proinflammatory chemokine
Macrophage Inflammatory Protein-3 beta (MIP-3 beta)	1.41	**2.17**	Proinflammatory cytokine
Interleukin-1 alpha (IL-1 alpha)	1.39	**2.15**	Proinflammatory cytokine

Interleukin-12 Subunit p70 (IL-12p70)	1.54	**2.07**	Proinflammatory cytokine
von Willebrand factor (vWF)	1.53	**2.01**	Blood coagulation protein
Interleukin-11 (IL-11)	**2.08**	1.50	Pleiotropic cytokine
Tissue Factor (TF)	0.60	*0.47*	Cytokine receptor
Fibrinogen	0.59	*0.37*	Coagulation Factor

Columns show fold differences in mouse cytokines and chemokines in virus-infiltrated tumorsafter 14 dpi of GLV-1h211- and GLV-1h210 injection compared to GLV-1h68-injected animals. Bold numbers indicate up-regulated antigens. Italic numbers indicate down-regulated antigens.

3.4.2 Assessment of immune cell infiltration in tumors after treatment with VACVs

To answer the question which factor is critical for immune infiltration into tumors (functional hEPO or virus titer; section 3.4.1), a better control for GLV-1h210 is needed. It should have the same virus replication efficiency as GLV-1h210 but no hEPO bioactivity function. GLV-1h68 is the parental strain for all EPO-VACVs and also served as a control. However, a minor difference in its virus genome, *lacZ* (pSEL) in GLV-1h68 compared with *hEPO* (p7.5) in GLV-1h210 could be a reason for the difference in virus replication [147]. For that purpose, a new control for GLV-1h210 was generated which contains an identical genomic sequence to GLV-1h210 except for 1 amino acid change in the hEPO protein sequence. Arginine at position 103 was replaced by alanine (R103R) and resulted in the new recombinant vaccinia virus strain GLV-1h209. This replacement makes hEPO in GLV-1h209 completely lose its natural bioactivity (erythropoiesis) (Fig 3.21E), while this protein is still expressed and secreted (Fig. 3.21C). The replication of GLV-1h209 and GLV-1h210 was identical in cell cultures (Fig. 3.21A) and no much differences in tumor xenografts (Fig. 3.21D). Tumor regression after virus treatments was not found to be significantly different between GLV-1h209 and GLV-1h68, but both strains showed impaired regression compared to GLV-1h210 (Fig. 3.21A). Taking together, the results indicated that GLV-1h209 can serve as a “perfect control” for GLV-1h210 to eliminate replication-dependent effects.

Virus replication in tumors was normalized to pfu/g tumor (Fig. 3.21D), and tumor sections were used to stain for MHC-II antigen (Fig. 3.22), a common cluster of differentiation marker expressed on the cell surfaces of monocytes, macrophages, dendritic cells and B cells. Interestingly, both tumors treated with GLV-1h210 and GLV-1h209 were found highly positive for MHC-II, while lower or very dim signals were observed in GLV-1h68- or untreated controls, respectively. No significant difference in MHC-II fluorescence intensity was found between GLV-1h210 and GLV-1h209 treatment groups (p = 0.43). In addition, tumor-protein samples from GLV-1h210- and GLV-1h209-treated animals were analyzed for immune-related antigen profiling. However, no differences in 58 tested antigens were found (data not shown). Those findings suggest that immune infiltration following EPO-VACVs administration was mostly influenced by the number of virus particles inside the tumors, but not hEPO expression.

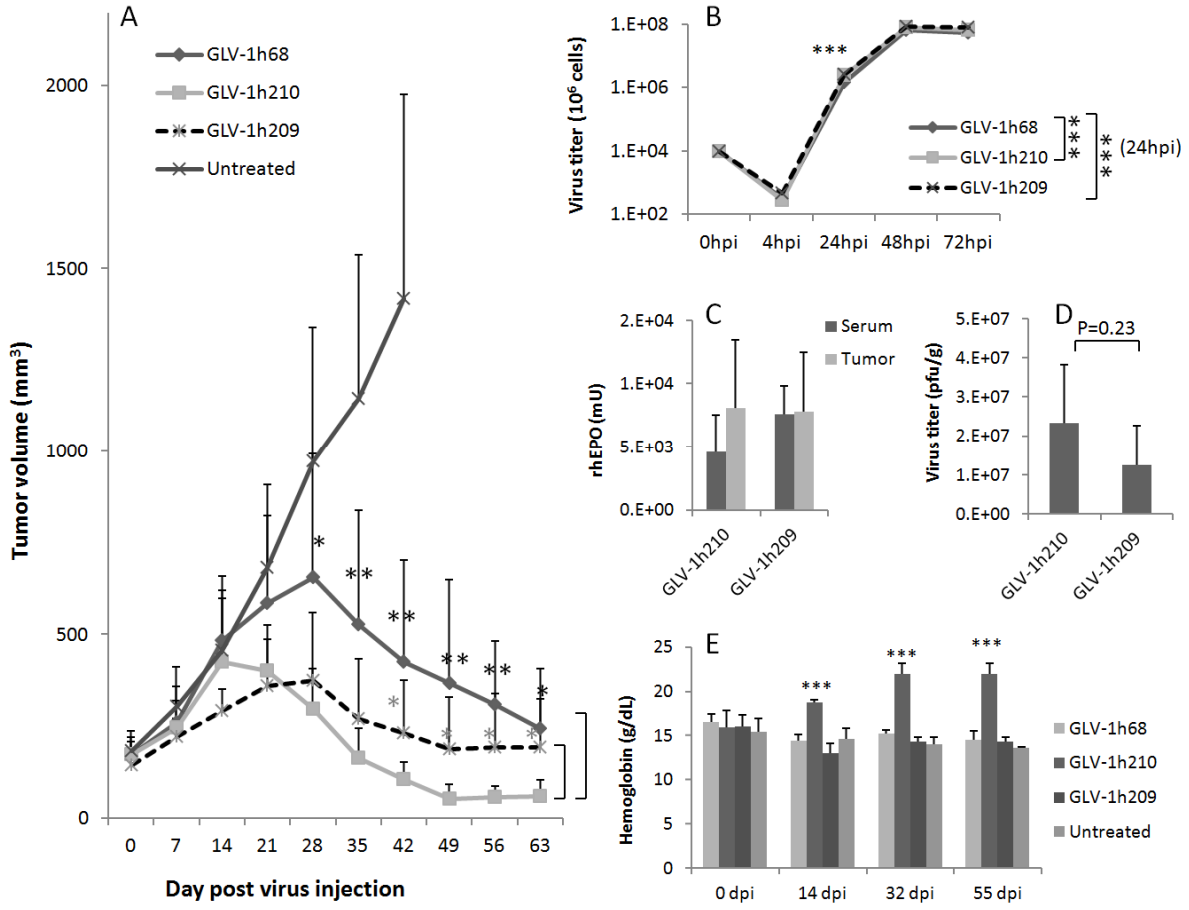

Fig. 3.21 Characterization of the EPO-VACV mutant (GLV-1h209) in culture and *in vivo*. (A) Tumor growth curves of A549 tumor-bearing mice after treatment with a single dose of

$2x10^6$ pfu/mouse of GLV-1h68, -1h210, -1h209 or untreated controls. Significant difference was highlighted when comparing oncolytic efficacy of GLV-1h210 and other viruses (n=8). The GLV-1h209 strain seemed to have a better effect on tumor inhibition compared to GLV-1h68 at early time points, however, they were similar at the end of the study and no significant differences between them was found at any points. (B) Virus replication in A549 cell culture at an MOI of 0.01 showed an identical replication of GLV-1h210 and GLV-1h209. Both viruses replicated better than GLV-1h68 at 24 hpi but similar at 48 and 72 hpi. Expression of hEPO (C) and virus replication (D) was found similar in GLV-1h209-treated and GLV-1h210-treated animals at 14 dpi (n=4). (E) Time point assessment of Hb levels in each treatment group (n=4-8). Significant differences were found between the GLV-1h210 treatment group and other groups ($p < 0.001$), whereas no differences among GLV-1h209, GL-1h68 and untreated control were observed.

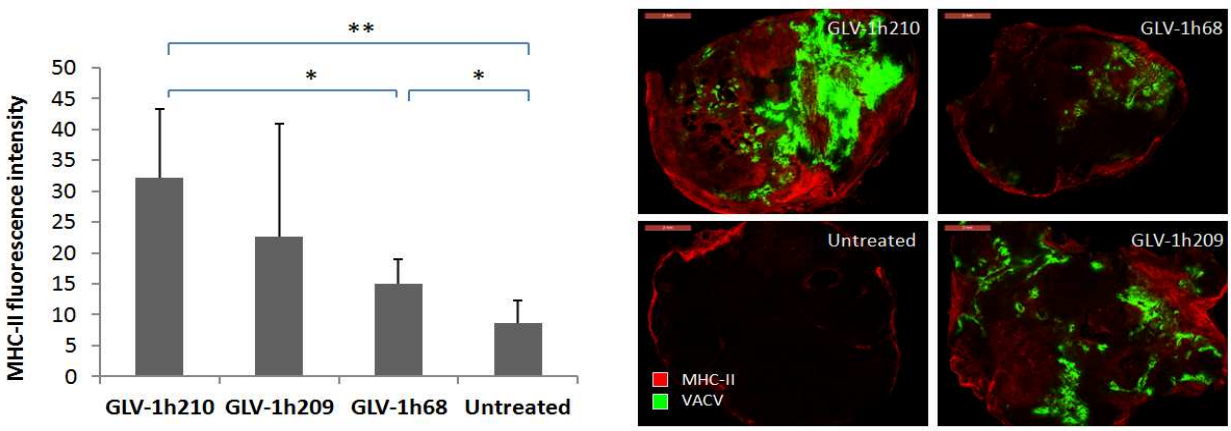

Fig. 3.22 Immune cell infiltraton in virus-infected tumors. Athymic nude mice bearing A549 tumors were injected with $5x10^6$ pfu of GLV-1h210, GLV-1h209 and GLV-1h68. At 14 dpi, tumors were excised and stained with anti-MHC-II antibodies. (left) Averaged MHC-II fluorescence intensity of n=5 tumors for each group is plotted with SDs (1 section for 1 tumor). (right) A representative MHC-II labeled section in each group overlaid with GFP as an indication for VACV replication with scale bars of 2 mm.

3.4.3 Assessment of tumor oxygenation after treatment with VACVs

Tumor hypoxia is an important factor associated with tumor prognosis and resistance to radio- or chemotherapies [148]. In culture, hypoxia affected virus replication and oncolytic efficiency. To evaluate how hEPO expressed by VACV is related to tumor oxygenation, tumor-bearing mice after 14 days of treatment with either GLV-1h210,

GLV-1h209, GLV-1h68 or no treatment were strained with hyoxic probes and their fluorescence intensity was measured. Unexpectedly, the hypoxic intensity in GLV-1h210-treated animals was higher than in other groups, while no difference was spotted among GLV-1h209, GLV-1h68 treatment groups and untreated controls. (Fig. 3.23)

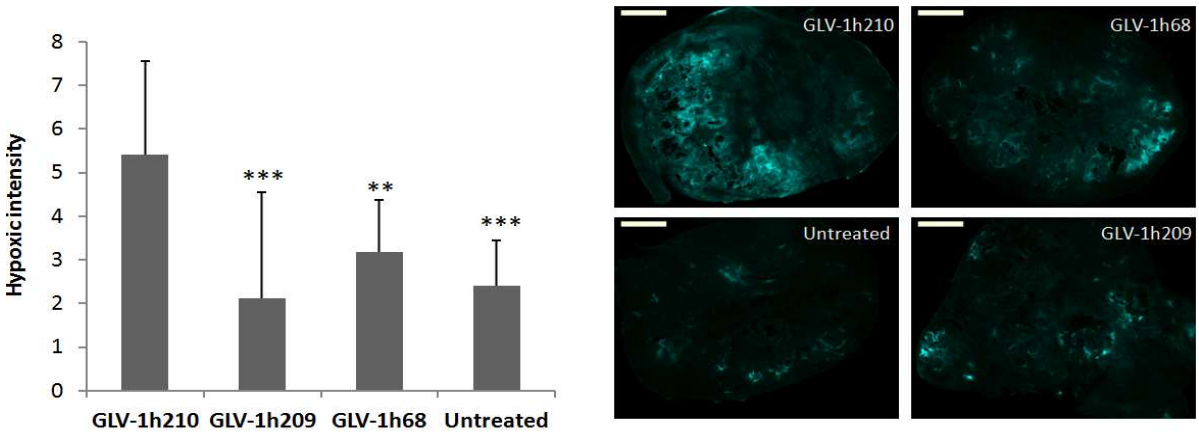

Fig. 3.23 Differences in tumor hypoxia after treatment with VACV strains. Athymic nude mice bearing A549 tumors were injected with $5x10^6$ pfu of GLV-1h210, GLV-1h209 and GLV-1h68. At 14 dpi, 2 hours before tumor excision, 60 mg/kg of pimonidazole was intraperitoneally injected (i.p.) into all mice. This chemical then formed adducts with thiol-containing tissue proteins under hypoxic condition (pO_2 < 10 mm Hg). Tumors were fixed with formaldehyde and processed with agarose-embedded sectioning. 100-μm-sections were cut and stained with mouse IgG1 monoclonal antibodies conjugated to Dylight-549 fluorophore (blue) which binds to pimonidazole adducts. (left) Fluorescence intensity indicating hypoxic intensity of virus-treated and untreated tumors was measured using ImageJ from 15 different sections in each group (3 sections for 1 tumor). The asterisks indicate significant differences between GLV-1h210 and other experimental groups. (right) a representative staining section for each group was shown with 2 mm scale bars. ** P < 0.01, *** P < 0.001.

3.4.4 Assessment of tumor vascularization after treatment with VACVs

Induced tumor blood vessel dilatation andpermeability following VACV infection has been reported recently [149]. Moreover, hEPO's involvement in activation of endothelial cells has also been addressed [150]. To investigate the dual effects of

VACV-mediated hEPO expression on tumor vascularization, we measured tumor blood vessel diameter, density as well as fluorescent intensity of A549 tumors infected with GLV-1h210, GLV-1h209, GLV-1h68 and untreated control at 14 dpi. Results (Fig. 3.24) revealed that blood vessel intensity was the highest in the GLV-1h210 treatment group and decreased in the order of GLV-1h209, GLV-1h68 treatment group and untreated controls (Fig. 3.24A). Interestingly, the strength of vessel intensity seemed to be caused byan increase in vessel diameter (Fig. 3.24B). Indeed, GLV-1h210-infected tumors showed significantly higher blood vessel diameter compared to all other groups ($p < 0.001$). The blood vessel diameters of GLV-1h209- and GLV-1h68-infected tumors were also higher than in untreated controls ($p < 0.001$). Meanwhile, blood vessel density was unchanged in all tested groups (Fig. 3.24C). Those findings suggested that functional hEPO could play a synergistic role with vaccinia virus in dilatation of virus-infected tumor vascularization, but not promoting the formation of new tumor blood vessels.

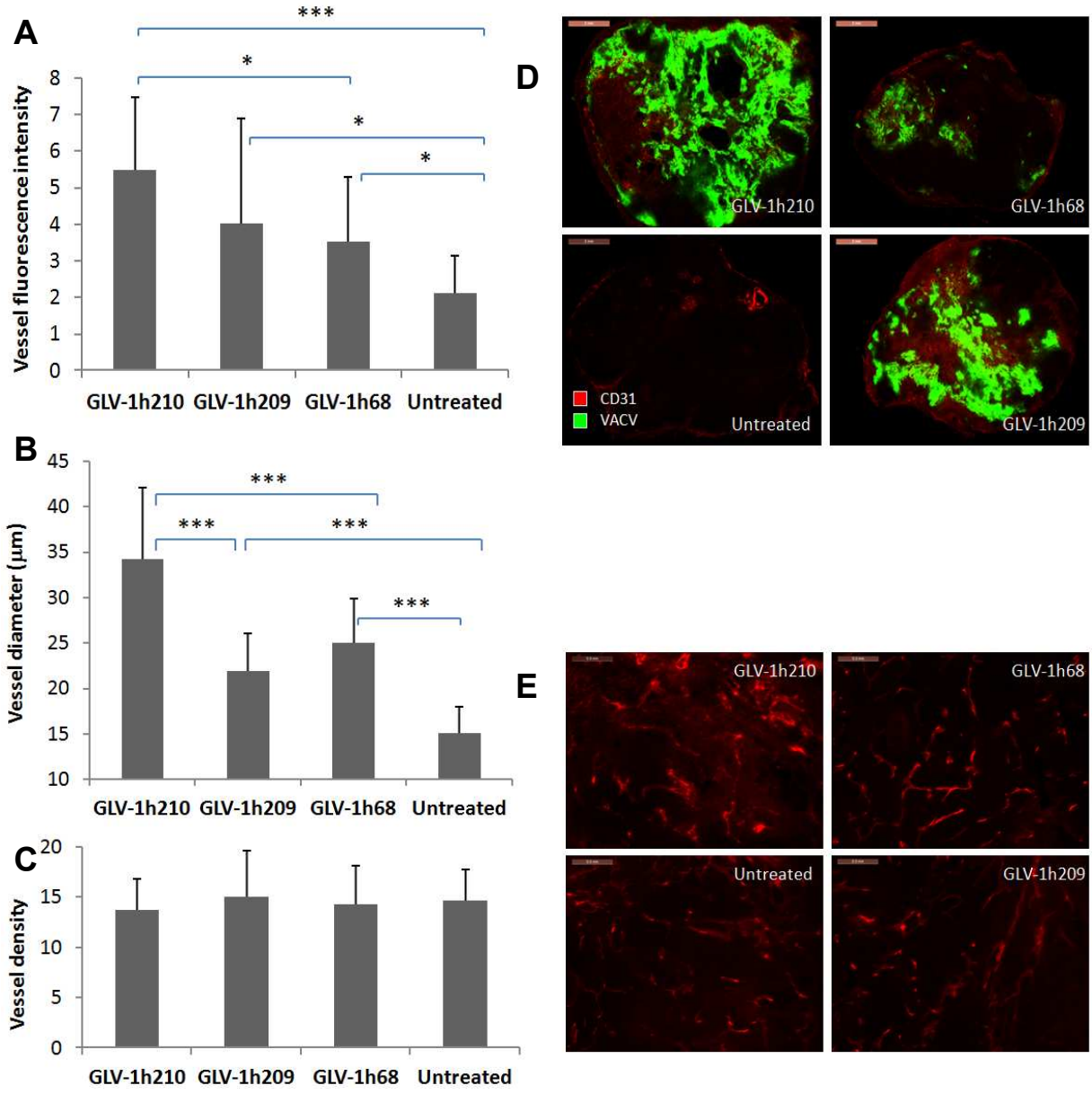

Fig. 3.24 The effect of hEPO-expressing viruses on tumor blood vessels. Athymic nude mice bearing A549 tumors were injected with $5x10^6$ pfu of GLV-1h210, GLV-1h209 and GLV-1h68. Tumors were excised at 14 dpi and blood vessels were stained with anti-CD31 antibodies (red). (A) Vessel fluorescence intensity, (B) vessel diameter, and (C) vessel density in the virus treated groups and untreated controls were measured and compared using ImageJ. Asterisks indicate significant difference between groups. Vessel intensity was measured on 15 different sections (3 sections for 1 tumor), vessel diameter and vessel density were measured on 30 different fields of 1.91 x 1.43 mm (2 fields for 1 section) in each group. Representative CD31 stainings of whole sections for blood intensity measurement were overlaid with GFP (VACV) with scale bars of 2 mm (D) and representative CD31-staining fields for blood diameter and blood density counting with scale bars of 0.3 mm (E) are shown. *** $P < 0.001$.

4. DISCUSSION

About 7.6 million people are estimated to die of cancer worldwide in 2012, and it will be the cause of an estimated 12 million deaths in 2030 [2, 151]. The current conventional therapies are facing several difficulties such as high toxicity or poor therapeutic efficacy once the cancer has become metastatic. The overall survival rate in patients with lung cancer is only 15% after 5 years, and 11% of deaths in the world population under the age of seventy has been estimated to result from cancer [1].

In attempting to enhance therapeutic efficacy, oncolytic viral therapies are emerging as promising treatment options which have been under intensive investigation recently. Many clinical trials in various types of cancer are being carried out with encouraging news that the first oncolytic agent has been approved in China (andenovirus H101). GLV-1h68 is a genetically engineered, attenuated vaccinia virus (VACV) derived from the LIVP strain [35] with the advantages of the inherent safety profile, natural tumor tropism, and multi-large transgene carrying capacity, making it suitable for development as an oncolytic agent. In preclinical models, GLV-1h68 has been successfully used to treat many types of cancer such as human breast carcinoma [35], pleural mesothelinoma [152], pancreatic carcinoma [65], squamous carcinoma [68], melanoma lymph node metastasis [153], human primary prostate carcinoma and metastasis [66]. Recently, the first phase I clinical trial with GL-ONC1 (the clinical version of GLV-1h68) in patients with advanced solid tumors was completed, demonstrating initial evidence of antitumor activity without toxicity concerns [154].

Cancer-related anemia occurs in about 50% of the people with solid cancers at the time of diagnosis [99]. The incidence is higher in groups receiving chemotherapy, with 1/3 developing anemia after 3 cycles of chemotherapy [155]. More than 60% cancer patients needed blood transfusions during or after cancer treatment [156]. Anemia affects normal mental and physical functional capacity with common side effects like fatigue, headache, or depression [157]. Moreover, anemia is associated with weaker response to chemotherapy and radiotherapy or poorer disease

prognosis [110, 158]. rhEPO has been approved for the treatment of cancer-related anemia since 1993. Enormous evidence has shown the benefits of hEPO in correcting anemia, and subsequently improving the health-related quality of life [99, 106, 155] or/and enhancing radio-, and chemo-therapy [107, 111]. Several recent clinical trials suggested that hEPO may promote tumor growth which raises questions concerning the safety of using rhEPO for cancer treatment [133-134]. In some models, rhEPO appeared to have anti- apoptotic effects, induce angiogenesis and promote tumor growth while in others, such effects were not indicated. The controversy is due to the lack of appropriate experimental designs to clarify the direct functional effects of rhEPO in tumor models.

Under this circumstance, this study was carried out to characterize the oncolytic capacities of four different EPO-VACV constructs in lung cancer cells (A549) in culture and in tumor xenografts. Concomitantly, the effects of locally expressed hEPO in tumors on virus replication, host immune infiltration, tumor vascularization and tumor growth were also evaluated.

4.1 The different expression levels of hEPO with four EPO-VACV constructs do not negatively affect oncolytic capacities of the viruses in cell culture.

In this study, the successful construction of four EPO-VACVs has been shown through either with Western blot or fluorescent microscopy. The replacement of the *lacZ* expression cassette with *hEPO* in the *J2R* locus was clearly confirmed by Western blot. The *hEPO* insertion did not affect the expression and fluorescent protein function of the marker genes (*ruc-gfp* and *gusA*) when compared to parental virus GLV-1h68. Moreover, the levels of *hEPO* transcription and translation were directly related to the strength of promoters used to drive *hEPO* expression in the EPO-VACVs once the promoters were fully activated (after 6 hpi). Yet at 6 hpi, pSL and pSEL did not seem to follow this rule. The transcriptional levels from pSL were higher than that from pSEL, but the order was reversed of the translational levels. Nevertheless, the parallel correlation between transcription and translation was not always observed [159], especially in mammalian cells where a mRNA has to pass through the complex systems of post-transcriptional and translational modification for

protein translation. VACV promoters are widely usable in mammalian cells, which allow the expression levels of transgenes to be controlled with time dependence [21]. Therefore, they are suitable for different purposes which require a low (reducing toxicity) or high protein expression [160]. In accordance with the results obtained by Baldick *et al.* [21], we did not detect any actions (transcription and translation) of late promoters (pSL) at 2 hpi while transcription driven by early (p7.5 and pSE) and early/late (pSEL) promoters had already started. Furthermore, protein expression was found to increase in the order of p7.5, pSE, pSL and pSEL with the ratio of about 1:2:20:20, respectively, in A549 cells at 24 hpi. hEPO expression levels from EPO-VACVs were in a similar order as the beta-galactosidase expression levels from WR strain-based vaccinia expressing *lacZ* in infected BS-C-1 cells (24 hpi), with the ratio of about 1:2:200:200 [161]. The disparity in the promoter strength of pSEL and pSL in two studies could be due to the different transgenes, host cells, and VACV strains as well as protein detection methods.

Non-small cell lung cancer accounts for 85% of lung cancer [2]. In order to determine the most responsive cell line for EPO-VACVs treatment, we compared the replication and cytotoxicity of all viruses in two lung cancer cell lines, A549 and NCI-H1299. It has been demonstrated that virus replication efficiency is inversely proportional to the strength of promoters linked to foreign genes [147]. This phenomenon was seen in NCI-H1299 and in A549 at some early time points (24-48 hpi). The stronger promoter-containing viruses [GLV-1h212 (pSEL) and GLV-1h213 (pSL)] showed slower replication efficiency compared to the weaker promoter-containing viruses [GLV-1h210 (p7.5) and GLV-1h211 (pSE)], however, they reached similar levels at 72 hpi. In general, all EPO-VACVs and GLV-1h68 demonstrated similar replication ability in the overall course of infection. The replication efficiency is linked to oncolytic capacity of the viruses in both cell lines. In addition, A549 cells were more susceptible to all tested viruses than NCI-H1299 cells with more than 95% cell death at 96 hpi.

In a study by Hiley *et al*. [162], it was suggested that hypoxia did not affect VACV replication and cytotoxicity in CFPac1 and MiaPaca2 cell lines. Furthermore, they also found a significant increase in virus protein expression in hypoxia. In contrast, in our study the replication and cytotoxicity highly decreased in hypoxia (2% O_2 adapted or unadapted) compared to normaxia (20% O_2). The gene expression of

gusA inserted into the virus genome decreased at both MOIs (1 and 0.01). Besides that, the decrease in viral oncolytic activity in hypoxia was independent from the tested viruses (with hEPO or without hEPO). In our study, hypoxia was maintained for the whole duration of the experiments. However, in the Hiley study, it is not clear if cells were maintained in hypoxic conditions after virus infection. If not, this might cause the discrepancy in the results. The difference in the cell lines could be also a factor contributing to the differences.

Taken together, the insertion of hEPO with different expression levels [with ratio about 1(p7.5) : 2(pSE) : 20(pSEL) : 20(pSEL)] did not show negative effects on the virus replication and oncolytic ability of EPO-VACVs, and the A549 cell line was more susceptible for EPO-VACVs infection than the HCI-H1299 cell line.

4.2 EPO-VACVs express functional hEPO with different patterns of isoforms in tumors and sera

The principle function of hEPO is to stimulate RBC formation. Therefore, we tested the functionality of virus-mediated host cell expression of hEPO by measuring Hb levels and RBCs at different time points after treatment with EPO-VACVs in the blood of virus-treated A549 tumor-bearing nude mice. As expected, all four EPO-VACVs significantly raised the number of RBCs compared to GLV-1h68 treatment or untreated controls. The increase was detected as early as 7 days after infection with each EPO-VACV at a single dose of $2x10^6$ pfu/mouse. The Hb baseline (14 - 16 (g/dl)) increased to ~ 20 (g/dl) after 2 weeks and reached a maximum level of about ~ 23 (g/dl) at 30 - 40 days after treatment with EPO-VACVs. VACV-mediated hEPO expression exclusively affected the number of RBCs but not WBCs (MON, LYM, NEU) or PLT. Furthermore, mean corpuscular volume (size of RBC) and corpuscular Hb (numbers of Hb in RBC) were unchanged compared to GLV-1h210-treated and untreated controls. These results confirmed functionality of hEPO expressed from EPO-VACVs-infected tumor cells. While treatment with GLV-1h68 alone or untreated controls significantly decreased in the levels of Hb during tumor growth.

It has been known that glycosylation affects *in vivo* activity and half-life of hEPO in sera [163], and results in differences in isoform patterns [90, 164]. hEPO is a

glycoprotein with 3 N-linked and 1 O-linked oligosaccharides accounting for 40% of the molecular weight. 3 N-linked oligosaccharides at the sites 24, 38 and 83 are important for protein stabilization and activity [81]. The attempts to delete any of these oligosaccharides resulted in the loss of the biological activity of hEPO [165] and faster clearance of this protein in serum [166]. Furthermore, the EPO isoforms were found to be tissue and species dependent. Because of this, we performed 2D-gel electrophoresis and subsequent Western blotting to determine how many EPO isoforms can be identified in tumors, sera, cells, or in supernatants of infected cells in culture after treatment with EPO-VACVs. In these studies, we were able to detect about 9-10 isoforms in cells, supernatants from infected cells and in tumor lysates. They all were similar in their isoform patterns with *pIs* ranging from 4.2 to 6.4, the bigger bands focused on the basic area but they were fewer in numbers compared to bands in the acidic area. The variance in *pI* isoforms occurred due to the differences in sialic acid residues in the molecules. Basic hEPO isoforms represent molecules which are lower (or non-sialic) in sialic acid residues. In contrast, the more acidic hEPO isoforms contain higher sialic acid residues [167-168]. Indeed, Darbepoetin alfa, containing up to 22 sialic acids, has isoforms shifted far beyond the acidic area (pI < 4) while in Epoetin alfa, containing up to 12 sialic acids, all isoforms existat pI > 4 [90]. Interestingly, we found only about 6 hEPO isoforms in the serum samples, focusing in the acidic area (*pIs*: 4.2 – 4.8), having similar isoform pattern to the commercially available Epoetin alfa. The absence of basic isoforms in the serum is possibly due to the body's clearance of during circulation. It has been mentioned that the sialoglycosylation plays a critical role for the protein folding, secretion and stabilization of hEPO in the circulation [169]. Furthermore, the binding of some acidic groups to the protein during hEPO circulation is another possibility for the shift of isoforms from the basic to acidic area.

4.3 EPO-VACVs enhance blood vessel dilatation and tumor regression without evidence of hEPO promoting tumor growth in the A549 tumor xenograft model

hEPO has been proven to be beneficial for the increase of Hb levels, improved health-related quality of life and enhanced radio-, and chemo-therapeutic efficacy

[158]. The previous work suggested that hEPO functions as an apoptosis inhibitor [135] or promoted tumor growth [170]. In this study, however, we did not observe any tumor-growth-promoting function of hEPO alone or in combination with GLV-1h68. In cell culture, the combination of GLV-1h68 with rhEPO did not show any difference in virus replication and cytotoxicity. A similar observation was seen in A549 tumor xenografts. Treatment with rhEPO (500 U/kg) for 9 consecutive days did not promote tumor growth when compared to untreated controls. In addition, the combination with GLV-1h68 showed a similar tumor growth curve as treatment with GLV-1h68 alone when clinical relevant doses were used. In another study (data not shown), rhEPO was injected thrice per week until termination of the experiment at day 50 post virus injection. The high dose (1000 U/kg) or low dose (100 U/kg) of rhEPO injected s.c. 1 week before, at the same time, or 1 week after GLV-1h68 administration did not show any difference in tumor growth as compared to GLV-1h68 alone.

Treatment with all EPO-VACVs demonstrated enhanced tumor regression compared to GLV-1h68 alone. As described before, the tumor growth after GLV-1h68 treatment occurred in three phases: growth, inhibition and regression [35]. Here, it was always observed that the tumor regression phase of EPO-VACVs appeared 1-2 weeks earlier compared to GLV-1h68, which resulted in better tumor therapeutic efficacy. The tumor regression was not affected by the level of hEPO expression among EPO-VACVs. Virus-mediated oncolysis is one of the most important factors for tumor regression [149]. Indeed, we found about 3-4 fold higher virus titers in tumors of mice treated with EPO-VAVCs compared to GLV-1h68 alone or GLV-1h68 in combination with rhEPO at 14 dpi, even though no big difference in virus replication and cytotoxicity among viruses was seen in cell cultures. This indicated that the effect of hEPO was not mediated directly on the tumor growth but somehow the local expression of hEPO affected the tumor microenvironment and virus spreading and subsequently led to better tumor regression.

The changed tumor microenvironment following rhEPO administration has been reported elsewhere (reviewed in [171]). However the effects of rhEPO on cancer cells are various. In endothelial cells, Rabatti *et al*. found EPOR expression, stimulation of Janus Kinase-2 (JAK-2) phosphorylation, production of matrix metalloproteinase-2 (MMP-2), and induction of neovascularization in the chick embryo chorioallantoic membrane (CAM) upon treatment with rhEPO [123]. In the

Lewis lung carcinoma tumor model, rhEPO treatment promoted tumor angiogenesis and tumor growth although this cell line does not express EPOR [172]. On the other hand, rhEPO was found to have no effect on anti-tumor apoptotic signaling in cell culture [141], or on the promotion of angiogenesis and tumor growth in xenograft models [122, 173] whether or not cancer cells were presented with EPOR [141].

All those discrepancies may result from the differences in cell lines, experimental conditions, or the dosage and intervals of rhEPO administration. But they may also derive from the lack of proper experimental designs which could test the direct effect of rhEPO on the tumors. hEPO has been reported to have multiple functions in the body. Besides erythropoiesis, it has tissue protective effects on the heart, brain, or the reproductive organs [94]. Therefore the systemic administration of rhEPO can cause cross-reactions and lead to confusions in result interpretation. In this study, hEPO was locally over-expressed in the VACV-specifically targeted tumors. However, we found that there was no difference in the tumor blood vessel density among mice treated with GLV-1h210 (functional hEPO) GLV-1h209 (no hEPO activity), GVL-1h68, or untreated control mice. The results indicated no neoangiogenesis effect of hEPO in A549 tumor xenografts. However, funtional hEPO caused enlarged tumor blood diameter. These findings are accordant with Tovari and colleagues' findings when they studied the effects of rhEPO on intratumoral blood vessels in two colorectal xenograft models [174]. The vessel enlargement could be an explanation for the enhanced tumor regression upon the treatment with GLV-1h210 expressing functional hEPO compared to the treatment with a non-functional mutant hEPO-expressing strain (GLV-1h209). Tumor blood dilatation can increase the vascular permeability, thus, facilitating the virus spreading to local and distant tumors [10, 149]. This is similar to the hyperthermia treatment strategy which has been used to improve virus delivery [175] as well as various therapeutic agents [176] to target tumors. To this date, the mechanism of hEPO on tumors is not well understood. The proposed pathways such as EPO → EPOR → JAK-2 / STAT5 / MAPK / PI3K are thought to be involved in tumor growth [177]. However, some investigators documented that despite no EPOR expression and downstream activation occurred, tumor growth was still observed, while others showed the opposite results [122, 172-173]. In another point of view, it was suggested that hEPO does not act via the regular dimer receptor (EPOR.EPOR) but via a dimer of one

EPO receptor and one common β receptor (EPOR.β_cR) [178]. Because of these conflicting findings, further studies in well-designed xenograft models of human cancer will be necessary to evaluate the effect of rhEPO on tumor growth.

4.4 The degree of tumor immune infiltration is proportionate to virus infection but is independent of hEPO expression

The innate immune infiltration following treatment with GLV-1h68 has been well elucidated in various tumor xenograft models [65-67, 149]. Immune cells play an important role in controlling tumor growth and rejection [179]. They seemed to have a synergistic interaction with virus in tumor elimination. Enormously elevated expression of immune cytokines/chemokines in tumors after treatment with GLV-1h211 and GLV-1h210 compared to GLV-1h68were observed, which could be a contributing factor to the better tumor regression found in mice treated with GLV-1h211 and GLV-1h210. Moreover, the levels of immune antigen expression were directly proportionate to the virus titers in tumors and the levels of hEPO expression. rhEPO is known as an immune modulator and treatment results in enhanced endogenous polyclonal immunoglobulins and B cell augment [126], T cell population [180], dendritic cells [181] or T cell elevation from sera of chronic renal failure patients [131]. Therefore, it was to test how the combination of virus and hEPO can affect tumor immune infiltration/expression and therapeutic outcomes.

To evaluate the effects of hEPO in tumor immune infiltration and cytokine expression, two different viruses (GLV-1h210 and GLV-1h209) with similar replication capacity in A459 cell culture were used. Both strains shared identical genome structure except for one amino acid change at the 103rd position (R103A). This replacement does not affect hEPO expression or secretion but disrupts its function. Xenograft tumors after 14 dpi were stained for MHC-II-positive cells (leucocytes, B cells, macrophages, and dendritic cells). Both, GLV-1h210 and GLV-1h209 treatment showed drastic positive staining compared to GLV-1h68 treatment or untreated controls, indicating the enhanced immune recruitment into GLV-210 or GLV-1h209-treated tumors. But there was no signiciant difference to be found between each other. The immune-related antigen profiling between them was also analyzed (data not shown). However, no significant difference (ratio > 2 or < 0.5) out

of 58 antigens was spotted. Those findings suggested that hEPO had no immune enhancing function in the A549 athymic nude mouse models. It is noteworthy that the athymic nude mice in this study were T cell-deficient, so other models with immunocompetent mice are required to be able to evaluate the involvement of T cell populations.

4.5 Toxicity concerns related to virus-mediated over-expression of hEPO

rhEPO is approved for the treatment of cancer-related anemia. It has been shown that it is beneficial in enhancing health-related quality of life, tumor oxygenation, chemo-, and radio-therapy. The recent clinical trials raised the question concerning the safety of using rhEPO which showed the lower survival rate in those groups with rhEPO treatment versus placebo [133-134]. However, those trials were found with some methodological limitations such as the imbalance baseline, high Hb starting points, and the interpretation reasons of death [97]. Besides, the outcome of a meta-analysis of 57 trials with 9353 patients was uncertain about the relationship of rhEPO administration and the survival rates [182]. Therefore, a clear statement on this issue has not been addressed to this date. However, the FDA has issued a warning concerning using rhEPO [183]. The use of rhEPO for correcting anemia in cancer patients has to be put under careful considerations and the use should not raise Hb level above 12 g/dl.

With EPO-VACVs, the virus-mediated expression of hEPO results in high accumulations of hEPO. This dose will be more than enough to stimulate the Hb levels in the animals. But in turn, this is a good model to examine the direct interaction among virus, hEPO, tumor and tumor microenvironment which is not currently well addressed. Unexpectedly, tumor oxygenation was found less prominent in tumors treated with EPO-VACVs, which is in disagreement with other findings, where they found enhanced tumor oxygenation subjected with hEPO [184]. In this case, however, it is hard to evaluate the effects of hEPO on tumor oxygenation because high-level RBC formation could block the blood microvessels inside the tumors. The use of those viruses for anemic models will gain more benefits from the increase of Hb levels. Other than that, VACVs encoding for hEPO did not show any different signs of toxicity compared to GLV-1h68, such as virus

distribution to animal organs or organs weight. The spleen is known as a site for filtering and removal of old RBCs or ion preservation, so spleen swelling is a part of biophysical function which has been predicted when coping with high production of RBCs [185].

GLV-1h210 with the lowest level of hEPO expression among four EPO-VACVs, showed a great improvement in animal weight and long-term overall survival compared to other EPO-VACVs, but similar to the non-hEPO-expressing virus strain GLV-1h68.

In conclusion, the four novel EPO-VACVs showed similar replication efficiency and cytotoxicity ability to the parental virus GLV-1h68 and mutant GLV-1h209 in A549 and NCI-H1299 cell cultures. *In vivo*, all EPO-VACVs were shown to significantly increase the number of RBCs, Hb levels, and virus replication in tumors as well as to enhance tumor regression in the A549 tumor xenograft model. Moreover, locally expressed hEPO did not promote tumor angiogenesis, tumor growth, and immune infiltration but was shown to cause enlarged tumoral microvessels which might facilitate virus spreading. It is conceivable that in a potential clinical application, anemic cancer patients could benefit from the EPO-VACVs, where they could serve as “wellness pills” to decrease anemic symptoms, while simultaneously destroying tumors.

ABBREVIATIONS

lacZ	β-galactosidase
gusA	β-glucuronidase
dpi	Day post virus injection
ELISA	Enzyme-linked immunosorbent assay
Hb	Hemoglobin
hpi	Hour post virus infection
hEPO	Human erythropoietin
kDa	KiloDalton
LEU	Leucocyte
LIVP	Lister vaccinia virus
MON	Monocyte
MOI	Multiplicity of infection
NEU	Neutrophil
PLT	Platelet
rhEPO	Recombinant human erythropoietin
RBC	Red blood cell
Ruc-GFP	*Renilla* luciferase-Aequorea – green fluorescent protein
U	Unit
VACV	Vaccinia virus
EPO-VACV	Vaccinia virus-encoding human erythrpoietin
WBC	White blood cell

ACKNOWLEDGEMENTS

It is my great pleasure to express my respect and gratitude to those who helped and supported me during my PhD's time, without the following people and institutions, this thesis could not have been completed.

This work was carried out at the Department of Biochemistry, Theodor Boveri Institute Biocenter, The University of Würzburg, Bavaria, Germany, and Genelux Corporation at the San Diego Science Center, San Diego, California, USA, between February 2009 and December 2012.

My special thanks to

Prof. Dr. Aladar A. Szalay for giving me a great opportunity to carry out such an interesting project under his supervision, to meet and to work with the great people in his group. His knowledge, vision and dedication to work have inspired me a lot in the difficult times and will be with me in the next steps of my future. I highly appreciate his recommendations, encouragements and a lot of support, which enabled me to finish the interesting but challenging project. I would also like to show my heartfelt gratitude to him for offering me an invaluable chance to experience the multiple cultures, to improve my English as well as to see how a successful educational institution is translated to the company.

Prof. Dr. Friedrich Grummt for his critical reading and corrections of my thesis. I am very thankful for his kindness and support especially during the initial time of my PhD program in the University of Würzburg when everything was new to me.

Dr. Nanhai G Chen for his substantial assistance, valuable suggestions, and useful discussions during most of my research time in San Diego. Thanks to his provision of initial data on this work, as well as his enormous help, my thesis is significantly improved in both content and language accuracy.

Dr. Qian Zhang, Dr. Rohit Duggal, Dr. Tony Yu, Dr. Jochen Stritzker for their interest in this project and their guidance in the construction of viruses, working with animals and many other experimental methods.

Dr. Alexa Frentzen and Lisa Bukel for the help with histology, Dr. Thu-ha Le for the help with 2D-gel electrophoresis, Jason Aguilar for the help with virus purification, and Dr. Barbara Härtl for the help with Q-PCR analysis. I am also grateful to the excellent technical support from Terry Trevino, Johanna Langbein, and Melody Jing.

I would like to extend my sincerest thanks and appreciation to all members of Wurzburg and Genelux family especially Dr. Ivaylo Gentschev, Dr. Ulrike Donat, Dr. Elisabeth Hofmann, Dr. Stephanie Weibel, Dr. Carolin Seubert, Dr. Dana Haddad, Dr. Victoria Raab, Dr. Julia Sturm, Marion Adelfinger, Michael Heß, Anna Seidensal, Jennifer Reinboth, Stephan Rudolph, Dr. Boris Minev, Dr. Mehmet Kilinc, Dr. Ulrike Geißinger, Dr. Huiqiang Wang, Ting Huang, Anu Pold, Katrin Schäffler, Desislava Tsoneva, Jacqueline Kramer, Lorenz Kirscher, Dr. Sunil Advani, Vannessa Cook, Uma Sukhwani, Ron Simus, Robin Crisler and, Terry Chamberlin, Kim Duffy, Thomas Hagood, and Camha Hoang for their friendly help and supports during my time in Wuerzburg and in San Diego. Especial thanks to Klaas Ehrig, Lisa Bukel, and Jason Aguilar for their critical reading and comments on this thesis.

I am very thankful to the Joint Graduate Education Program (JGEP) between “Hanoi and Greifswald”, and the financial support from the Vietnam Ministry of Education and Training (MOET). Without this program, I would not have gotten a chance to spend my doctoral years at the University of Würzburg.

To my farther, though I cannot touch you now, I know you are a part of me, and always there, supporting and encouraging me in every step of my life; to my mother, thank you for your unconditional love and strength to overcome the hardest time in our life; to my wife, thank you for sharing your life with me, taking a good care of our beloved daughter without me. I know that it wasn’t an easy time for you but I believe we will make our beautiful journey together ahead; to my grandparents, masters, sister, brother, and all my friends… thank you so much for being a part of my life.

San Diego, October 20, 2012

CURRICULUM VITAE

Personal information:

Name:	Duong Hoang Nguyen
Date of birth:	August 17, 1982
Place of birth:	Nghe An province, Vietnam
Address:	3922 Jewell Street Apt M307 San Diego, California 92109, USA

Education:

09/1996 – 06/2000	Quynh Luu I high school, Nghe An province, Vietnam
09/2000 – 06/2004	Bachelor of biotechnology, Vietnam National University, Hanoi
10/2004 – 01/2009	Researcher at Molecular Microbiology lab, Institute of Biotechnology (IBT), Vietnam Academy of Science and Technology (VAST)
09/2006 – 06/2008	Master of Science in Biology, Thai Nguyen University and Vietnam Academy of Science and Techonology, Vietnam
01/2007 – 02/2008	Diploma in Biology, Joint Graduate Education Program between Hanoi National University, Vietnam and Greifswald University, Germany
02/2009 – 12/2012	Doctoral studies supervised by Professor Aladar A. Szalay, University of Wuerzburg, Germany and Genelux Corporation, San Diego, USA

LIST OF PUBLICATIONS

1. Nguyen Thi Kim Cuc, Nguyen Thi Tuyet Mai, Pham Viet Cuong, Nguyen Hoang Duong, Le Thanh Hoa, (2005). **Isolation and sequencing the segments VP2 gene of infectious bursal disease virus (IBDV) from infected chickens in Binh Duong and Hung Yen provinces (Vietnam)**. *Vietnam J. of Science and Technology. 43(4), 22-28.*

2. Pham Viet Cuong, Nguyen Hoang Duong, Nguyen Thi Kim Cuc, Le Thanh Hoa (2006) **Expression of surface antigen (VP2) of Gumboro virus in *E. coli* BL21 (DE3).** *Vietnam J. of Science and Technology*. *44(4), 71-76.*

3. Boonhiang Promdonkoy, Wanwarang Pathaichindachote, Duong Hoang Nguyen, Noppawan Nounjan, Patcharee Promdonkoy, Chartchai Krittanai and Mongkon Audtho (2008). **Effects of amino acid substitutions in a loop connecting beta-6 and beta-7 of a cytolytic toxin from *Bacillus thuringiensis.*** 41st Annual Meeting of the Society for Invertebrate Pathology and 9th International Conference on *Bacillus thuringiensis.* University of Warwick, Coventry, United Kingdom.

4. Pham Viet Cuong, Le Van Duyet, Nguyen Hoang Duong, Nguyen Thi Kim Cuc (2008) **Influence of some culture parameters on growth of *Aspergillus niger* and glucosamine obtainment from their cell walls.** *Vietnam J. of Science and Technology*. *46(5), 29-35.*

5. Nguyen Hoang Duong, Pham Viet Cuong, Nguyen Thi Kim Cuc (2008) **Cloning and construction of NagA-expression vector in eukaryotic system.** *Vietnam J. of Science and Technology*. *46(6), 91-96.*

6. Nguyen Hoang Duong, Pham Viet Cuong, Le Quang Huan (2008) **Expression and purification of *her2* gene fragment**. *J. of Biotechnology. 6(4A): 599-604.*

7. Duong H Nguyen, Nanhai G Chen, Qian Zhang, Ha T Le, Jason Aguilar, Yong A Yu, Aladar A Szalay (2012) **Vaccinia virus-encoded expression of human erythropoietin in colonized human lung cancer xenografts results in enhanced oncolytic virotherapy and overproduction of red blood cells in mice.** Submitted to the journal of Cancer Research

REFERENCES

1. *World Health Organization, Globocan 2008, IARC, 2010.* *http://globocan.iarc.fr/factsheets/populations/factsheet.asp?uno=900.*

2. *American Cancer Society, Cancer factors & figures 2012.* http://www.cancer.org/acs/groups/content/@epidemiologysurveilance/documents/document/acspc-031941.pdf.

3. Shchelkunov, S.N., S.S. Marennikova, and R.W. Moyer, *Orthopoxviruses pathogenic for humans*. 2005, New York, NY: Springer. xxiii, 425 p.

4. Plaut, M. and S.S. Tinkle, *Risks of smallpox vaccination: 200 years after Jenner.* J Allergy Clin Immunol, 2003. **112**(4): p. 683-5.

5. WHO, *Factsheet. http://www.who.int/mediacentre/factsheets/smallpox/en/.*

6. Moss, B., *Vaccinia virus: a tool for research and vaccine development.* Science, 1991. **252**(5013): p. 1662-7.

7. Southam, C.M., *Present status of oncolytic virus studies.* Trans N Y Acad Sci, 1960. **22**: p. 657-73.

8. Hunter-Craig, I., et al., *Use of vaccinia virus in the treatment of metastatic malignant melanoma.* Br Med J, 1970. **2**(5708): p. 512-5.

9. Nanhai G Chen, A.A.S., *Oncolytic vaccinia virus: a theranostic agent for cancer.* Future Virol, 2010. **5**(6): p. 763-784.

10. Kirn, D.H. and S.H. Thorne, *Targeted and armed oncolytic poxviruses: a novel multi-mechanistic therapeutic class for cancer.* Nat Rev Cancer, 2009. **9**(1): p. 64-71.

11. Goebel, S.J., et al., *The complete DNA sequence of vaccinia virus.* Virology, 1990. **179**(1): p. 247-66, 517-63.

12. Harrison, S.C., et al., *Discovery of antivirals against smallpox.* Proc Natl Acad Sci U S A, 2004. **101**(31): p. 11178-92.

13. Ichihashi, Y., S. Matsumoto, and S. Dales, *Biogenesis of poxviruses: role of A-type inclusions and host cell membranes in virus dissemination.* Virology, 1971. **46**(3): p. 507-32.

14. Smith, G.L., A. Vanderplasschen, and M. Law, *The formation and function of extracellular enveloped vaccinia virus.* J Gen Virol, 2002. **83**(Pt 12): p. 2915-31.

15. Townsley, A.C., et al., *Vaccinia virus entry into cells via a low-pH-dependent endosomal pathway.* J Virol, 2006. **80**(18): p. 8899-908.

16. Lin, C.L., et al., *Vaccinia virus envelope H3L protein binds to cell surface heparan sulfate and is important for intracellular mature virion morphogenesis and virus infection in vitro and in vivo.* J Virol, 2000. **74**(7): p. 3353-65.

17. Hsiao, J.C., C.S. Chung, and W. Chang, *Vaccinia virus envelope D8L protein binds to cell surface chondroitin sulfate and mediates the adsorption of intracellular mature virions to cells.* J Virol, 1999. **73**(10): p. 8750-61.

18. Chung, C.S., et al., *A27L protein mediates vaccinia virus interaction with cell surface heparan sulfate.* J Virol, 1998. **72**(2): p. 1577-85.

19. Carter, G.C., et al., *Entry of the vaccinia virus intracellular mature virion and its interactions with glycosaminoglycans.* J Gen Virol, 2005. **86**(Pt 5): p. 1279-90.

20. Oda, K.I. and W.K. Joklik, *Hybridization and sedimentation studies on "early" and "late" vaccinia messenger RNA.* Journal of Molecular Biology, 1967. **27**(3): p. 395-419.

21. Baldick, C.J., Jr. and B. Moss, *Characterization and temporal regulation of mRNAs encoded by vaccinia virus intermediate-stage genes.* J Virol, 1993. **67**(6): p. 3515-27.

22. Munyon, W., E. Paoletti, and J.T. Grace, Jr., *RNA polymerase activity in purified infectious vaccinia virus.* Proc Natl Acad Sci U S A, 1967. **58**(6): p. 2280-7.

23. Gershon, P.D. and B. Moss, *Early transcription factor subunits are encoded by vaccinia virus late genes.* Proc Natl Acad Sci U S A, 1990. **87**(11): p. 4401-5.

24. Broyles, S.S. and B. Moss, *DNA-dependent ATPase activity associated with vaccinia virus early transcription factor.* J Biol Chem, 1988. **263**(22): p. 10761-5.

25. Ahn, B.Y. and B. Moss, *RNA polymerase-associated transcription specificity factor encoded by vaccinia virus.* Proc Natl Acad Sci U S A, 1992. **89**(8): p. 3536-40.

26. Patel, D.D. and D.J. Pickup, *The second-largest subunit of the poxvirus RNA polymerase is similar to the corresponding subunits of procaryotic and eucaryotic RNA polymerases.* J Virol, 1989. **63**(3): p. 1076-86.

27. Broyles, S.S., *Vaccinia virus transcription.* J Gen Virol, 2003. **84**(Pt 9): p. 2293-303.

28. Rosales, R., G. Sutter, and B. Moss, *A cellular factor is required for transcription of vaccinia viral intermediate-stage genes.* Proc Natl Acad Sci U S A, 1994. **91**(9): p. 3794-8.

29. Guerra, S., et al., *Cellular gene expression survey of vaccinia virus infection of human HeLa cells.* J Virol, 2003. **77**(11): p. 6493-506.

30. Rice, A.P. and B.E. Roberts, *Vaccinia virus induces cellular mRNA degradation.* J Virol, 1983. **47**(3): p. 529-39.

31. Zeh, H.J. and D.L. Bartlett, *Development of a replication-selective, oncolytic poxvirus for the treatment of human cancers.* Cancer Gene Ther, 2002. **9**(12): p. 1001-12.

32. Moss, B., *Poxvirus entry and membrane fusion.* Virology, 2006. **344**(1): p. 48-54.

33. McCart, J.A., et al., *Systemic cancer therapy with a tumor-selective vaccinia virus mutant lacking thymidine kinase and vaccinia growth factor genes.* Cancer Res, 2001. **61**(24): p. 8751-7.

34. Smith, G.L. and B. Moss, *Infectious poxvirus vectors have capacity for at least 25 000 base pairs of foreign DNA.* Gene, 1983. **25**(1): p. 21-8.

35. Zhang, Q., et al., *Eradication of solid human breast tumors in nude mice with an intravenously injected light-emitting oncolytic vaccinia virus.* Cancer Res, 2007. **67**(20): p. 10038-46.

36. Mastrangelo, M.J., et al., *Intratumoral recombinant GM-CSF-encoding virus as gene therapy in patients with cutaneous melanoma.* Cancer Gene Ther, 1999. **6**(5): p. 409-22.

37. Sinkovics, J.G. and J.C. Horvath, *Natural and genetically engineered viral agents for oncolysis and gene therapy of human cancers.* Arch Immunol Ther Exp (Warsz), 2008. **56 Suppl 1**: p. 3s-59s.

38. Hruby, D.E. and L.A. Ball, *Mapping and identification of the vaccinia virus thymidine kinase gene.* J Virol, 1982. **43**(2): p. 403-9.

39. Puhlmann, M., et al., *Vaccinia as a vector for tumor-directed gene therapy: biodistribution of a thymidine kinase-deleted mutant.* Cancer Gene Ther, 2000. **7**(1): p. 66-73.

40. Buller, R.M., et al., *Decreased virulence of recombinant vaccinia virus expression vectors is associated with a thymidine kinase-negative phenotype.* Nature, 1985. **317**(6040): p. 813-5.

41. Katsafanas, G.C. and B. Moss, *Vaccinia virus intermediate stage transcription is complemented by Ras-GTPase-activating protein SH3 domain-binding protein (G3BP) and cytoplasmic activation/proliferation-associated protein (p137) individually or as a heterodimer.* J Biol Chem, 2004. **279**(50): p. 52210-7.

42. Thorne, S.H., et al., *Rational strain selection and engineering creates a broad-spectrum, systemically effective oncolytic poxvirus, JX-963.* Journal of Clinical Investigation, 2007. **117**(11): p. 3350-8.

43. Oie, M., H. Shida, and Y. Ichihashi, *The function of the vaccinia hemagglutinin in the proteolytic activation of infectivity.* Virology, 1990. **176**(2): p. 494-504.

44. Guo, Z.S., et al., *The enhanced tumor selectivity of an oncolytic vaccinia lacking the host range and antiapoptosis genes SPI-1 and SPI-2.* Cancer Res, 2005. **65**(21): p. 9991-8.

45. Kirn, D.H., et al., *Targeting of interferon-beta to produce a specific, multi-mechanistic oncolytic vaccinia virus.* PLoS Med, 2007. **4**(12): p. e353.

46. Greer, L.F., 3rd and A.A. Szalay, *Imaging of light emission from the expression of luciferases in living cells and organisms: a review.* Luminescence, 2002. **17**(1): p. 43-74.

47. Wang, Y., et al., *Renilla luciferase- Aequorea GFP (Ruc-GFP) fusion protein, a novel dual reporter for real-time imaging of gene expression in cell cultures and in live animals.* Mol Genet Genomics, 2002. **268**(2): p. 160-8.

48. Hess, M., et al., *Bacterial glucuronidase as general marker for oncolytic virotherapy or other biological therapies.* J Transl Med, 2011. **9**: p. 172.

49. Acres, B., et al., *Directed cytokine expression in tumour cells in vivo using recombinant vaccinia virus.* Ther Immunol, 1994. **1**(1): p. 17-23.

50. Chen, B., et al., *Low-dose vaccinia virus-mediated cytokine gene therapy of glioma.* Journal of Immunotherapy, 2001. **24**(1): p. 46-57.

51. Sturm, J.B., et al., *Functional hyper-IL-6 from vaccinia virus-colonized tumors triggers platelet formation and helps to alleviate toxicity of mitomycin C enhanced virus therapy.* J Transl Med, 2012. **10**(1): p. 9.

52. Breitbach, C.J., et al., *Intravenous delivery of a multi-mechanistic cancer-targeted oncolytic poxvirus in humans.* Nature, 2011. **477**(7362): p. 99-102.

53. Chen, B., et al., *Evaluation of cytokine toxicity induced by vaccinia virus-mediated IL-2 and IL-12 antitumour immunotherapy.* Cytokine, 2001. **15**(6): p. 305-14.

54. Campoli, M., et al., *Immunotherapy of malignant disease with tumor antigen-specific monoclonal antibodies.* Clin Cancer Res, 2010. **16**(1): p. 11-20.

55. Wang, S.Y. and G. Weiner, *Complement and cellular cytotoxicity in antibody therapy of cancer.* Expert Opin Biol Ther, 2008. **8**(6): p. 759-68.

56. Cassard, L., et al., *Fc gamma receptors and cancer.* Springer Semin Immunopathol, 2006. **28**(4): p. 321-8.

57. Frentzen, A., et al., *Anti-VEGF single-chain antibody GLAF-1 encoded by oncolytic vaccinia virus significantly enhances antitumor therapy.* Proc Natl Acad Sci U S A, 2009. **106**(31): p. 12915-20.

58. Hengartner, M.O., *The biochemistry of apoptosis.* Nature, 2000. **407**(6805): p. 770-6.

59. Timiryasova, T.M., et al., *Vaccinia virus-mediated expression of wild-type p53 suppresses glioma cell growth and induces apoptosis.* Int J Oncol, 1999. **14**(5): p. 845-54.

60. Timiryasova, T.M., et al., *Radiation enhances the anti-tumor effects of vaccinia-p53 gene therapy in glioma.* Technol Cancer Res Treat, 2003. **2**(3): p. 223-35.

61. Mulryan, K., et al., *Attenuated recombinant vaccinia virus expressing oncofetal antigen (tumor-associated antigen) 5T4 induces active therapy of established tumors.* Mol Cancer Ther, 2002. **1**(12): p. 1129-37.

62. Gil, M., et al., *Targeting a mimotope vaccine to activating Fcgamma receptors empowers dendritic cells to prime specific CD8+ T cell responses in tumor-bearing mice.* J Immunol, 2009. **183**(10): p. 6808-18.

63. Eder, J.P., et al., *A phase I trial of a recombinant vaccinia virus expressing prostate-specific antigen in advanced prostate cancer.* Clin Cancer Res, 2000. **6**(5): p. 1632-8.

64. Worschech, A., et al., *The immunologic aspects of poxvirus oncolytic therapy.* Cancer Immunol Immunother, 2009. **58**(9): p. 1355-62.

65. Yu, Y.A., et al., *Regression of human pancreatic tumor xenografts in mice after a single systemic injection of recombinant vaccinia virus GLV-1h68.* Mol Cancer Ther, 2009. **8**(1): p. 141-51.

66. Gentschev, I., et al., *Regression of human prostate tumors and metastases in nude mice following treatment with the recombinant oncolytic vaccinia virus GLV-1h68.* J Biomed Biotechnol, 2010. **2010**: p. 489759.

67. Gentschev, I., et al., *Significant Growth Inhibition of Canine Mammary Carcinoma Xenografts following Treatment with Oncolytic Vaccinia Virus GLV-1h68.* J Oncol, 2010. **2010**: p. 736907.

68. Yu, Z., et al., *Oncolytic vaccinia therapy of squamous cell carcinoma.* Mol Cancer, 2009. **8**: p. 45.

69. Gnant, M.F., et al., *Systemic administration of a recombinant vaccinia virus expressing the cytosine deaminase gene and subsequent treatment with 5-fluorocytosine leads to tumor-specific gene expression and prolongation of survival in mice.* Cancer Res, 1999. **59**(14): p. 3396-403.

70. Touchefeu, Y., G. Vassaux, and K.J. Harrington, *Oncolytic viruses in radiation oncology.* Radiother Oncol, 2011. **99**(3): p. 262-70.

71. Advani, S.J., et al., *Preferential Replication of Systemically Delivered Oncolytic Vaccinia Virus in Focally Irradiated Glioma Xenografts.* Clin Cancer Res, 2012.

72. Mansfield, D., et al., *Oncolytic Vaccinia virus and radiotherapy in head and neck cancer.* Oral Oncol, 2012.

73. Gridley, D.S., et al., *Evaluation of radiation effects against C6 glioma in combination with vaccinia virus-p53 gene therapy.* Int J Oncol, 1998. **13**(5): p. 1093-8.

74. Wong, H.H., N.R. Lemoine, and Y. Wang, *Oncolytic Viruses for Cancer Therapy: Overcoming the Obstacles.* Viruses, 2010. **2**(1): p. 78-106.

75. Ottolino-Perry, K., et al., *Intelligent design: combination therapy with oncolytic viruses.* Mol Ther, 2010. **18**(2): p. 251-63.

76. Lun, X.Q., et al., *Efficacy of systemically administered oncolytic vaccinia virotherapy for malignant gliomas is enhanced by combination therapy with rapamycin or cyclophosphamide.* Clin Cancer Res, 2009. **15**(8): p. 2777-88.

77. Komatsu, N., et al., *In vitro development of erythroid and megakaryocytic cells from a UT-7 subline, UT-7/GM.* Blood, 1997. **89**(11): p. 4021-33.

78. Hoke, A., *Erythropoietin and the Nervous System* 2005: Springer. 360.

79. Davis, J.M., et al., *Characterization of recombinant human erythropoietin produced in Chinese hamster ovary cells.* Biochemistry, 1987. **26**(9): p. 2633-8.

80. Wen, D., et al., *Erythropoietin structure-function relationships. Identification of functionally important domains.* J Biol Chem, 1994. **269**(36): p. 22839-46.

81. Wasley, L.C., et al., *The importance of N- and O-linked oligosaccharides for the biosynthesis and in vitro and in vivo biologic activities of erythropoietin.* Blood, 1991. **77**(12): p. 2624-32.

82. Koury, M.J. and M.C. Bondurant, *The molecular mechanism of erythropoietin action.* Eur J Biochem, 1992. **210**(3): p. 649-63.

83. Lin, F.K., et al., *Cloning and expression of the human erythropoietin gene.* Proc Natl Acad Sci U S A, 1985. **82**(22): p. 7580-4.

84. Jacobs, K., et al., *Isolation and characterization of genomic and cDNA clones of human erythropoietin.* Nature, 1985. **313**(6005): p. 806-10.

85. Recny, M.A., H.A. Scoble, and Y. Kim, *Structural characterization of natural human urinary and recombinant DNA-derived erythropoietin. Identification of des-arginine 166 erythropoietin.* J Biol Chem, 1987. **262**(35): p. 17156-63.

86. Lai, P.H., et al., *Structural characterization of human erythropoietin.* J Biol Chem, 1986. **261**(7): p. 3116-21.

87. Sytkowski, A.J., *Erythropoietin: blood, brain and beyond*. 2004: WILEY-VCH Verlag GmbH & Co. KGaA.

88. Lasne, F. and J. de Ceaurriz, *Recombinant erythropoietin in urine.* Nature, 2000. **405**(6787): p. 635.

89. Macdougall, I.C., et al., *Pharmacokinetics of novel erythropoiesis stimulating protein compared with epoetin alfa in dialysis patients.* J Am Soc Nephrol, 1999. **10**(11): p. 2392-5.

90. Caldini, A., et al., *Epoetin alpha, epoetin beta and darbepoetin alfa: two-dimensional gel electrophoresis isoforms characterization and mass spectrometry analysis.* Proteomics, 2003. **3**(6): p. 937-41.

91. Catlin, D.H., et al., *Comparison of the isoelectric focusing patterns of darbepoetin alfa, recombinant human erythropoietin, and endogenous erythropoietin from human urine.* Clinical Chemistry, 2002. **48**(11): p. 2057-9.

92. Grodberg, J., K.L. Davis, and A.J. Sykowski, *Alanine scanning mutagenesis of human erythropoietin identifies four amino acids which are critical for biological activity.* Eur J Biochem, 1993. **218**(2): p. 597-601.

93. Boissel, J.P. and H.F. Bunn, *Erythropoietin structure-function relationships.* Prog Clin Biol Res, 1990. **352**: p. 227-32.

94. Arcasoy, M.O., *The non-haematopoietic biological effects of erythropoietin.* Br J Haematol, 2008. **141**(1): p. 14-31.

95. Jelkmann, W., *Molecular biology of erythropoietin.* Intern Med, 2004. **43**(8): p. 649-59.

96. Ebert, B.L. and H.F. Bunn, *Regulation of the erythropoietin gene.* Blood, 1999. **94**(6): p. 1864-77.

97. Spivak, J.L., *The anaemia of cancer: death by a thousand cuts.* Nat Rev Cancer, 2005. **5**(7): p. 543-55.

98. Nosaka, T., et al., *STAT5 as a molecular regulator of proliferation, differentiation and apoptosis in hematopoietic cells.* Embo J, 1999. **18**(17): p. 4754-65.

99. Bohlius, J., et al., *Cancer-Related Anemia and Recombinant Erythropoietin--An Updated Overview.* Nature Clinical Practice Oncology, 2006. **3**: p. 152-164.

100. Kasper, C., et al., *Recombinant human erythropoietin in the treatment of cancer-related anaemia.* Eur J Haematol, 1997. **58**(4): p. 251-6.

101. Groopman, J.E. and L.M. Itri, *Chemotherapy-induced anemia in adults: incidence and treatment.* J Natl Cancer Inst, 1999. **91**(19): p. 1616-34.

102. Caro, J.J., et al., *Anemia as an independent prognostic factor for survival in patients with cancer: a systemic, quantitative review.* Cancer, 2001. **91**(12): p. 2214-21.

103. Auguste, P., et al., *Molecular mechanisms of tumor vascularization.* Crit Rev Oncol Hematol, 2005. **54**(1): p. 53-61.

104. Cella, D., *The effects of anemia and anemia treatment on the quality of life of people with cancer.* Oncology (Williston Park), 2002. **16**(9 Suppl 10): p. 125-32.

105. LT, G., *Risks of blood transfusion.* Crit Care Med, 2003. **31**: p. 678-686.

106. Glaspy, J.A., *Erythropoietin in Cancer Patients.* Annu Rev Med, 2008.

107. Littlewood, T.J., et al., *Effects of epoetin alfa on hematologic parameters and quality of life in cancer patients receiving nonplatinum chemotherapy: results of a randomized, double-blind, placebo-controlled trial.* J Clin Oncol, 2001. **19**(11): p. 2865-74.

108. Seidenfeld, J., et al., *Epoetin treatment of anemia associated with cancer therapy: a systematic review and meta-analysis of controlled clinical trials.* J Natl Cancer Inst, 2001. **93**(16): p. 1204-14.

109. Bohlius, J., et al., *Erythropoietin for patients with malignant disease.* Cochrane Database Syst Rev, 2004(3): p. CD003407.

110. Vaupel, P. and A. Mayer, *Hypoxia and anemia: effects on tumor biology and treatment resistance.* Transfus Clin Biol, 2005. **12**(1): p. 5-10.

111. Lavey, R.S. and W.H. Dempsey, *Erythropoietin increases hemoglobin in cancer patients during radiation therapy.* Int J Radiat Oncol Biol Phys, 1993. **27**(5): p. 1147-52.

112. Kelleher, D.K., et al., *Blood flow, oxygenation, and bioenergetic status of tumors after erythropoietin treatment in normal and anemic rats.* Cancer Res, 1996. **56**(20): p. 4728-34.

113. Stuben, G., et al., *Recombinant human erythropoietin increases the radiosensitivity of xenografted human tumours in anaemic nude mice.* J Cancer Res Clin Oncol, 2001. **127**(6): p. 346-50.

114. Ehrenreich, H., et al., *Erythropoietin: a candidate compound for neuroprotection in schizophrenia.* Mol Psychiatry, 2004. **9**(1): p. 42-54.

115. Yu, X., et al., *Erythropoietin receptor signalling is required for normal brain development.* Development, 2002. **129**(2): p. 505-16.

116. Brines, M.L., et al., *Erythropoietin crosses the blood-brain barrier to protect against experimental brain injury.* Proc Natl Acad Sci U S A, 2000. **97**(19): p. 10526-31.

117. Demers, E.J., R.J. McPherson, and S.E. Juul, *Erythropoietin protects dopaminergic neurons and improves neurobehavioral outcomes in juvenile rats after neonatal hypoxia-ischemia.* Pediatr Res, 2005. **58**(2): p. 297-301.

118. Chong, Z.Z. and K. Maiese, *Erythropoietin involves the phosphatidylinositol 3-kinase pathway, 14-3-3 protein and FOXO3a nuclear trafficking to preserve endothelial cell integrity.* Br J Pharmacol, 2007. **150**(7): p. 839-50.

119. McPherson, R.J. and S.E. Juul, *Recent trends in erythropoietin-mediated neuroprotection.* Int J Dev Neurosci, 2008. **26**(1): p. 103-11.

120. Calvillo, L., et al., *Recombinant human erythropoietin protects the myocardium from ischemia-reperfusion injury and promotes beneficial remodeling.* Proc Natl Acad Sci U S A, 2003. **100**(8): p. 4802-6.

121. Sepodes, B., et al., *Recombinant human erythropoietin protects the liver from hepatic ischemia-reperfusion injury in the rat.* Transplant International, 2006. **19**(11): p. 919-26.

122. Hardee, M.E., et al., *Human recombinant erythropoietin (rEpo) has no effect on tumour growth or angiogenesis.* Br J Cancer, 2005. **93**(12): p. 1350-5.

123. Ribatti, D., et al., *Human erythropoietin induces a pro-angiogenic phenotype in cultured endothelial cells and stimulates neovascularization in vivo.* Blood, 1999. **93**(8): p. 2627-36.

124. Monestiroli, S., et al., *Kinetics and viability of circulating endothelial cells as surrogate angiogenesis marker in an animal model of human lymphoma.* Cancer Res, 2001. **61**(11): p. 4341-4.

125. Yuan, R., et al., *Erythropoietin: a potent inducer of peripheral immuno/inflammatory modulation in autoimmune EAE.* PLoS ONE, 2008. **3**(4): p. e1924.

126. Katz, O., et al., *Erythropoietin enhances immune responses in mice.* Eur J Immunol, 2007. **37**(6): p. 1584-93.

127. Prutchi Sagiv, S., et al., *Erythropoietin effects on dendritic cells: potential mediators in its function as an immunomodulator?* Exp Hematol, 2008. **36**(12): p. 1682-90.

128. Anagnostou, A., et al., *Erythropoietin receptor mRNA expression in human endothelial cells.* Proc Natl Acad Sci U S A, 1994. **91**(9): p. 3974-8.

129. Sela, S., et al., *The polymorphonuclear leukocyte--a new target for erythropoietin.* Nephron, 2001. **88**(3): p. 205-10.

130. Fraser, J.K., et al., *Expression of specific high-affinity binding sites for erythropoietin on rat and mouse megakaryocytes.* Exp Hematol, 1989. **17**(1): p. 10-6.

131. Trzonkowski, P., et al., *Treatment with recombinant human erythropoietin is associated with rejuvenation of CD8+ T cell compartment in chronic renal failure patients.* Nephrol Dial Transplant, 2007. **22**(11): p. 3221-7.

132. Mittelman, M., et al., *Erythropoietin induces tumor regression and antitumor immune responses in murine myeloma models.* Proc Natl Acad Sci U S A, 2001. **98**(9): p. 5181-6.

133. Henke, M., et al., *Erythropoietin to treat head and neck cancer patients with anaemia undergoing radiotherapy: randomised, double-blind, placebo-controlled trial.* Lancet, 2003. **362**(9392): p. 1255-60.

134. Leyland-Jones, B., et al., *Maintaining normal hemoglobin levels with epoetin alfa in mainly nonanemic patients with metastatic breast cancer receiving first-line chemotherapy: a survival study.* J Clin Oncol, 2005. **23**(25): p. 5960-72.

135. Dolznig, H., et al., *Apoptosis protection by the Epo target Bcl-X(L) allows factor-independent differentiation of primary erythroblasts.* Curr Biol, 2002. **12**(13): p. 1076-85.

136. Mirmohammadsadegh, A., et al., *Role of erythropoietin receptor expression in malignant melanoma.* Journal of Investigative Dermatology, 2010. **130**(1): p. 201-10.

137. Acs, G., et al., *Erythropoietin and erythropoietin receptor expression in human cancer.* Cancer Res, 2001. **61**(9): p. 3561-5.

138. Kumar, S.M., et al., *Erythropoietin activates the phosphoinositide 3-kinase/Akt pathway in human melanoma cells.* Melanoma Res, 2006. **16**(4): p. 275-83.

139. Mohyeldin, A., et al., *Erythropoietin signaling promotes invasiveness of human head and neck squamous cell carcinoma.* Neoplasia, 2005. **7**(5): p. 537-43.

140. Lai, S.Y., et al., *Erythropoietin-mediated activation of JAK-STAT signaling contributes to cellular invasion in head and neck squamous cell carcinoma.* Oncogene, 2005. **24**(27): p. 4442-9.

141. Sinclair, A.M., et al., *Erythropoietin receptor transcription is neither elevated nor predictive of surface expression in human tumour cells.* Br J Cancer, 2008. **98**(6): p. 1059-67.

142. Swift, S., et al., *Absence of functional EpoR expression in human tumor cell lines.* Blood, 2010. **115**(21): p. 4254-63.

143. Mosmann, T., *Rapid colorimetric assay for cellular growth and survival: application to proliferation and cytotoxicity assays.* J Immunol Methods, 1983. **65**(1-2): p. 55-63.

144. Pfaffl, M.W., *A new mathematical model for relative quantification in real-time RT-PCR.* Nucleic Acids Research, 2001. **29**(9): p. e45.

145. O'Farrell, P.H., *High resolution two-dimensional electrophoresis of proteins.* J Biol Chem, 1975. **250**(10): p. 4007-21.

146. Storring, P.L., et al., *Epoetin alfa and beta differ in their erythropoietin isoform compositions and biological properties.* Br J Haematol, 1998. **100**(1): p. 79-89.

147. Chen, N.G., et al., *Replication efficiency of oncolytic vaccinia virus in cell cultures prognosticates the virulence and antitumor efficacy in mice.* J Transl Med, 2011. **9**: p. 164.

148. Vaupel, P., *Hypoxia and aggressive tumor phenotype: implications for therapy and prognosis.* Oncologist, 2008. **13 Suppl 3**: p. 21-6.

149. Weibel, S., et al., *Viral-mediated oncolysis is the most critical factor in the late-phase of the tumor regression process upon vaccinia virus infection.* Bmc Cancer, 2011. **11**: p. 68.

150. Ribatti, D., et al., *Erythropoietin as an angiogenic factor.* European Journal of Clinical Investigation, 2003. **33**(10): p. 891-6.

151. *National Institute of Health. Global cancer research programs.* http://www.cancer.gov/researchandfunding/priorities/global-research-activities.

152. Kelly, K.J., et al., *Novel oncolytic agent GLV-1h68 is effective against malignant pleural mesothelioma.* Hum Gene Ther, 2008. **19**(8): p. 774-82.

153. Kelly, K.J., et al., *Real-time intraoperative detection of melanoma lymph node metastases using recombinant vaccinia virus GLV-1h68 in an immunocompetent animal model.* Int J Cancer, 2009. **124**(4): p. 911-8.

154. Joanna Vitfell Pedersen, L.K., Salma Alam, Martina Puglisi, Lauren Britton, Salem Sassi, David Mansfield, Timothy Yap, Johann De-Bono, Kevin Harrington, *Preliminary results of a Phase 1 study of intravenous administration of GL-ONC1 Vaccinia virus in patients with advanced solid cancer with real time imaging. The Royal Marsden Hospital.*

http://www.ncri.org.uk/ncriconference/2010abstracts/abstracts/C122.htm. 2012.

155. Glaspy, J., et al., *Comparable efficacy of epoetin alfa for anemic cancer patients receiving platinum- and nonplatinum-based chemotherapy: a retrospective subanalysis of two large, community-based trials.* Oncologist, 2002. **7**(2): p. 126-35.

156. Engert, A., *Recombinant human erythropoietin in oncology: current status and further developments.* Annals Oncology, 2005. **16**: p. 1584-1595.

157. Curt, G.A., et al., *Impact of cancer-related fatigue on the lives of patients: new findings from the Fatigue Coalition.* Oncologist, 2000. **5**(5): p. 353-60.

158. Harris, A.L., *Hypoxia--a key regulatory factor in tumour growth.* Nat Rev Cancer, 2002. **2**(1): p. 38-47.

159. Lee-Chen, G.J. and E.G. Niles, *Transcription and translation mapping of the 13 genes in the vaccinia virus HindIII D fragment.* Virology, 1988. **163**(1): p. 52-63.

160. Chen, N., et al., *A novel recombinant vaccinia virus expressing the human norepinephrine transporter retains oncolytic potential and facilitates deep-tissue imaging.* Mol Med, 2009. **15**(5-6): p. 144-51.

161. Chakrabarti, S., J.R. Sisler, and B. Moss, *Compact, synthetic, vaccinia virus early/late promoter for protein expression.* Biotechniques, 1997. **23**(6): p. 1094-7.

162. Hiley, C.T., et al., *Lister strain vaccinia virus, a potential therapeutic vector targeting hypoxic tumours.* Gene Ther, 2010. **17**(2): p. 281-7.

163. Yamaguchi, K., et al., *Effects of site-directed removal of N-glycosylation sites in human erythropoietin on its production and biological properties.* J Biol Chem, 1991. **266**(30): p. 20434-9.

164. Storring, P.L. and R.E. Gaines Das, *The International Standard for Recombinant DNA-derived Erythropoietin: collaborative study of four recombinant DNA-derived erythropoietins and two highly purified human urinary erythropoietins.* Journal of Endocrinology, 1992. **134**(3): p. 459-84.

165. Jones, S.S., et al., *Human erythropoietin receptor: cloning, expression, and biologic characterization.* Blood, 1990. **76**(1): p. 31-5.

166. Spivak, J.L. and B.B. Hogans, *The in vivo metabolism of recombinant human erythropoietin in the rat.* Blood, 1989. **73**(1): p. 90-9.

167. Watson, E., A. Bhide, and H. van Halbeek, *Structure determination of the intact major sialylated oligosaccharide chains of recombinant human erythropoietin expressed in Chinese hamster ovary cells.* Glycobiology, 1994. **4**(2): p. 227-37.

168. Imai, N., et al., *Physicochemical and biological characterization of asialoerythropoietin. Suppressive effects of sialic acid in the expression of biological activity of human erythropoietin in vitro.* Eur J Biochem, 1990. **194**(2): p. 457-62.

169. Noguchi, C.T., et al., *Cloning of the human erythropoietin receptor gene.* Blood, 1991. **78**(10): p. 2548-56.

170. Yasuda, Y., et al., *Erythropoietin regulates tumour growth of human malignancies.* Carcinogenesis, 2003. **24**(6): p. 1021-9.

171. Hardee, M.E., et al., *Erythropoietin biology in cancer.* Clin Cancer Res, 2006. **12**(2): p. 332-9.

172. Okazaki, T., et al., *Erythropoietin promotes the growth of tumors lacking its receptor and decreases survival of tumor-bearing mice by enhancing angiogenesis.* Neoplasia, 2008. **10**(9): p. 932-9.

173. LaMontagne, K.R., et al., *Recombinant epoetins do not stimulate tumor growth in erythropoietin receptor-positive breast carcinoma models.* Mol Cancer Ther, 2006. **5**(2): p. 347-55.

174. Tovari, J., et al., *Recombinant human erythropoietin alpha targets intratumoral blood vessels, improving chemotherapy in human xenograft models.* Cancer Res, 2005. **65**(16): p. 7186-93.

175. Chang, E., et al., *Targeting vaccinia to solid tumors with local hyperthermia.* Hum Gene Ther, 2005. **16**(4): p. 435-44.

176. Song, C.W., et al., *Implications of increased tumor blood flow and oxygenation caused by mild temperature hyperthermia in tumor treatment.* Int J Hyperthermia, 2005. **21**(8): p. 761-7.

177. Elliott, S., E. Pham, and I.C. Macdougall, *Erythropoietins: a common mechanism of action.* Exp Hematol, 2008. **36**(12): p. 1573-84.

178. Sytkowski, A.J., *Does erythropoietin have a dark side? Epo signaling and cancer cells.* Sci STKE, 2007. **2007**(395): p. pe38.

179. Hicks, A.M., et al., *Transferable anticancer innate immunity in spontaneous regression/complete resistance mice.* Proc Natl Acad Sci U S A, 2006. **103**(20): p. 7753-8.

180. Prutchi-Sagiv, S., et al., *Erythropoietin treatment in advanced multiple myeloma is associated with improved immunological functions: could it be beneficial in early disease?* Br J Haematol, 2006. **135**(5): p. 660-72.

181. Rocchetta, F., et al., *Erythropoietin enhances immunostimulatory properties of immature dendritic cells.* Clin Exp Immunol, 2011. **165**(2): p. 202-10.

182. Bohlius, J., et al., *Erythropoietin or darbepoetin for patients with cancer.* Cochrane Database Syst Rev, 2006. **3**: p. CD003407.

183. Fox, J.L., *FDA likely to further restrict erythropoietin use for cancer patients.* Nat Biotechnol, 2007. **25**(6): p. 607-8.

184. Blackwell, K.L., et al., *Human recombinant erythropoietin significantly improves tumor oxygenation independent of its effects on hemoglobin.* Cancer Res, 2003. **63**(19): p. 6162-5.

185. Kato, M., Y. Kato, and Y. Sugiyama, *Mechanism of the upregulation of erythropoietin-induced uptake clearance by the spleen.* Am J Physiol, 1999. **276**(5 Pt 1): p. E887-95.